Extraction of oil from algae for biofuel production by thermochemical liquefaction

Anro Barnard (B.Eng, Chemical)

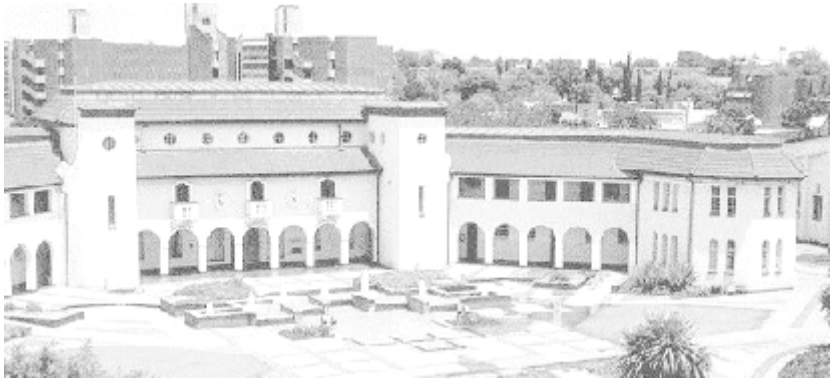

Dissertation submitted in fulfilment of the requirements for the degree of Master of Engineering in the School of Chemical and Minerals Engineering of the North-West University, Potchefstroom Campus

Supervisor: **Prof. S. Marx**

Co-supervisor: **Dr. P. van der Gryp**

November 2009

Abstract

The extraction of oil from microalgae was investigated. The study focused on the hydrothermal liquefaction of the microalgae *Microcystis aeruginosa, Cyclotella meneghinia* and *Nitzschia pusilla*. *M. aeruginosa* was collected from the Hartebeespoort dam, while *C. meneghinia* and *N. pusilla* were cultured in the laboratory.

The experiments were conducted in a high pressure autoclave with an inert atmosphere. Sodium carbonate was studied as a potential catalyst. The hydrothermal liquefaction of *M. aeruginosa, C. meneghinia* and *N. pusilla* was carried out at various reaction temperatures and catalyst loads. For the liquefaction of *M. aeruginosa* the residence times were also varied. The reaction temperatures ranged from 260 to 340 °C, while the catalyst loads varied between 0 and 10 wt% Na_2CO_3. The residence time was varied between 15 and 45 minutes.

The study showed that hydrothermal liquefaction of *M. aeruginosa* produced a maximum oil yield of 15.60 wt% at 300 °C, whereas the thermochemical liquefaction of *C. meneghinia* and *N. pusilla* produced maximum yields of 16.03 wt% and 15.33 wt%, respectively, at 340 °C. The residence time did not influence thermochemical liquefaction of the algae, while an increase in the catalyst load reduced the oil yield.

The reaction conditions had no effect on the elemental composition or the calorific value of the thermochemical liquefaction oil. The calorific value of the hydrothermal liquefaction oils ranged from 28.57 to 35.90 $MJ.kg^{-1}$.

Hydrothermal liquefaction of microalgae produced oil that can be used as substitute for coal in simple gasification processes. The study showed that microalgal blooms, such as the *M. aeruginosa* blooms of the Hartebeespoort dam, can be used for the extraction of oil through hydrothermal liquefaction.

Keywords: Hydrothermal liquefaction, *Microcystis aeruginosa*, microalgae

Uittreksel

Die ekstraksie van olie vanuit alge is bestudeer. Die studie het gefokus op die hidrotermiese vervloeiing van die alge *Microcystis aeruginosa, Cyclotella meneghinia* en *Nitzschia pusilla*. *M. aeruginosa* is vanuit die Hartebeespoortdam versamel, terwyl *C. meneghinia* en *N. pusilla* in die laboratorium gekweek is.

Eksperimente is uitgevoer in ’n hoë-druk outoklaaf in ’n inerte atmosfeer. Natriumkarbonaat is bestudeer as ’n potensiële katalisator. Die hidrotermiese vervloeiing van *M. aeruginosa, C. meneghinia* en *N. pusilla* is uitgevoer by verskillende reaksietemperature en katalisatorladings. Die verblyfstye is ook gevarieer vir die vervloeiing van *M. aeruginosa*. Die reaksietemperatuur vir die eksperimente is gevarieer tussen 260 en 340 °C, terwyl die katalisatorladings gevarieer is tussen 0 en 10 massa persentasie natriumkarbonaat. Die verblyfstyd van die eksperimente is gevarieer tussen 15 en 45 minute.

Die studie het gevind dat hidrotermiese vervloeiing van *M. aeruginosa* ’n maksimum olie-opbrengs van 15.60 massa persentasie by 300 °C lewer, terwyl die termochemiese vervloeiing van die *C. meneghinia* en *N. pusilla* maksimum olie-opbrengste van onderskeidelik 16.03 en 15.33 massa persentasie gelewer het by 340 °C. Die verblyfstyd het nie die termochemiese vervloeiing van die alge beïnvloed nie, terwyl ’n toename in die katalisatorlading ’n afname in die olie-opbrengs veroorsaak het.

Die reaksie toestande het geen invloed op die elementele samestelling en of hittewaarde van termochemiese vervloeiingsolie gehad nie. Die hittewaarde van die olie wat verkry is vanuit die termochemiese vervloeiing van die alge het gevarieer tussen 28.57 en 35.90 $MJ.kg^{-1}$.

Die hidrotermiese vervloeiing van alge het olie geproduseer wat gebruik kan word as ’n plaasvervanger vir steenkool in eenvoudige vergassingsprosesse. Die studie het gevind dat algopbloeie soos die opbloei van *M. aeruginosa* in die Hartebeespoortdam gebruik kan word vir die ekstraksie van olie deur gebruik te maak van hidrotermiese vervloeiing.

Sluitelwoorde: Hidrotermiese vervloeiing, *Microcystis aeruginosa*, alge

Declaration

I, Anro Barnard, hereby declare to be the sole author of the report entitled:

EXTRACTION OF OIL FROM ALGAE FOR BIOFUEL PRODUCTION BY THERMOCHEMICAL LIQUEFACTION

For the fulfilment of the requirements for the degree of Master of Engineering in the School of Chemical and Minerals Engineering of the North-West University, Potchefstroom Campus.

Anro Barnard

Potchefstroom

20 November 2009

Acknowledgements

"*But Jesus beheld them, and said unto them, with men this is impossible; but with God all things are possible.*" ~ Matthew 19:26

"*We give thanks to you, Lord God Almighty, the One who is and who was, because you have taken your great power and have begun to reign.*" ~ Revelation 11:17

I would like to show my appreciation to the following persons for their invaluable contributions to my study:

- First and foremost my Heavenly Farther, because without Him this study would not have been possible.
- Prof. Sanette Marx for her leadership and advice.
- Dr. Percy van der Gryp for his guidance with the articulation of my results and the writing of my dissertation.
- My parents, André and Mareé Barnard, for their unwavering support throughout my studies.
- Christel Schutte for her patience, understanding and support.
- Dr. Arthurita Venter for her advice and guidance regarding the algae.
- Dr. George Obiero for his assistance with the gas chromatography.
- Prof. Rui Krause and Patrick Komane from the Department of Chemical Technology at the University of Johannesburg for the elemental analyses.
- Jan Kroeze and Adrian Brock for their technical expertise and help without which the experimental work would not have been possible.
- Dr. Johan Jordaan for the use of the gas chromatograph at the School for Chemistry at the Potchefstroom campus of the North-West University.
- SASOL and SANERI for their financial support.

Table of Contents

NOMENCLATURE

Symbols	Description	Unit
K	Number of factors	
n_c	Number of replicates of the centre point	
n_t	Total number of points	
P_c	Critical pressure	Mpa
R^2	Measure of the variation around the mean that is explained by the model	
T_c	Critical temperature	°C
x_i	Coded variable	
y	Response of the regression model	
Y_i	Response variables	

Greek symbols	Description	Unit
α	Distance of axial point from centre point	
β_i	Regression coefficient	
δ	Hildebrand solubility parameter	($Mpa^{1/2}$)
δ_p	Polar cohesion parameter	($Mpa^{1/2}$)
δ_h	Hydrogen bonding cohesion parameter	($Mpa^{1/2}$)
δ_d	Dispersion cohesion parameter	($Mpa^{1/2}$)
δ_t	Total cohesion parameter	($Mpa^{1/2}$)
ε	Error of model	
ε_r	Dielectric constant	
μ	Dipole moment	Debye (D)
ξ_i	Natural variable	-
T_c	Critical temperature	°C
P_c	Critical pressure	Mpa
x_i	Coded variable	

Abbreviation	Definition
A	Asphaltene
ANOVA	Analysis of variance
CCD	Central Composite Design
DGDG	Digalactosyl-diacylglycerol
DGTS	Diacylglyceryl-N,N,N-trimethylhomoserine
FID	Flame ionization detector
GC	Gas chromatograph
GHG	Greenhouse gasses
IEA	International Energy Agency
IPCC	Intergovernmental Panel on Climate Change
JPoI	Johannesburg Plan of Implementation
MGDG	Monogalactosyl-diacylglycerol
MSHA	Mine Safety and Health Administration
NEMP	National Eutrophication Management Programme
NIOSH	The National Institute for Occupational Safety and Health
nPAH	Nitrated polyaromatic hydrocarbons
NREL	National Renewable Energy Laboratory
NSPU	National Scientific Programmes Unit
PA	Preasphaltene
PAH	Polyaromatic hydrocarbons
PtdCho	Phosphatidylcholine
PtdEtn	Phospatidylethanolamine
PtdGro	Phospatidylclycerol
RSM	Response surface methodology
SEM	Scanning electron microscope
SQDG	Sulfoquinovosyl-diacylglycerol
TMSH	Trimethyl Sulfonium Hydroxide
USA	United States of America

LIST OF FIGURES

LIST OF TABLES

Chapter 1. – Introduction

This chapter provides a broad overview of the contents of the study. Section 1.1 discusses the background and motivation for the investigation, while Section 1.2 lists the aims and objectives of the study. Section 1.3 provides the scope of the investigation.

1.1 Background and Motivation

1.1.1 Current energy situation

In 2007, eighty percent of the global energy demand was fulfilled by utilization of fossil fuels, whereas renewable energy and nuclear power contributed only 13.5% and 6.5% respectively to the total energy needs (Asif & Muneer, 2007: 1389). The current energy situation has four major concerns, namely (i) the depletion of the fossil fuel reserves, (ii) global warming, (iii) energy security and (iv) a rising energy cost (Asif & Muneer, 2007: 1397).

In 2007 the World Coal Institute predicted that at the present production levels, the coal, oil and gas reserves, i.e. fossil fuel reserves, will last for 147, 41 and 63 years, respectively (World Coal Institute, 2007). The combustion of these fossil fuels for energy production produces carbon dioxide emissions, which the Intergovernmental Panel on Climate Change (IPCC) found to constitute 77% of the total Greenhouse Gasses (GHG) emitted globally (IPCC, 2007). Greenhouse gases such as carbon dioxide (CO_2), methane (CH_4), water vapour and fluorinated gases are responsible for global warming. Global warming is defined as an increase in the temperature of the lower atmosphere due to an increase in the concentration of greenhouse gases. These greenhouse gases allow heat from the sun to enter the atmosphere, but not to escape from the atmosphere (Yeseul *et al.,* 2008). Therefore, it is important to reduce the amount of CO_2 emissions in order to alleviate the effects of global warming on the temperature. This can be accomplished by reducing the combustion of fossil fuels, i.e. by reducing the global reliance on fossil fuels.

The economies of countries are dependent on secure supplies of energy (Asif & Muneer, 2007: 1401). In the current energy situation, many countries only have a singular source of energy, which reduces the energy security of the country. The global reliance on fossil fuels produces a high demand, which in turns results in high energy prices. A rise in the oil price affects the gross domestic product (GDP) and financial markets. A $10 increase in the oil price would reduce the GDP of a country by 0.5% and result in $225 billion losses. Renewable energy can help nations to avoid these costly macroeconomic losses that arise due to a rise in the oil price (Chang *et al.,* 2009: 5797).

The demand for oil increases dramatically due to an exponential growth in the world population. In conjunction with the depletion of fossil fuels, this suggests that the energy supply in the future has to come from renewable sources of energy such as solar, wind, hydroelectric, biomass and geothermal power (Demirbaş, 2001: 1362). Demirbas and co-workers (2009: 1746) considered biomass to be the renewable energy source with the highest potential to contribute to the energy needs of the industrialized as well as developing countries worldwide.

1.1.2 The use of biomass for energy production

The contribution of renewable energy sources to the total energy demand is expected to increase very significantly to between 30 and 80% in 2100. As a source of renewable energy, biomass contributes 62.1% of the energy obtained from renewable energy sources (Demirbaş, 2005: 173 - 174). Therefore there is a big potential for the development of renewable energy from biomass.

In essence petroleum is formed by plant decomposition over long periods of time. In order to produce oil-like products from biomass, the process of plant decomposition through deoxygenation must be accelerated. Figure 1.1 depicts a generalization of the overall sequence of transformations for energy production by biomass (Walton & Paudler, 1981: 650).

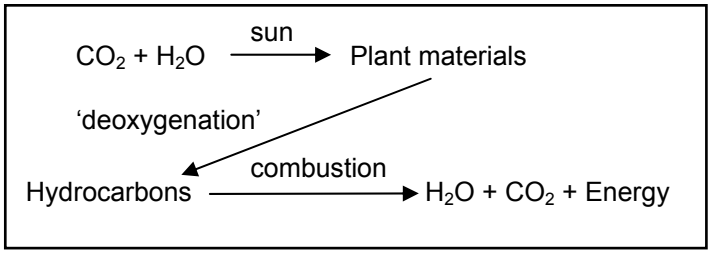

Figure 1.1: Generalization of overall sequence of transformations.

In order to produce a complete solar cycle, the deoxygenation process should involve materials that can be generated by utilizing energy from the sun (Walton & Paudler, 1981: 650). Biomass is the solution to completing the solar cycle. Biomass is plant matter which is created by photosynthesis and may therefore be considered as effectively stored solar energy and a renewable source of carbon (Demirbaş, 2001: 1358 – 1360).

The use of biomass as source of energy has many advantages to the environment. Terrestrial vegetation annually captures 500 billion tonnes of CO_2 through photosynthesis (Skjårnes *et al.*, 2007: 406). This is 20 times more than the amount of CO_2 that is released annually from fossil fuel consumption. The capturing of CO_2 indirectly by planting vegetation is, however, inadequate to solve the problem of growing CO_2 emissions (Skjårnes *et al.,* 2007: 405). The problem of growing CO_2 emissions can be addressed by introducing biomass as a source of energy. The combustion of biomass only releases the CO_2 that was absorbed while the plant was growing and does not introduce any additional CO_2 into the atmosphere (Demirbaş, 2001: 1358 – 1359). This phenomenon makes biomass CO_2 neutral (Demirbaş, 2001: 1365) and results in a net reduction of greenhouse gases by substituting biomass for fossil fuels (Demirbaş, 2001: 1365; Minowa et al., 1995: 1735).

The utilization of biomass improves energy security by decreasing the reliance on oil and providing an alternative source of energy (Demirbaş, 2001: 1365). The Herfindahl index relates the market size to risk dependency, i.e. it can quantify the dependency of a country on an energy source. A greater number of fuel supplies or suppliers lower the risk of dependency. A country that is only dependent on one supplier (or country) for 95% of their transportation petroleum, has a related dependency index of 0.90. Replacing 10% of the petroleum in the market with biofuels (produced domestically, or imported from another region) will result in a dependency index of 0.74 (IEA, 2004: 173). This shows that even a small

contribution of biomass to the fuel supply of a country can significantly alleviate the dependence of a country on oil imports.

The introduction of biomass as a source of energy has the ability to meet the shortcomings presented by the current energy situation. The use of biomass for energy production has many added advantages, for example energy from biomass (1) contributes to the reduction of poverty in developing countries, (2) meets energy needs at all times, (3) can deliver energy in any form required by people, (4) is carbon dioxide neutral and (5) helps to restore unproductive and degraded lands, which increases biodiversity, soil fertility and water retention (Demirbas *et al.,* 2009: 1746). Biomass may be used directly (burning wood) or indirectly (conversion into liquid or gaseous fuel) and has the ability of producing various types of fuels such as solid, liquid and gaseous fuels (Demirbaş, 2001: 1358).

The use of biomass as an energy source also has some disadvantages that may arise. In South Africa the Biofuels Industrial Strategy of South Africa proposed a 2% penetration of biofuels into the national liquid fuel supply by 2013 to reduce the emissions of greenhouse gasses in South Africa according to the Kyoto Protocol (Biofuels Industrial Strategy of the Republic of South Africa, 2007: 6). In order to achieve this, the Biofuels Industry of South Africa suggested using sugar cane and sugar beet crops for bioethanol production whereas sunflower, canola and soybean crops were suggested for biodiesel production (Biofuels Industrial Strategy of the Republic of South Africa, 2007: 3).

The use of food crops for the production of biofuel will lead to an increase in food prices, which may contribute to world hunger (Nebehay, 2007). The production of energy from food resources has a significant effect on the prices of the feedstock. This is illustrated by a doubling in the grain prices due to the small amount of grain (mainly sugarcane, maize and oilseeds) that is currently being used for biofuel production (Gressel, 2007: 247). Increases in the food prices due to biofuel production is not localised to South Africa. The interdependency of the international markets will result in an increase in the world grain price when there is for instance only an increased use of grain in the United States of America (USA) for the production of biofuel (Sugrue & Douthwaite, 2007: 1). This rise in grain prices will be carried through the food chain and will result in a rise in all food prices. In turn a low availability of grain for emergency food aid will be produced (Gressel, 2007: 247). In South Africa the very poor living in rural areas spend over 62% of their income on

food, whereas those living in towns spend over 51% of their income on food (Sugrue & Douthwaite, 2007: 4). An increase in the food prices will therefore affect South Africa severely.

It is of the utmost important to use alternative feedstocks that do not form part of the food supply for the production of biofuels (Nebehay, 2007). Peat (Panayotova-Björnbom *et al*, 1979; Björnbom *et al.*, 1981), wood (Boocock *et al.,* 1979; Eager *et al.,* 1982), algae (Herro, 2008; Inoues et al., 1994) and sewage sludge (Boocock *et al.,* 1992; Yokoyama *et al.,* 1987) are examples of biomass that does not form part of the food supply and have been studied as possible energy sources.

1.1.3 Biomass suitable for the production of energy

Algae are oil rich sources of biomass and do not form part of the food supply of a nation (Herro, 2008). Algae also have the ability to efficiently take a waste form of carbon (CO_2) and convert it into natural liquid oil (Widjaja *et al.,* 2009: 13). Ross and co-workers (2008: 6494) stated that aquatic biomass, such as algae, has higher photosynthetic efficiencies (6 to 8%) than their terrestrial counterparts (1.8 to 2.2%) and can therefore convert solar energy more effectively than terrestrial biomass (Ross *et al.,* 2008: 6494). In Table 1.1 the use of terrestrial biomass as source of high-lipid material for biodiesel production is compared with the use of microorganisms, such as microalgae (Rittmann, 2008: 210). Table 1.2 shows the annual production of biofuels obtained from an average hectare of canola, soybeans, sugar beets, sunflower and algae.

Table 1.1: Comparison of terrestrial biomass and photosynthetic microorganisms as source of high-lipid material for biodiesel production.

Feature	**High-lipid plants**[a]	**Photosynthetic microorganisms**[b]
Doubling time	Relatively long, weeks.	Relatively short, ~ 1 day.
Needs arable land?	Yes.	No.
Harvesting	Seasonal, 1 or 2 crops per year.	Continuous.
Biomass quality – homogeneity	Heterogeneous, with leaves, stems, seeds, roots, etc.	Homogeneous.
Biomass quality – lignocellulose	Yes.	No.
Water use	High due to evapotranspiration.	Low to moderate if controlled.
Fertilizer use	High use rate and subject to runoff.	Amenable to nutrient capture and recycling.

a. High-lipid plants considered here are soybeans and sunflowers.

b. Photosynthetic microorganisms include algae and cyanobacteria.

Table 1.2: Biodiesel production from crops of canola, soybeans, sugar beets and algae.

Crop	**Production (litres)**
Canola[a]	1 500
Soybeans[b]	655
Algae[b]	47 000
Sugar beets[a]	5 000
Sunflower[c]	770 – 961

a) Soetaert, 2008: 5.

b) Herro, 2008.

c) Kondili and Kaldellis, 2007: 2143.

Table 1.2 indicates that algae are a viable source of biomass for the production of biodiesel. From Table 1.1 it can be seen that algae have numerous advantages over terrestrial biomass. Rosenberg and co-workers (2008: 430) state that algae have the unique ability of combining the renewable energy-capturing of photosynthesis with the high yields obtained from microbial cultivation. This makes algae potentially valuable organisms for economical, industrial-scale production processes (Rosenberg *et al.,* 2008: 430).

1.1.4 Extraction of oil from algae

As mentioned previously, algae are oil rich sources of biomass. The oil contained in the algal cells may be extracted in a variety of different ways, including pyrolysis and thermochemical liquefaction (Skjånes *et al.*, 2007: 410). In Figure 1.2 the various conversion pathways for the utilization of algae is depicted (Amin, 2009: 1835).

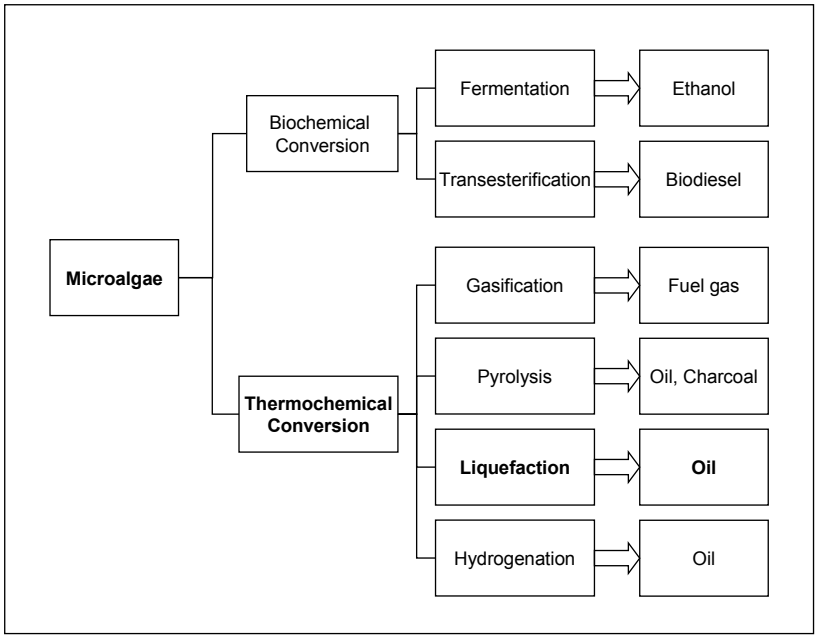

Figure 1.2: Energy conversion processes from microalgae.

The variety of products listed in Figure 1.2 indicates the versatility of algae as a source of renewable biofuel. Pyrolysis, liquefaction and hydrogenation are identified as pathways for oil extraction from algae. An evaluation of the energy conversion processes listed in Figure 1.2 showed that hydrothermal processing, i.e. liquefaction, is the best suited process for the extraction of the oil from algae. Hydrothermal processing (liquefaction) offers various advantages over the other biofuel production methods, which include high throughputs, high energy and separation efficiency, the ability to use mixed feedstocks and the production of direct replacements for existing fuels. Liquefaction also has no need to maintain specialized microbial cultures or enzymes and the high temperatures used during liquefaction produce biofuels that are free of biologically active organisms or compounds, including bacteria, viruses and even prion proteins (Peterson *et al.,* 2008: 22 – 33).

Various persons investigated the thermochemical liquefaction of different algal cells with great success (Inoues *et al*., 1994; Dote *et al*., 1994; Sawayama *et al*., 1995;

Minowa *et al*., 1995; Matsui *et al*., 1997, Yang *et al*., 2004). Table 1.3 lists previous work done on the liquefaction of algae.

Table 1.3: Previous work done on the liquefaction of algae

Year	Algae	Temperature (°C)	Observation	Reference
1994	*Botryococcus braunii* Berkeley strain	200 – 340	Maximum oil recovery of 78 wt% obtained at 200 °C with the use of a catalyst. The oil consisted of low molecular weight hydrocarbons, botryococcenes and polar substances.	Inoues *et al*., 1994: 273.
1994	*Botryococcus braunii* Kützing Berkeley strain	200 – 340	Thermochemical liquefaction produced a greater amount of oil than the amount of hydrocarbons contained in the cells. The oil obtained was comparable with petroleum oil	Dote *et al.*, 1994: 1855.
1995	*Botryococcus braunii* Berkeley strain	300	Thermochemical liquefaction sufficiently recovered the oil in the algal cells. Thermochemical liquefaction produced an oil yield of 64% on a dry basis at 300 °C.	Sawayama *et al*., 1995: 730 – 731.
1995	*Dunaliella tertiolecta*	250 – 340	Oil comparable to fuel oil was obtained from the liquefaction process. Thermochemical liquefaction of *Dunaliella tertiolecta* is a net energy producer.	Minowa *et al*., 1995: 1735 – 1738.
1997	*Spirulina* sp.	300 – 425	Thermochemical liquefaction conducted with water delivered a yield of 78.3 wt% without a catalyst. The oil had a lower calorific value than the oil obtained from thermochemical liquefaction using toluene.	Matsui *et al*., 1997: 1048.
2004	*Microcystis viridis*	300 – 340	The oil obtained from the thermochemical liquefaction process had the potential to be used as an energy resource and could be classified as heavy oil.	Yang *et al*., 2004: 32.

The process of thermochemical liquefaction has of yet not been studied for the extraction of oil from algae that are readily available in South Africa. This shortcoming will be addressed by studying the extraction of oil from microalgae available in South Africa using thermochemical liquefaction.

1.2 Aims and Objectives

i. Extraction of oil from microalgae available in South Africa through thermochemical liquefaction.

ii. Determination of the effect of operating conditions (temperature, catalyst load and reaction time) of the thermochemical liquefaction process on the yield and characteristics of the extracted oil.

iii. Development of a process for the extraction of oil from algae.

iv. Identification of the best source of algae for thermochemical liquefaction.

1.3 Scope of the investigation

In order to fulfil the aims and objectives set out in section 1.2, the following is required from the various sections of the report:

- Chapter 2 – Literature Study
    - A literature study on the thermochemical liquefaction process and the variables that influence the thermochemical liquefaction process.
    - A study on the previous work done with the thermochemical liquefaction of biomass.
    - A study on the various types of algae that occur as well as the characteristics of the various algal types.
    - A study on the production of biodiesel.
    - A study on the biodiesel policy of South Africa.

- Chapter 3 - Experimental
    - Planning and description of the experimental setup.
    - Description of the reagents used.
    - Identification of the manipulated variables of the system as well as the response variables.
- Chapter 4 – Results and Discussion
    - Results from a central composite design of thermochemical liquefaction experiments conducted on *Microcystis aeruginosa* collected from the Hartebeespoort dam.
    - Results from thermochemical liquefaction experiments conducted on cultivated *Cyclotella meneghinia*.
    - Results from thermochemical liquefaction experiments conducted on cultivated *Nitzschia pusilla*.
    - Processing the measured variables in order to determine the effect of the operating conditions on the quality of the oil obtained from the thermochemical liquefaction process as well as the oil yield.
- Chapter 5 – Conclusions and Recommendations

1.4 References

Amin, S. 2009. Review on biofuel oil and gas production processes from microalgae. Energy Conversion and Management, 50(7): 1834 – 1840.

Asif, M. & Muneer, T. 2007. Energy supply, its demand and security issues for developed and emerging economies. Renewable and Sustainable Energy Reviews, 11: 1388 – 1413.

Biofuels Industrial Strategy of the Republic of South Africa. 2007. http://www.fanrpan.org/documents/d00472/Biofuels_industry_RSA_Dec2007.pdf. Date of access: 18 March 2008.

Björnbom, P., Granath, L., Kannel, A., Karlsson, G., Lindström, L. & P-Björnbom, E. 1981. Liquefaction of Swedish peats. Fuel, 60: 7 – 13.

Boocock, D.G.B., Mackay, D., McPherson, M., Nadeau, S. & Thurier, R. 1979. Direct hydrogenation of hybrid poplar wood to liquid and gaseous fuels. The Canadian Journal of Chemical Engineering, 57: 98 – 101.

Boocock, D.G.B., Konar, S.K., Leung, A. & Ly, L.D. 1992. Fuels and chemicals from sewage sludge 1: The solvent extraction and composition of a lipid from a raw sewage sludge. Fuel, 71: 1283 – 1289.

Chang, T., Huang, C. & Lee, M. 2009. Threshold effect of the economic growth rate on the renewable energy development from a change in energy price: Evidence from OECD countries. Energy Policy, 37: 5796 – 5802.

Demirbaş, A. 2001. Biomass resource facilities and biomass conversion processing for fuels and chemicals. Energy Conversion and Management, 42: 1357 – 1378.

Demirbaş, A. 2005. Potential applications of renewable energy sources, biomass combustion problems in boiler power systems and combustion related environmental issues. Progress in Energy and Combustion Science, 31: 171 – 192.

Demirbaş, F.M., Balat, M. & Balat, H. 2009. Potential contribution of biomass to the sustainable energy development. Energy Conversion and Management, 50(7): 1746 – 1760.

Dote, Y., Sawayama, S., Inoue, S., Minowa, T. & Yokoyama, S. 1994. Recovery of liquid fuel from hydrocarbon-rich microalgae by thermochemical liquefaction. Fuel, 73(12): 1855 – 1857.

Eager, R.L., Mathews, J.F. & Pepper, J.M. 1982. Liquefaction of Aspen Poplar Wood. The Canadian Journal of Chemical Engineering, 60: 289 – 294.
Gressel, J. 2007. Transgenics are imperative for biofuel crops. Plant Science, 174(3): 246 – 263.

Herro, A. 2008. Better than corn? Algae Set to Beat Out Other Biofuel Feedstocks. World Watch, 21(1): 4.

IEA **see** International Energy Association

Inoue, S., Dote, Y., Sawayama, S., Minowa, T., Ogi, T. & Yokoyama, S. 1994. Analysis of oil derived from liquefaction of Botryococcus Braunii. Biomass and Bioenergy, 6(4): 269 – 274.

Intergovernmental Panel on Climate Change. 2007. Climate Change 2007: Synthesis Report. http://www.ipcc.ch/pdf/assessment-report/ar4/syr/ar4_syr.pdf. Date of access: 8 April 2008.

International Energy Agency. 2004. Biofuels for transport: An international perspective. France. 210 p.

IPCC **see** Intergovernmental Panel on Climate Change

Kondili, E.M. & Kaldellis, J.K. 2007. Biofuel implementation in East Europe: Current status and future prospects. Renewable and Sustainable Energy Reviews, 11: 2137 – 2151.

Matsui, T., Nishihara, A., Ueda, C., Ohtsuki, M., Ikenaga, N. & Suzuki, T. 1997. Liquefaction of micro-algae with iron catalyst. Fuel, 76(11): 1043 – 1048.

Minowa, T., Yokoyama, S., Kishimoto, M. & Okakura, T. 1995. Oil production from algal cells of Dunaliella tertiolecta by direct thermochemical liquefaction. Fuel, 74(12): 1735 – 1738.

Nebehay, S. 2007. Biofuels could lead to mass hunger deaths: U.N. envoy. Reuters, 14 June.

Panayotova-Björnbom, E., Björnbom, P., Cavalier, J.C. & Chornet, E. 1979. The combined dewatering and liquid phase hydrogenolysis of raw peat using carbon monoxide. Fuel Processing Technology, 2: 161 – 169.

Peterson, A.A., Vogel., F., Lachance, R.P., Fröling, M., Antal., M.J. & Tester, J.W. 2008. Thermochemical biofuel production in hydrothermal media: A review of sub- and supercritical water technologies. Energy and Environmental Science, 1: 32 – 65.

Rittmann, B.E. 2008. Opportunities for Renewable Bioenergy Using Microorganisms. Biotechnology and Bioengineering, 100(2): 203 – 212.

Rosenberg, J.N., Oyler, G.A., Wilkinson, L. & Betenbaugh, M.J. 2008. A green light for engineered algae: redirecting metabolism to fuel a biotechnology revolution. Current Opinion in Biotechnology, 19: 430 – 436.

Ross, A.B., Jones, J.M., Kubacki, M.L. & Bridgeman, T. 2008. Classification of macroalgae as fuel and its thermochemical behaviour. Bioresource Technology, 99: 6494 – 6504.

Sawayama, S., Inoue, S., Dote, Y. & Yokoyama, S. 1995. CO_2 fixation and oil production through microalga. Energy Conversion and Management, 36(6 – 9): 729 – 731.

Skjånes, K., Lindblad, P. & Muller, J. 2007. BioCO_2 – A multidisciplinary, biological approach using solar energy to capture CO_2 while producing H_2 and high value products. Biomolecular Engineering, 24: 405 – 413.

Soetaert, W. 2008. Second generation biofuels. http://www.ef4.be/documents/evenements/biocarburants/041_gent.pdf. Date of access: 8 April 2008.

Sugrue, A. & Douthwaite, R. 2007. Biofuel production and the threat to South Africa's food security. (Brief delivered to the Regional Hunger and Vulnerability Programme in April 2007.) http://www.wahenga.net/uploads/documents/news/Brief_11_Biofuels.pdf. Date of access: 9 July 2009.

Walton, T.E. & Paudler, W.W. 1981. Conversion of cellulose to hydrocarbons. Fuel, 60: 650 – 654.

Widjaja, A., Chien, C. & Ju, Y. 2009. Study of increasing lipid production from fresh water microalgae Chlorella vulgaris. Journal of the Taiwan Institute of Chemical Engineers, 40: 13 – 20.

World Coal Institute. 2007. Coal Facts. http://www.worldcoal.org/pages/content/index.asp?PageID=188. Date of access: 7 May 2008.

Yang, Y.F., Feng, C.P., Inamori, Y. & Maekawa, T. 2004. Analysis of energy conversion characteristics in liquefaction of algae. Resources, Conservation and Recycling, 43: 21 – 33.

Yeseul, K., Granger, E., Puckett, K., Hasar, C. & Francel, L. 2008. Global Warming: Definition. http://web.mit.edu/12.000/www/m2010/finalwebsite/background/globalwarming/definition.html. Date of access: 8 April 2008.

Yokoyama, S., Suzuki, A., Murakami, M., Ogi, T., Koguchi, K. & Nakamura, E. 1987. Liquid fuel production from sewage sludge by catalytic conversion using sodium carbonate. Fuel, 66: 1150 – 1155.

Chapter 2. – Literature Study

2.1 Algae

In this section the various characteristics of algae will be discussed. Section 2.1.1 states a short introduction of the study of algae. Section 2.1.2 discusses the occurrence and the distribution of the algae, whereas Section 2.1.3 elaborates on the classification of algae.

In Section 2.1.4 the food reserves that are stored in the algal cells are discussed and Section 2.1.5 states the lipid content of various algal cells. Section 2.1.6 describes the suitability of algae for oil production.

2.1.1 Introduction to algae

It is difficult to give a precise definition of algae due to the large variation in their structure. Algal cells always have single-cellular reproductive organs and may vary in size from a 0.5 micron unicellular organism to large seaweed. In between these two extremes there are thousands of species of unicellular, colonial, filamentous, frond-like and bushy plants which display great complexity and geometric design (Prescott, 1969: 4 – 5).

The study of algae is termed phycology or algology (Van den Hoek *et al*., 1995: 9). The defining factor that distinguishes algae from other chlorophyll containing plants is their reproduction, which differs from that of other green plants in that the organisms reproduce through gametes that are either produced by the algal organism itself (unicellular) or through unicellular containers (multicellular algae) (Bold & Wynne, 1978: 1).

2.1.2 Occurrence and Distribution of Algae

Algae are able to live completely submersed in water or exposed to the atmosphere and may be found in fresh water, seawater and also brackish water. This versatility of algae results in their occurrence from deserts to snowfields (Bold & Wynne, 1978: 2 – 3).

Algae are highly selective of their habitats and require specific chemical and physical conditions (Prescott, 1969: 16) to grow and reproduce. Some algae can tolerate a wide pH range, while others are limited to either an acidic or alkaline environment (Bold & Wynne, 1978: 3). Table 2.1 lists some algae that are able to live in extreme conditions (Prescott, 1969: 17).

Table 2.1: Algae able to live in extreme conditions.

Algae	**Extreme condition**
Blue-green algae (sometimes termed as thermal)	Hot water up to 80°C.
Diatoms	Warm water up to 40°C.
Chlamydomonas spp., *Scotiella* spp.and *Raphidonema* spp.	Ice and snow.

Some algae are able to live at the interface between water and the atmosphere (Bold & Wynne, 1978: 3), while other algae may associate with fungi. The association of algae with fungi produces lichens, which are composite organisms that form a characteristic crust-like or branching growth on rocks or tree trunks. Lichens are of considerable biological interest and in some instances the fungi act like parasites on the algal cells (Prescott, 1969: 18).

Algae may be distributed in a variety of ways. Marine algae are distributed by tides, currents and agitation by wind. The movement of ships and animals (such as aquatic birds) also contribute to the distribution of marine algae as well as bursting bubbles and air currents. Algae growing in and on soil are distributed by air currents (Bold & Wynne, 1978: 5 – 6).

2.1.3 Classification of algae

A variety of algal classes exists. The following characteristics of the algae are used to classify them:

1. Pigments: Type (chemical composition) and the amounts.
2. Reserve food products or products produced during photosynthesis and their chemistry.
3. Flagellation: The type and number of flagella, their insertion and morphology. Flagella are long, threadlike appendages consisting of certain cells or unicellular

organisms that function as an organ for locomotion. Morphology refers to the structure of an organism or one of its parts.

4. Cell wall: The chemistry and physical features of the cell wall.
5. The presence (Eukaryotic algae) or the absence (Akaryotic algae) of a true nucleus.
6. Life history and reproduction: The reproductive organs and methods (Prescott, 1969: 6).

In order to determine whether an organism may be classified as an alga it is examined according to the criteria mentioned above. A combination of these criteria may disprove the characterization of an organism as algae or determine the classification of a certain species. In order to sufficiently classify algal species, an elaborate life history is required (Prescott, 1969: 6). Algae are divided into nine main categories as follows:

1. Phylum Chlorophyta (Green Algae).
2. Phylum Euglenophyta (Euglenoid Algae).
3. Phylum Chrysopyta (Yellow-green Algae).
4. Phylum Pyrrhophyta (Dinoflagellates).
5. Phylum Phaeophyta (Brown Algae, Brown Seaweeds).
6. Phylum Rhodophyta (Red Algae).
7. Phylum Cyanophyta (Blue-Green Algae).
8. Phylum Cryptophyta (Blue and Red Flagellates).
9. Phylum Chloromonadophyta (Chloromonads).

The large variation in the structure of the algae produces an array of algal classes. Aquatic algae are able to survive suspended (planktonic) or attached. They may also live on the bottom (benthic) of the ocean or on various other substances. In Table 2.2 the classification of the various benthic algae is given in regard to the substance that it lives on. Aquatic plankton consists of plants and animals, as well as bacteria and fungi. Plankton may also be classified into various groups by their occurrence. Table 2.3 gives the classification of plankton according to their occurrence (Prescott, 1969: 17). The attached and bottomdwelling organisms are collectively termed as benthos (Bold & Wynne, 1978: 3).

Table 2.2: Classification of benthic algae.

Algal classification	Substance
Epilithic[a]	Stones
Epipelic[a]	Mud or sand
Epiphytic[a]	Plants
Epizoic[a]	Animals (on outside)
Endozoic[b]	Animals (on inside)
Edaphic[a]	In and on soil
Corticolous[a]	Tree bark

a. Bold & Wynne, 1978: 3.

b. Prescott, 1969: 17.

Table 2.3: Classification of plankton according to their occurrence.

Class of plankton	Occurrence
Euplanton (true plankton)	Float free in open water.
Tychoplankton	Not attached to anything, but still lives among algal mixtures near the shore and in weed beds.
Potamoplankton	Found in rivers.
Heleoplankton	Found in ponds.

Marine algae and desert soil algae may be categorized by the habitats that they grow in. The categorization of marine and desert soil algae by their growth habitat, is given in Tables 2.4 and 2.5, respectively (Bold & Wynne, 1978: 3 – 4).

Table 2.4: Categorization of marine algae by their growth habitat.

Category of marine algae	Growth habitat
Subaerial/supralittoral	Grow above the water level and in the spray zone. They may be edaphic, epilithic, epiphytic, epizoic, corticolous or parasitic.
Intertidal	Exposed periodically to the water and the atmosphere due to variations in the water level caused by tidal changes.
Sublittoral	Permanently submersed. Grow at various depths depending on the turbidity of the water.

Table 2.5: Categorization of desert sand algae by their growth habitat.

Category of desert soil algae	Growth habitat
Endedaphic	Living in soil.
Epidaphic	Living on the soil surface.
Hypolithic	On the lower surface of stones on soil.
Rock algae	
Chasmolithic	Growing in rock fissures.
Endolithic	Rock penetrating algae.

It is clear that a variety of algal classes exists. This is due to the variety of classification methods used to classify the algae.

2.1.4 Food reserves in algae

Similar to other photosynthetic plants, algae produce food that is fit for human consumption. The process of photosynthesis produces sugar according to the following reaction (Tiffany, 1958: 14 – 15):

$$6CO_2 + 12H_2O \rightarrow C_6H_{12}O_6 + 6O_2 + 6H_2O$$

The sugar is used to produce starches, fats and proteins in the protoplasm of algal cells and the production thereof may occur at any time. The protoplasm may be defined as the substance that constitutes the living matter of cells and it manifests the vital life functions of a cell. The production of starches requires sugar molecules to lose water molecules (Tiffany, 1958: 18).

Fats are produced through a two stage process. Firstly the sugar undergoes a reduction in the oxygen content in relation to the hydrogen, which forms glycerine and a fatty acid. The fatty acid and the glycerine then combine to produce a fat. This stage is accompanied by a loss of water (Tiffany, 1958: 18).

Under optimal growth conditions algae produce fatty acids mainly for esterification into glycerol-based membrane lipids, which constitute approximately 5 – 20 wt% of the dry cell weight. Hydrocarbons are another type of lipid that may be found in algal cells and normally constitute less than 5 wt% of the dry cell weight (Hu *et al.,* 2008: 622).

In order for algae to produce proteins they require mineral salts that contain nitrogen, sulphur and sometimes phosphorus. The sugar and nitrogen form an amino acid through a process of reduction. This reduction process may also occur with sulphur and sugar (Tiffany, 1958: 18). In Figure 2.1 the foods that are produced and used by algae are depicted (Tiffany, 1958: 14).

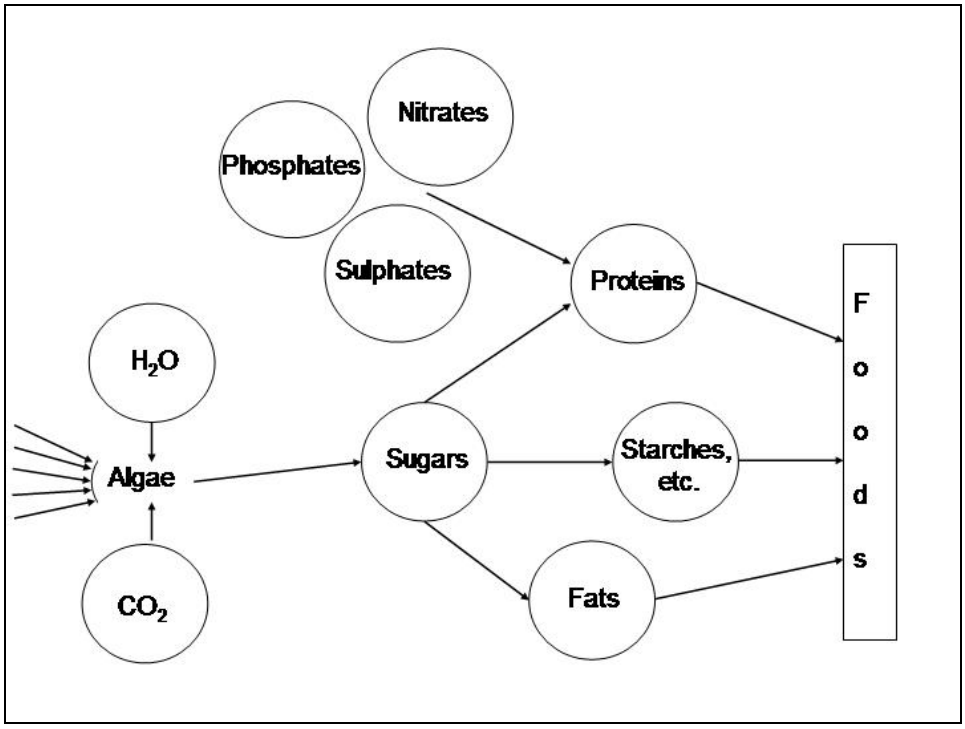

Figure 2.1: Foods produced and used by algae.

In the algal cells fats are stored mostly in spores and in other algal cells that are in a resting stage (Miller, 1962: 357). According to Miller (1962: 358) the acids that occur in the fats range from C_{12} to C_{24}. Miller (1962: 358) also discovered that the even numbered acids are the only acids that occur at significant levels and that these fatty acids may occur as mono-, di-, or triglycerides or, less frequently, free in the algal cells. The triglycerides are fatty acids in which all three hydroxyl groups of the glycerol are esterified. These lipids are regarded as energy storage products (Williams, 1979: 100). The following saturated straight-chain fatty acids occur frequently in algal cells:

- Lauric acid (C_{12}).
- Myristic acid (C_{14}).
- Palmitic acid (C_{16}).
- Stearic acid (C_{18}) (Miller, 1962: 358).

Collyer and Fogg (1955: 256 – 257) suggested that the accumulation of fat in algal cells are dependent on the environment in which the species are normally found and not on the tendency of the organism to synthesize fat. Therefore the fat content of the algal cells may be varied by various changes in the environment (Collyer & Fogg, 1955: 266). Collyer and Fogg (1955: 266) determined that the availability of nitrogen is the primary limiting factor that leads to the accumulation of fat. The fat accumulates when the nitrogen concentration falls below a certain level. A deficiency of water may also be a factor that influences the accumulation of fat in algal cells (Collyer & Fogg, 1955: 266).

Survival tactics of the algae may explain the accumulation of fat during a shortage in the availability of water. Collyer and Fogg (1955: 266) ascribes this phenomenon to a decrease in the chemical potential of the water dipoles within the protoplasm, which in turn would favour an increase in the formation of non-polar groups. These non-polar groups are formed at the expense of hydrophilic groups (Collyer & Fogg, 1955: 267). The effect of other factors on the accumulation of fat has been investigated, but none of them influences the accumulation of fat to such an extent as nitrogen and water deficiency (Collyer & Fogg, 1955: 267).

According to the National Renewable Energy Laboratory (NREL) (1998: 142 – 143), the rate of synthesis of all cell components including lipids, proteins and carbohydrates decreases in nutrient-stressed cells. The rate of lipid synthesis however remains higher than the synthesis rates of proteins and carbohydrates. This results in a net accumulation of lipid in nutrient-starved cells (National Renewable Energy Laboratory, 1998: 142 – 143).

2.1.5 Lipid content of some algal cells

The National Renewable Energy Laboratory (NREL) (1998: 30) conducted experiments under various conditions in order to determine the lipid content of seven algal species. This was done under nitrogen sufficiency and nitrogen deficiency conditions as well as at different salinity levels (National Renewable Energy Laboratory, 1998: 30).

From the NREL study (1998: 30) it was found that *Botryococcus braunii* contained a high lipid level. Fifty five percent of the organic mass of the *B. braunii* are lipids for the nitrogen deficient cells. The majority of these lipids were in the form of

hydrocarbons, which included C_{29} to C_{34} aliphatic hydrocarbons and a variety of branched and unsaturated isoprenoids (National Renewable Energy Laboratory, 1998: 30). It was found that glycerolipids were less abundant than hydrocarbons. The glycerolipids were primarily composed of $C_{16:0}$ and various C_{18} fatty acids. The *B. braunii* algae, however, have the disadvantage of growing slowly and only double in 72 hours.

Table 2.6 shows the influence of nitrogen on the lipid content of some algae used by the NREL (National Renewable Energy Laboratory, 1998: 30)

Table 2.6: Lipid content of various algae under various conditions.

		Lipid content (wt%)	
Algal phylum	**Algae**	**Sufficient Nitrogen**	**Nitrogen Deficient**
Chlorophyte	*Ankistrodesmus sp*	24.5	40.3
	Dunaliella sp.	25.3	9.2
	Nannochloris sp.	20.8	35.5
Chrysophyte	*Isochrysis sp.*	7.1	26.0

Table 2.6 shows that nitrogen deficiency led to an increase in the lipid content of the *Ankistrodesmus* sp., *Isochrysis* sp. and *Nannochloris* sp.. The nitrogen deficiency, however, resulted in a decrease in the lipid content of the *Dunaliella* sp. (National Renewable Energy Laboratory, 1998: 30).

An elevation in the NaCl concentration of the medium had little effect on the lipid content of *B. braunii* cells, but this elevation caused a slight decrease in the lipid content of *Dunaliella salina* (National Renewable Energy Laboratory, 1998: 30). The NREL (1998: 31) also identified the major fatty acids contained in the various microalgae. Table 2.7 lists the major fatty acids of various microalgae as identified by the NREL. The fatty acids listed in bold are present at levels of 15% or higher (National Renewable Energy Laboratory, 1998: 31).

Table 2.7: Major fatty acids of various microalgae.

Strain	Nitrogen-sufficient cells	Nitrogen-deficient cells
Ankistrodesmus	16:0, 16:4, **18:1, 18:3**	16:0, **18:1,** 18:3
Botryococcus braunii	**16:0, 18:1,** 18:2, **18:3**	16:0, **18:1, 18:3,** 20:5
Dunaliella bardawil	Not determined	12:0, 14:0/14:1, **16:0, 18:1**, 18:2, 18:3
Dunaliella salina	14:0/14:1, **16:0,** 16:3, 16:4, 18:2, **18:3**	**16:0,** 16:3, 18:1, 18:2, **18:3**
Isochyrsis sp.	14:0/14:1, 16:0, 16:1, **18:1,** 18:3, **18:4**, 22:6	**14:0/14:1, 18:1,** 18:2 18:3, 18:4, 22:6
Nannochloris sp.	14:0/14:1, 16:0, 16:1, 16:2, 16:3, 20:5	Not determined
Nitzschia sp.	14:0/14:1, 16:0, 16:1, 16:2, 16:3, 20:6	Not determined

2.1.6 Suitability of algae for oil production

Carbohydrates, proteins and lipids are the major components of primary biomass, i.e. plant biomass. The dominant component in biomass obtained from higher plants is structural carbohydrates. In microalgae the major component is proteins (Ginzburg, 1993: 249).

Two aspects should be taken into consideration when evaluating the most suitable biomass component for the production of hydrocarbons, namely materials and thermodynamics. It must be kept in mind that, from a materials consideration, the percentage of hydrogen and carbon that is contained in the biomass component determines the maximum amount of hydrocarbons that can be obtained from that component (Ginzburg, 1993: 249). The heat of formation gives an indication of the energy content of the material and thus determines the thermodynamics of the component. The heat of formation of hydrocarbon is 11 $kcal.g^{-1}$, whereas the heat of formation for carbohydrate is only 4 $kcal.g^{-1}$. This indicates that carbohydrates only have one-third of the energy content of lipids, per unit mass of hydrocarbons (Ginzburg, 1993: 249). Proteins and lipids, on the other hand, have about half and two-thirds of the energy content of hydrocarbons, respectively. Theoretically carbohydrates are therefore the least desirable component for oil production from both the material and thermodynamic point of view. Lipids are most preferable compared to carbohydrates and proteins (Ginzburg, 1993: 249).

Ginzburg (1993: 249) determined that it is often difficult to convert lipids into hydrocarbons by means of a thermal reaction. In order to obtain a high lipid content in algal cells the cultures must be very old or stressed, which results in more time required for the production of the lipids (Ginzburg, 1993: 249). Young, vigorously growing algal cultures have high protein content and can be subjected to pyrolysis for oil production. Pyrolysis is a method of liquefaction that produces high-quality hydrocarbons from proteins (Ginzburg, 1993: 249).

Ginzburg (1993: 250) studied *Dunaliella* algae and determined that they have a very high growth potential:

a) "simple systems" produce 50 tons of organic dry weight per hectare per year;
b) more elaborate systems produced up to three times higher yields of dry organic weight on a medium scale;
c) sophisticated systems have the ability to produce a 100-fold increase in biomass per day (Ginzburg, 1993: 249).

Hu and co-workers (2008: 622) also listed the potential advantages of algae as feedstocks for biofuels due to their ability to:

- produce and accumulate large quantities of neutral lipids or oils (20 – 50 wt%).
- grow at high rates (may exhibit 1 to 3 doublings per day).
- thrive in conditions where there are no competing demands, for instance in saline/brackish water or coastal seawater.
- tolerate marginal land that are not suitable for conventional agriculture.
- use nutrients like phosphorous and nitrogen from a variety of wastewater sources, which adds the benefit of the bio-remediation of wastewater.
- capture CO_2 from flue gases that are emitted from fossil fuel-fired power plants as well as other sources, reduces the emission of CO_2.
- produce value-added co-products or by-products (e.g. biopolymers, proteins, polysaccharides, pigments, animal feed, fertilizer and H_2).
- grow in photo-bioreactors throughout the year with an annual biomass productivity which exceeds that of terrestrial plants approximately tenfold on an area basis (Hu *et al.,* 2008: 622).

In comparison with traditional oil crops, algae also show a remarkable increase in the oil yield per hectare. Table 2.8 lists the oil yield per hectare for a variety of oil crops including algae (Chisti, 2007: 296).

Table 2.8: Oil yield comparison for some oil crops.

Crop	Oil yield ($L.ha^{-1}$)
Corn	172
Soybean	446
Canola	1190
Jatropha	1892
Coconut	2689
Oil palm	5950
Microalgae[a]	136 900
Microalgae[b]	58 700

a) 70 wt% oil in biomass.

b) 30 wt% oil in biomass.

A study conducted by Chisti (2007: 294) shows that microalgae seem to be the only source of renewable biodiesel that has the ability of meeting the global demand for transport fuels. This illustrates the suitability of algae for oil production and therefore for biodiesel production.

2.1.7 Possible disadvantages of algae for biofuel production

Algae and other sources of biomass have high moisture contents (between 20 and 50%) and therefore require an external source of energy for drying (Lédé, 1999: 4). This aspect can be addressed by the selection of a suitable processing technique, such as thermochemical liquefaction, which utilizes water as a reaction medium (Rezzoug & Capart, 2002: 632).

Algae and other sources of biomass are dependent on the dispersion energy provided by the sun on the surface of the earth. Biomass is therefore affected by the seasonal changes in the availability of the energy provided by the sun. Biomass is also dispersed on the earth surface, which results in high transport costs and large volumes of storage (Lédé, 1999: 4). Culturing techniques for algae, i.e. raceway ponds and tubular photobioreactors, optimizes the utilization of the energy available from the sun and increases the biomass concentrations (Amin, 2009: 2).

The oil obtained from microalgae contains polyunsaturated fatty acids with four or more double bonds. These fatty acids and fatty acid methyl esters are susceptible to oxidation during storage. This reduces their acceptability for use as biodiesel, since these oils will not comply with biodiesel standards. The extent of the unsaturation of

microalgal oil and its fatty acid content can however be recuded by simple hydrogenation of the oil (Chisti, 2007: 300 – 301). Simple processing of the microalgal oil therefore makes it suitable for use as a source of biofuel.

2.2 Biofuels Industrial Strategy of South Africa

In 2002 South Africa hosted the World Summit on Sustainable Development, which resulted in the Johannesburg Plan of Implementation (JPol). JPol commits South Africa to the development of renewable energy technologies, which includes biofuels (Biofuels Industrial Strategy of the Republic of South Africa, 2007: 6). The Biofuels Industrial Strategy of South Africa proposed a 2% penetration of biofuels into the national liquid fuel supply. In order to achieve this, it was suggested to use sugar beet and sugar cane crops for the production of bioethanol and sunflower, canola and soybean crops for the production of biodiesel (Biofuels Industrial Strategy of the Republic of South Africa, 2007: 3).

In order to integrate the biofuels with the current liquid fuel supply, the Biofuels Industrial Strategy of South Africa proposed a blending ratio of 2% biodiesel and 8% bioethanol (Biofuels Industrial Strategy of the Republic of South Africa, 2007: 12). The use of the proposed crops for biofuel production will require 1.4% (300 000 ha) of the national arable land (Biofuels Industrial Strategy of the Republic of South Africa, 2007: 14). A 100% petrol tax exemption and a 50% diesel fuel levy exemption have been suggested, which result in a support of R 1.21 per litre for bioethanol and a R 0.53 per litre support of biodiesel (Biofuels Industrial Strategy of the Republic of South Africa, 2007: 4).

South Africa is in need of an alternative biofuel initiative, because the feedstock proposed by the Biofuel Industrial Strategy of South Africa is not the best choice. The use of food crops for the production of biofuels will have disastrous consequences. Gressel (2007: 247) states that the production of energy from food resources has a significant effect on the prices of the feedstock. At present, the small amount of grain (mainly sugarcane, maize and oilseeds) currently being used to produce biofuel has caused a doubling in the grain prices. This rise in grain prices will be carried through the food chain, which will result in a rise in all food prices and in low availability of grain for emergency food aid (Gressel, 2007: 247).

Alternate feedcrops should therefore be investigated for the production of biofuels. Algae are oil rich sources of biomass, which does not form part of the food supply of a nation (Herro, 2008). In Table 2.9 the annual production of biofuels obtained from an average hectare of feedcrop that forms part of the food supply is compared with the annual production of biofuels from algae.

Table 2.9: Biodiesel production from crops of canola, soybeans, sugar beets and algae.

Crop	Production (litres)
Canola[a]	1 500
Soybeans[b]	655
Sugarbeets[a]	5 000
Sunflower[c]	770 – 961
Algae[b]	47 000

a) Soetaert, 2008: 5.

b) Herro, 2008.

c) Kondili and Kaldellis, 2007: 2143.

Table 2.9 indicates that algae are a viable feedstock for the production of biofuel. Algae have the ability to be grown on marginal land (Herro, 2008) and do not form part of the food supply of a nation, which resolves the issue of food security.

2.3 Biodiesel

This section gives an overview of biodiesel. Section 2.3.1 contains a short introduction to biodiesel, whereas Section 2.3.2 describes the process used to produce the biodiesel. Section 2.3.3 states the safety aspects related to biodiesel.

2.3.1 Introduction to biodiesel

Biodiesel may be defined as a fuel for conventional diesel engines that is made from plant or animal oil or fats and that has been chemically transformed into alkyl esters (Carter *et al*., 2005: 13). Burning of biodiesel does not produce carcinogenic substances such as polyaromatic hydrocarbons (PAH) or nitrated polyaromatic hydrocarbons (nPAH) (Lin, C. & Li, R., 2009: 130).

Diesel engines are not equipped to run on pure vegetable oil due to the high viscosity of the oil (Carter *et al*., 2005: 13). The oil must therefore be altered in order to

reduce its viscosity. The process used to chemically alter the oil in order to reduce its viscosity is called transesterification (Carter *et al*., 2005: 13).

2.3.2 Transesterification

Transesterification is a process that transforms one ester (glyceryl esters) into another ester (methyl esters). This is done by the addition of methanol or ethanol to the triglyceride. The addition of the alcohol removes the glycerol structure and replaces it with a smaller methyl group. During transesterification the large molecule is therefore split into methyl esters and glycerol products (Carter *et al*., 2005: 57). Figure 2.2 depicts the transesterification process.

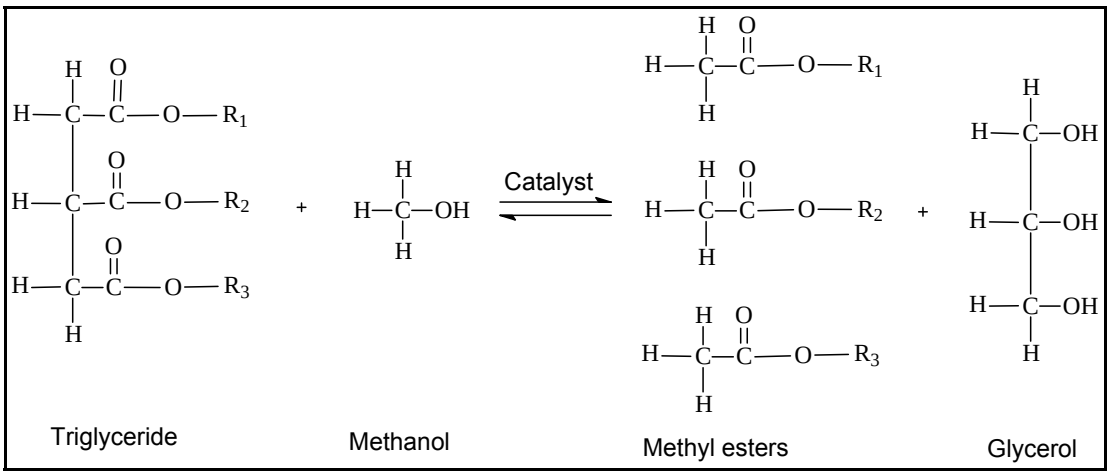

Figure 2.2: Schematic representation of the transesterification process.

The transesterification reaction is reversible, which means that, during the reaction, some of the products combine to form triglycerides and alcohol (methanol or ethanol). This reverse reaction will continue until equilibrium has been reached between the products and the reagents. At equilibrium there is an amount of triglycerides that has not reacted (Carter *et al.,* 2005: 57).

In order to maximize the conversion of the triglycerides, equilibrium must be avoided. This may be achieved by continually removing the products as they are formed or by adding an excess of alcohol (methanol or ethanol) in order to force the reaction towards completion (Carter *et al.,* 2005: 58). Stoichiometrically, 3 moles of alcohol are required for each mole of triglyceride in order to produce 1 mole of glycerol and 3 moles of methyl esters. In industry an excess of 3 moles of alcohol is used for each

mole of triglyceride in order to maximize the conversion of triglycerides (Fukuda *et al.,* 2001: 408).

The transesterification reaction requires a catalyst. Alkaline catalysts such as Potassium or Sodium Hydroxide (Carter *et al.,* 2005: 58) may be used, as well as acid catalysts (Chisti, 2007: 295). Alkali-catalyzed transesterification reactions occur approximately 4000 times faster than acid catalyzed reactions, therefore alkali-catalyzed transesterification reactions are commercially more favourable (Fukuda *et al.,* 2001: 407). The alcohol that is preferred for transesterification reactions is methanol, due to its inexpensive cost. Alkali-catalyzed transesterification is carried out at 60 °C under atmospheric pressure. The temperature constraint is as a result of the boiling point of methanol being 65 °C. Under these conditions the transesterification reaction takes approximately 90 min to reach completion (Chisti, 2007: 295).

After the reaction is completed, the catalyst and the excess methanol are left over and must be separated from the products (Carter *et al.,* 2005: 58). This is done by washing the biodiesel with water (Chisti, 2007: 296).

2.3.3 Safety aspects of biodiesel

Bio-crude oil is classified as a Class 3 substance – Flammable liquid. The presence of Class 6.1 – Toxic substances (phenols, etc.) in bio-crude complicates the classification of bio-crude oil. Packages that contain bio-crude oil must therefore bear labels that conform to model No. 3 (Class 3 – Flammable liquid) and model No. 6.1 (Class 6.1 – Toxic substances). Figure 2.3 depicts the labels required for bio-crude oil packaging (Peacocke & Bridgwater, 2001: 1490).

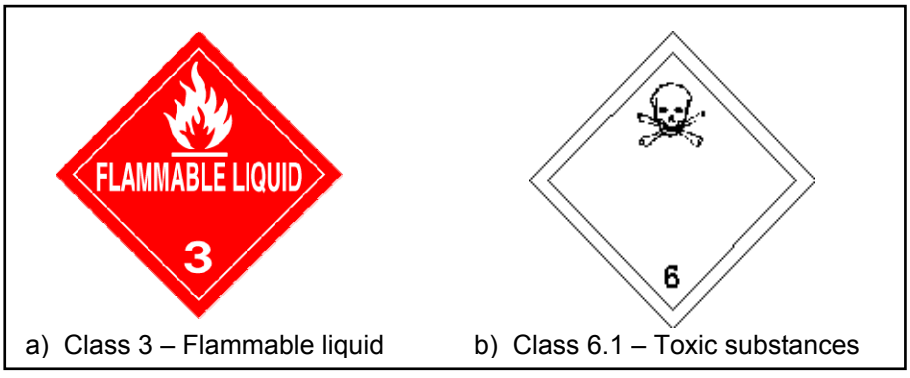

a) Class 3 – Flammable liquid b) Class 6.1 – Toxic substances

Figure 2.3: Labels required for bio-crude oil packaging.

Spills of biodiesel/bio-crude oil should be treated with care. Small quantities (up to 1L) may be cleaned immediately by a person wearing correct personal protective clothing (rubber gloves, eye and face protection). Large spills (above 1L) require evacuation of the area before cleaning commences, as well as the use of a NIOSH/MSHA approved respirator (Peacocke & Bridgwater, 2001: 1496).

2.4 Hydrothermal processing of biomass

This section gives a description of hydrothermal processing. In Section 2.4.1 a brief introduction is given regarding hydrothermal processing. Section 2.4.2 gives a brief introduction of thermochemical liquefaction as well as an historical overview of the liquefaction of biomass.

Section 2.4.3 discusses the process of thermochemical liquefaction in more detail, whereas Section 2.4.4 states the various reactions that occur during thermochemical liquefaction. The products that are formed during liquefaction in subcritical water is discussed in Section 2.4.5. Section 2.4.6 states the influence of the various operating conditions on the thermochemical liquefaction process.

2.4.1 Introduction to hydrothermal processing

Hydrothermal processing is defined as processing of biomass in a water-rich phase at temperatures above 200 °C and at sufficient pressures to keep the water in either a liquid or supercritical state. The high pressures of the hydrothermal processing procedures avoid energy losses due to phase change of water to steam (Peterson *et al.,* 2008: 32). Hydrothermal processing offers various advantages including high throughputs, high energy and separation efficiency, the ability to use mixed feedstocks and the production of direct replacements for existing fuels. Hydrothermal processing also has no need to maintain specialized microbial cultures or enzymes (Peterson *et al.,* 2008: 32 – 33). The high temperatures used during hydrothermal processing produce biofuels that are free of biologically active organisms or compounds, including bacteria, viruses and even prion proteins (Peterson *et al.,* 2008: 33).

Hydrothermal processing is attractive for biomass conversion for three main reasons:

a) The presence of water.

The feedstocks that are used for hydrothermal processing contain large amounts of water and by carrying out reactions under pressure the phase change of water is avoided, i.e. the energy loss accompanied by a phase change is avoided (Peterson *et al.,* 2008: 34).

b) Versatility of chemistry.
   A variety of feedstocks may be processed during hydrothermal processing. Lignocellulose, fatty acids and protein derivatives may be transformed into a wide range of gasified and liquefied fuel products (Peterson *et al.,* 2008: 34).

c) Enhanced reaction rates and efficient separations.
   The interphase mass transfer resistances are substantially reduced or eliminated by operating at the hydrothermal or supercritical conditions. Energy savings may also result from working in a dense supercritical vapour or near-critical liquid phase system with improved selectivity to more desirable energy products (Peterson *et al.,* 2008: 35).

   The physical properties of water vary significantly with changes in temperature and pressure. This may result in efficient separations of product and by-product streams, which can reduce the energy that is required for purification of the products (Peterson *et al.,* 2008: 35).

Hydrothermal processing can be divided into the following three main regions: liquefaction, catalytic gasification and high-temperature gasification. Figure 2.4 depicts the three main regions of hydrothermal processing (Peterson *et al.,* 2008: 35).

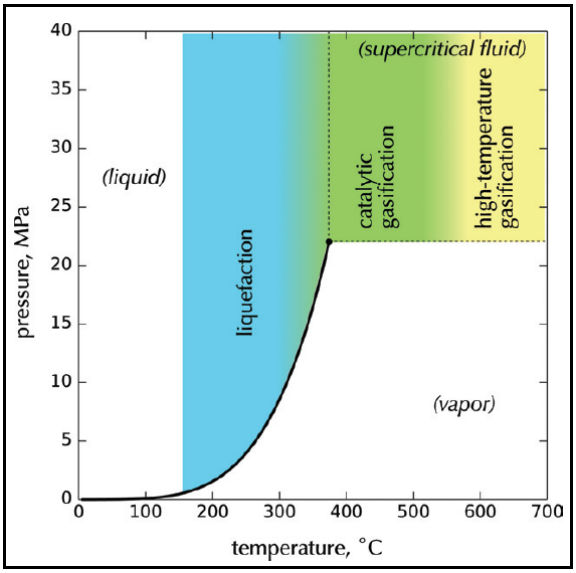

Figure 2.4: Hydrothermal processing regions imposed on the phase diagram of water.

Hydrothermal conversion via liquefaction pathways generally occurs at temperatures ranging from 200 to 370 °C, with pressures between approximately 4 and 20 MPa. These conditions are sufficient to keep the water in a liquid state (Peterson *et al.,* 2008: 35).

The three main regions of hydrothermal processing take advantage of substantial changes in the properties of water that occur near the critical point of water at 374 °C (T_c) and 22 MPa (P_c). Moving from subcritical to supercritical temperatures at pressures above P_c, the rate of hydrolysis as well as the phase partitioning and the solubility of components can be controlled so that more chemically and energetically favourable pathways may be released to gaseous and liquid biofuels (Peterson *et al.,* 2008: 36).

Water is highly compressible near its critical point. The density of water decreases for instance nearly two orders of magnitudes without a change in phase from liquid-like (about 800 $kg.m^{-3}$) to a dense gas-like (about 150 $kg.m^{-3}$) state as the temperature is increased from 300 to 450 °C (Peterson *et al.,* 2008: 36). The change in density of the water is connected with other macroscopic properties to reveal changes at molecular level. These changes may be attributed to changes in solvation power, the degree of hydrogen bonding, polarity, dielectric strength, molecular diffusivity and/or viscosity (Peterson *et al.,* 2008: 26). The ability to modify the solvation properties of water in the highly compressible near-critical region makes

it possible to use the partitioning of products or by-products into separate phases in order to separate and purify the products (Peterson *et al.,* 2008: 36).

2.4.2 Introduction to thermochemical liquefaction

Thermochemical liquefaction of biomass is a process which entails heating the biomass to a high temperature in the presence of a catalyst and under pressure. During this process the biomass is converted to a mixture of gas (2 – 10 wt%), char (5 – 40 wt%) and oil (up to 40 wt%) (Erzengin & Küçük, 1998: 1203). Thermochemical liquefaction of biomass may be described as the dissolution of biomass in a liquid medium. The liquid medium may simply be water with some added minerals (acids, bases, salts and catalysts) (Rezzoug & Capart, 2002: 632).

The products obtained from liquefaction of biomass have many potential applications. Biopolymers, polyurethane, phenolic resins, adhesives and fuel or fuel additives may be produced from the liquefaction products. In order to produce fuel or fuel additives, the primary bio-oil must, however, be upgraded to reach the specifications (heating value and viscosity) of petroleum fuel (Rezzoug & Capart, 2002: 632). The objective of biomass liquefaction is to transform a carbonaceous solid material into pumpable oils. The original carbonaceous solid material is bulky and has a low energy concentration, whereas the product oil has physico-chemical properties which permit storage and transferability through pumping systems. The product oil may be used in direct combustion furnaces or as feedstock for the production of fuels and chemicals by hydrotreatment (Chornet & Overend*,* 1985: 967).

The thermochemical liquefaction process therefore produces oil products with increased H/C ratios and decreased O/C ratios (Xu & Lancaster, 2008: 1572). Chornet and Overend (1985: 968) determined that the H/C ratio may be increased by the addition of H_2. The addition of H_2 also decreases the O/C ratio through the formation of H_2O. They also stated that oxygen removal may occur via internal dehydration and decarboxylation reactions which occur during the initial pyrolytic stages (Chornet & Overend*,* 1985: 968).

A disadvantage of the thermochemical liquefaction process is that the process produces oil derived from protein. This oil may contain sulphur and nitrogen (Boocock *et al.,* 1992: 1283; Inoue *et al.,* 2001: 1219). The sulphur and nitrogen content of the oil requires flue gas treatment to remove NO_x gases after burning

(Minowa *et al.,* 1994: 582). Thermochemical liquefaction is also carried out in an autoclave, which takes some time to obtain reaction temperature (Matsumura *et al.,* 2005: 272). This may have significant implications for the energy efficiency of the process. The chemical pathways, kinetics and interactions between most of the components in the biomass are not charaterized (Peterson *et al.,* 2008: 38). This poses a problem in the optimization and kinetic studies of thermochemical liquefaction.

Thermochemical liquefaction has been used in the past to process various types of biomass. Table 2.10 lists the previous work done on the thermochemical liquefaction of biomass.

Table 2.10: Previous work done on thermochemical liquefaction of biomass.

Year	Feedstock	Catalyst	Observations	Reference
1979	Peat	Potassium carbonate	Increases in temperature increased the yield of the bitumen. No catalyst is needed for peat with high ash content.	Panayotova-Björnbom *et al*, 1979: 168.
1979	Poplar wood	Raney nickel catalyst	The oils that were produced from the liquefaction had heating values of up to 40.8 $MJ.kg^{-1}$. The product oils were derived from the lignin, whereas the gaseous products were derived from the cellulose.	Boocock *et al.,* 1979: 98.
1980	Poplar wood	Raney nickel catalyst	Liquefaction at 340 °C produces oils with typically 77 wt% carbon, 7.5 – 8.5 wt% hydrogen and 12 – 13 wt% oxygen. The viscosity of the oils ranged from 5000 to 8000 mPa.s and they had higher heating values of around 35 $MJ.kg^{-1}$.	Boocock *et al.,* 1980: 466.
1981	Peat	Potassium carbonate	The yield of butimen depends on the input material and the operating conditions. Catalyst is not always needed.	Björnbom *et al.*, 1981: 7.
1981	Cellulose	Sodium carbonate	Reaction temperature had the most significant effect on the yield of the oil. The oil must be processed before use as a fuel due to its corrosive nature.	Donovan *et al.,* 1981: 898.
1981	Microcrystalline cellulose	Iodine	A 58 wt% oil yield was obtained. The oxygen content of the oil was much less than that of the starting material, which illustrates the effectiveness of the deoxygenation procedure.	Walton & Paudler, 1981: 650 – 651.
1982	Sugar cane bagasse	Sodium formate or calcium hydroxide	The use of formate is more advantage than using CO in the presence of a base and results in higher yields at lower temperatures. The product oil has a oxygen content of 20 to 30 wt% and a heat of combustion of 28 000 $kJ.kg^{-1}$.	Schuchardt & De Assis Pereira Matos, 1982: 106.

Table 2.10 continued

Year	Feedstock	Catalyst	Observations	Reference
1982	Aspen poplar wood	Sodium carbonate, Potassium carbonate and Sodium hydroxide	The oils obtained from the thermochemical liquefaction process have approximately 80 wt% hydrogen plus carbon content as well as higher heating values ranging from 32.2 to 36.0 $MJ.kg^{-1}$. Oil yields obtained from freshly cut (green) wood are 5 wt% higher than those from dried wood.	Eager *et al.,* 1982: 289.
1984	Wood powder	Potassium carbonate and nickel carbonate	Obtained heavy oils with approximately 80 wt% hydrogen and carbon content. Heats of combustion of oils ranged from 29.3 to 33.4 $MJ.kg^{-1}$. 24% carbon recovery in form of oil.	Yokoyama *et al.,* 1984: 155.
1985	α-cellulose	Raney nickel and potassium hydroxide	A 100% conversion of the cellulose feed was obtained with oil yields greater than 50%. The oxygen content of the oil decreased with an increase in the temperature. Too high temperature resulted in hydrocracking of the product oil to gases.	Vasilakos & Austgen, 1985: 304.
1985	Aspen poplar	Sodium carbonate, potassium carbonate and sodium hydroxide	The water to wood ratio is the most important variable for the liquefaction process. Freshly cut wood delivers approximately 5 wt% higher oil yields. Batch operations resulted in oil yields between 33.6 and 44.0 wt%. Semi-continuous operations produced oil yields between 36 and 44 wt%.	Eager *et al.,* 1985: 1051.
1986	Peat	Potassium carbonate	Residue had decreased oxygen content and a higher calorific value	Björnbom *et al.,* 1986: 1051.
1986	Lignocellulosic material	Palladium	The highest oil yield obtained from the liquefaction experiments were 64 wt%. The calorific values of the oils ranged between 26.3 and 32.5 $MJ.kg^{-1}$.	Meier *et al.,* 1986: 910.

Table 2.10 continued

Year	Feedstock	Catalyst	Observations	Reference
1987	Sewage sludge	Sodium carbonate	Sewage sludge can be liquefied under nitrogen pressure above 275 °C. The catalyst load and reaction temperature affects the yield of the heavy oil. Oil obtained with heating value of 30 $MJ.kg^{-1}$.	Yokoyama *et al.,* 1987: 1155.
1988	Wood (*Populus deltoides*)	-	Ethylene glycol interacts with the cellulose and protects them from dehydration and carbonization. This produces an oil yield ranging between 40 to 55 wt%, whereas with creosote as solvent an oil yield of between 51.3 and 61.3 wt% is obtained.	Vanasse *et al.,* 1988: 119.
1990	Rye straw	Red mud and CoO-MoO_3	Red mud can only liquefy biomass in the presence of sulphur. Red mud is a cheap catalyst for liquefaction. CoO-MoO_3 exhibit higher hydrodeoxygenation activities.	Klopries *et al*., 1990: 455.
1990	Peat	-	The oil obtained from liquefaction of peat may be analyzed with infra-red detection in order to determine the functional groups	Karlsson, 1990: 613.
1992	Sewage sludge	-	Major fatty acids present in oil were palmitic, stearic and oleic acids. The process was able to remove oils from the sewage sludge.	Boocock *et al.,* 1992: 1283.
1994	Stillage from sweet potato, barley, rice and buckwheat	Sodium carbonate	Yield of oil was depended on the type of stillage, the catalyst load and the reaction temperature. Oil yield obtained from 33 – 58 wt% under optimum conditions (300 °C and 12 MPa N_2). Oil calorific values of 33 – 37 $MJ.kg^{-1}$ and viscosities of 300 – 2000 mPas.	Minowa *et al.,* 1994: 582.
1994	*Botryococcus braunii*	Sodium carbonate	More oil was obtained than the amount of hydrocarbons contained in the algal cells. The oil was similar to petroleum oil with a heating value of approximately 50 $MJ.kg^{-1}$. The maximum recovery was obtained at 300 °C.	Dote *et al.,* 1994: 1855.

Table 2.10 continued

Year	Feedstock	Catalyst	Observations	Reference
1994	*Botryococcus braunni*	Sodium carbonate	A maximum of 78 wt% recovery was obtained from the liquefaction process at 200 °C.	Inoue *et al.,* 1994: 274.
1995	*Botryococcus braunii*	Sodium carbonate	Algae are able to capture CO_2 from the atmosphere. Thermochemical liquefaction of *B. braunii* produced an oil yield of 64 wt% at 300 °C. The oil had a heating value of 49 $MJ.kg^{-1}$.	Sawayama *et al.,* 1995: 729.
1995	*Dunaliella tertiolecta*	Sodium carbonate	The liquefaction of *D. tertiolecta* produced oil comparable to fuel oil. The process is a net energy producer. The sodium carbonate is not necessary for the liquefaction of *D. tertiolecta*.	Minowa *et al.,* 1995b: 1735.
1995	Garbage	Sodium carbonate	Oil with a calorific value of 36 $MJ.kg^{-1}$ was obtained. The oil yield was dependent on the catalyst addition and the reaction temperature.	Minowa *et al.,* 1995a: 120.
1996	Albumin	Sodium carbonate	The catalyst prevented the distribution of nitrogen to the oil. Above 200 °C the nitrogen in the albumin was distributed to the aqueous phase.	Dote *et al.*, 1996: 497.
1997	Cellulose, eucalyptus wood and sugar cane	FeS	The biomass produced bio-oils with lower oxygen content than obtained from pyrolysis.	Rocha *et al.,* 1997: 91.
1997	*Spirulina* sp.	$Fe(CO)_5$-S	The catalyst produced an increase in the oil yield. Oil obtained in a water solvent had lower heating values than oil obtained in a tetrahydrofuran solvent.	Matsui *et al.,* 1997: 1043.
1998	Sunflower stalk	Sodium hydroxide	The oil yield increased as the reaction temperature was increased. The catalyst had a positive effect on the yields.	Erzengin & Küçük, 1998: 1205 – 1206.

Table 2.10 continued

Year	Feedstock	Catalyst	Observations	Reference
1998	Indonesian biomass residues	Sodium carbonate	Energy density of oil increased more than 50% in comparison with the feedstock. Liquefaction process is not a net energy producer, but does have the potential to become a net energy producer.	Minowa *et al.,* 1998: 523.
1999	*Botryococcus braunii* and *Dunaliella tertiolecta*	Sodium carbonate	*B. braunii* was determined to be more suitable for the production of liquid fuel than *D. tertiolecta* due to higher heating value and lower energy inputs.	Sawayama *et al.,* 1999: 33.
1999	Sawdust	-	A hydrogen donor solvent increased the oil yield above 300°C. Optimal operating time is 30 minutes with H_2 gas.	Yan *et al.,* 1999: 143.
2000	Lignite with sawdust	-	The addition of sawdust to the lignite influenced the total conversion negatively.	Karaca & Bolat, 2000: 54.
2002	*Pinus pinaster* (Pine wood)	Iron powder, Co-Mo and Ni-Mo	Ni-Mo catalyst was determined to be the best catalyst. Reaction temperature above 350 °C produces oil with a heating value similar to that of conventional petroleum fuel.	Rezzoug & Capart, 2002: 643.
2002	Lignite with sawdust	-	The initial H_2 pressure does not affect the yield and total conversion. A higher sawdust/lignite ratio increases the oil and gas yields as well as the total conversion.	Karaca & Bolat, 2002: 111 – 115.
2003	Wood (*Pinus pinaster*)	Sulphuric acid	The maximum liquefied wood yield, approximately 95 wt%, was calculated to be obtained at a temperature of 250 °C, reaction time of 40 min and acidity of 0.7 wt% sulphuric acid (on wood basis).	Rezzoug & Capart, 2003: 781.

Table 2.10 continued

Year	Feedstock	Catalyst	Observations	Reference
2003	Wood (*Cunninghamia lanceolata*)	-	A maximum heavy oil yield of approximately 24 wt% was obtained at a reaction temperature of 320 °C, a reaction time of 10 min, a biomass loading of 8 g and a water quantity of 100 ml. The higher values of the oils ranged from 27.063 to 30.221 $kJ.g^{-1}$.	Qu *et al.,* 2003: 597.
2004	Wood	Potassium carbonate	Potassium carbonate reduces the formation of residue. *Franxinus mandshurica* produced a 31% y(on an organics basis) ield of oil oat 573.15 K.	Zhong & Wei, 2004: 1740.
2004	*Microcystic viridis*	Sodium carbonate	The oil contained n-alkane of C_{17} – C_{18} and was therefore classified as heavy oil. The oil had a heating value of 28 – 30 $kJ.g^{-1}$.	Yang *et al.,* 2004: 32.
2007	Sawdust	-	The atmosphere in the autoclave influenced the conversion, with H_2 producing the best conversion. An increase in temperature increased the conversion of the liquefaction products, while the initial atmospheric pressure influences the conversion negligibly.	Wang *et al.*, 2007a: 1593.
2007	Sawdust	Molybdenum	The solvent used for liquefaction process is important. High temperatures are more favourable for thermal decomposition, hydrogenation and hydrocracking reactions.	Wang *et al.,* 2007b: 187.
2007	Silver birch	Sodium carbonate	The oil yield increased with an increase in temperature up to a maximum of 53.3 wt% at 380 °C and decreased again at temperatures higher than 380 °C.	Qian *et al.,* 2007: 201.
2007	Rice straw	-	A maximum oil yield of 39.7 wt% was obtained for a 2-propanol:water volume ratio of 5:5 at 573 K.	Yuan *et al.,* 2007: 2081.

Table 2.10 continued

Year	Feedstock	Catalyst	Observations	Reference
2008	Legume straw, corn stalk, cotton stalk and wheat stalk	-	The order of the conversion of the biomass was: cotton stalk > corn stalk > wheat straw > legume straw. Only the oils produced from legume straw and corn stalk may be classified as bio-petroleum. The oils mainly contained aromatic compounds and long-chain alkanes (C_{13} – C_{23}).	Wang *et al.,* 2008: 2785.
2008	*Pinus banksiana* (Jack pine)	FeS or $FeSO_4$	The catalysts increased the oil yield. The oil yields also increased with increases in residence time, initial H_2 pressure and reaction temperature. The catalyst suppressed the formation of gases and water.	Xu & Etcheverry, 2008: 344.
2008	Secondary pulp/paper sludge power	Sodium carbonate	An increased operating temperature, reaction time and initial biomass concentration produced an increase in the conversion. The process delivered heavy oil with a higher heating value bigger than 35 $MJ.kg^{-1}$.	Xu & Lancaster, 2008: 1571.
2008	Soybean stalk	-	Liquefaction of soybean stalk produced a bio-petroleum with a H/C ratio of 1.9 and a higher heating value of 44.22 $MJ.kg^{-1}$.	Li *et al.,* 2008: 204.
2008	Cherry and cypress wood	Potassium carbonate	Cherry wood (cellulose rich) produced more acetic acid than cypress wood. The oil yields from the two wood species were similar (near 50 wt%).	Bhaskar *et al.*, 2008: 2236.

2.4.3 Thermochemical liquefaction process

A generalized conceptual liquefaction process for thermochemical liquefaction involves the following:

- Feedstock preparation at a suitable moisture content and size range (typically < 0.5 mm);
- Creating a slurry of the feedstock within a liquid carrier (oil recycle cut, specific solvent or simply an aqueous system);
- Preheating the slurry through heat exchangers to temperatures near the reaction conditions;
- Adding a reducing gas (H_2 or H_2/CO at ≤ 300 bar);
- Reactor system for the main reaction;
- Separation of the products by using a multistage let-down system which normally uses vapour-liquid equilibrium to separate light, middle and heavy condensates from the non-condensable gases;
- Solid-liquid separation of the heavy condensate with distillation, centrifugation and/or extraction;
- Recycling or recovering of the liquid carrier if it is of any value (Chornet & Overend, 1985: 967).

Figure 2.5 depicts a generalized biomass liquefaction flow diagram (Chornet & Overend, 1985: 969).

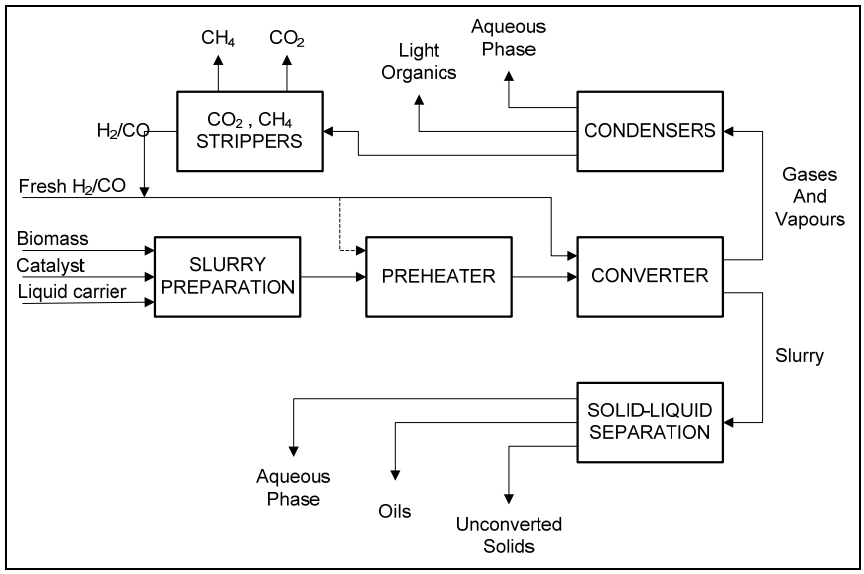

Figure 2.5: Generalized biomass liquefaction flow diagram.

2.4.4 Reactions during thermochemical liquefaction

Liquefaction of carbonaceous material takes place through an intricate sequence of structural and chemical changes, which involve the following:

- solvolysis, which produces substructures similar to a submicroscopic aggregation of molecules;
- depolymerization to smaller and soluble molecules;
- thermal decomposition which leads to new molecular rearrangements through dehydration, decarboxylation, C-O and C-C bond ruptures;
- hydrogenolysis (in the presence of hydrogen);
- hydrogenation of functional groups (Chornet & Overend, 1985: 968; Xu & Lancaster, 2008: 1572).

The extent of the reactions stated above will vary according to the original material, the severity of the liquefaction conditions and the presence of interacting media and catalysts (Chornet & Overend, 1985: 968). The reactions may also be divided into the following two main categories, namely substrate-solvent interactions and thermal decomposition sequences (Chornet & Overend, 1985: 977). Chornet and co-workers (1985: 839) hypothesized that the liquefaction of biomass occurs according to the following process steps:

i. the polymeric structures in the biomass material are solubilized;
ii. the solubilized polymers are split into smaller units;
iii. the smaller units are stabilized by either increased solvolytic action or addition of an external reducing agent or autogenous reactions.

Wang and co-workers (2007b: 191) proposed the mechanism of liquefaction as being divided into two steps. The first step entails the formation of preasphaltene (PA), asphaltene (A) and residue 1 through decomposition of the biomass. The second step is the conversion of the PA, A and residue 1 into oil and gas 1 by hydrogenation/hydrocracking reactions or into gas 2 and residue 2 by polycondensation (Wang *et al*, 2007b: 191). Figure 2.6 depicts the process of biomass liquefaction (Wang *et al*, 2007b: 191).

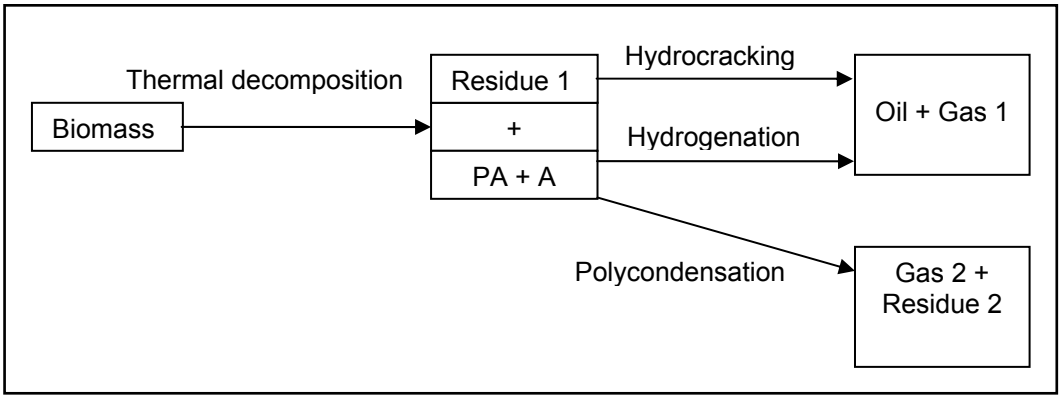

Figure 2.6: Biomass liquefaction process.

In order to produce fuels from biomass the 40 – 60 wt% oxygen content of the biomass feedstock must be reduced. The removal of the oxygen heteroatom occurs most readily by dehydration and decarboxylation. Dehydration removes oxygen in the form of water, whereas decarboxylation removes oxygen in the form of carbon dioxide. Water and carbon dioxide make ideal compounds in which to remove oxygen without losing heating value to the oxygen-containing chemicals removed, since they are fully oxidized and have no residual heating value (Peterson *et al.,* 2008: 38). The removal of water leads to the remaining product being carbon, whereas the removal of carbon dioxide produces a product with a higher H/C ratio and therefore a higher heating value (Goudriaan *et al.,* 2001: 1314). According to McKeough (1983: 445), two basic routes exist for the removal of oxygen, which are as follows:

Route A – Abstraction by reducing gas

$$O_{feed} + H_2 \rightarrow H_2O$$

or

$$O_{feed} + CO \rightarrow CO_2$$

Route P – Pyrolytic evolution

$$feed \xrightarrow{\Delta} CH_x + residue + CO, CO_2, H_2O, etc.$$

Both of these reaction pathways have certain disadvantages. The abstraction route consumes valuable reducing gas, while the pyrolytic evolution route has a loss of feed carbon or feed hydrogen (McKeough, 1983: 445).

Deoxygenization and liquefaction occur simultaneously during liquefaction. This causes the O-H bonds to dissociate and the C-H bonds to recombine into hydrocarbons. CO and CO_2 are also released from the C-O bonds. This results in a higher calorific value relative to those of the feedstocks (Li *et al.,* 2008: 200).

Decarboxylation reactions not only decrease the oxygen content of the feedstock, but also increase the H/C ratio, which leads to more attractive fuels (Peterson *et al.,* 2008: 38). At elevated temperatures and pressures, dehydration reactions occur in hydrothermal media even though an excess of water is present (Peterson *et al.,* 2008: 38).

2.4.4.1 Substrate-media interactions

In an aqueous medium (acidic or basic) the chemistry involved with liquefaction is similar to that of pulping processes in the initial stages of the liquefaction process. In an acidic medium, rapid acid hydrolysis of the glycosidic bonds takes place when the temperature is brought up above 230 °C (Chornet & Overend, 1985: 978). If the acidic conditions are maintained, secondary hydrolysis products are also formed. If acid hydrolysis is therefore not controlled at high temperatures it will lead to a complex mixture of aldehydes and acids. These aldehydes and acids will react at higher temperatures via pyrolytic processes (Chornet & Overend, 1985: 978).

Liquefaction in a basic medium produces an intricate mixture of phenolic derivatives, acids, gaseous hydrocarbons, CO_2, CO and H_2. 'Bitumen' is also produced, which may be the sum of the condensation products that are obtained from unoccupied C_5 sites produced during hydrolysis, as well as the free radicals induced by thermal excitations (Chornet & Overend, 1985: 979).

In an organic medium the chemistry of the liquefaction process is reliant on the nature of the interactions between the medium and the substrate. The first step towards liquefaction, i.e. solvation, will take place through the electron-donor-electron-acceptor coupling that takes place between the medium and the substrate (Chornet & Overend, 1985: 979). In order to obtain good solvation, good penetration of the medium is required within the feedstock. This is applicable for aqueous and organic media (Chornet & Overend, 1985: 979).

2.4.4.2 Thermal decomposition reactions (Pyrolysis)

Hydrolytic (or solvolytic) reactions compete with pyrolytic events from the start of the liquefaction process. Increased temperatures bring about electronic excitations, which generate enough free radicals to initiate subsequent thermal decompositions, which in turn lead to the formation of some volatiles and char (Chornet & Overend, 1985: 981).

A reducing medium (hydrogen) is necessary to:

- hydrogenate or deoxygenate terminal O-containing functional groups;
- limit the extent of condensation reactions induced by the free radicals; and
- hydrocrack the lignin and the tar material formed in the early stages of the thermal treatment (Chornet & Overend, 1985: 981).

The depolymerization process that takes place during liquefaction involves primary hydrogenolysis, secondary hydrogenolysis, cracking (C-C bond cleavage) and ring saturation. Cracking produces a loss of hydroxyl as H_2O and methoxyl as methyl alcohol whereas ring saturation produces cyclohexyl derivatives (Chornet & Overend, 1985: 982).

The intermediate free radicals that are formed at higher temperatures have a tendency to form condensed macromolecules, which lead to tar and eventually the formation of char. Splicing of the reducing medium (H_2) produces atomic species which have the ability to stabilize the free radical intermediates and thereby prevent condensation. During the stabilization of the free radical intermediates the H-transfer from the catalyst to the free radical intermediates is, however, problematic. Aldol condensation may also occur between two carbohydrate molecules. This takes place at temperatures ranging from 250 to 400 °C and produces an undefined high molecular weight viscous material (Chornet & Overend, 1985: 982).

C-C cleavage and splitting of C=O and C-OH bonds are two main functions that are required in the hydrocracking reactions. Hydrocracking also requires a suitable catalyst with hydrogenating ability to increase the H/C ratio (Chornet & Overend, 1985: 984).

2.4.4.3 Reactions of lipids

Fats and oils are non-polar compounds, which are similar to hydrocarbon fuels in their chemical structures. Therefore fats and oils can undergo reactions which convert them into suitable substitutes for conventional hydrocarbons (Peterson *et al.,* 2008: 44). The reactions of water and lipids are influenced strongly by their phase behaviour. When water is heated isobarically, at pressures higher than its critical pressure, the dielectric constant of the water decreases severely from room temperature to temperatures above the critical temperature of water. This causes the solvation properties of the water to be similar to the solvation properties of the organic solvents (Peterson *et al.,* 2008: 44). These conditions also cause a decrease in the hydrogen bonding between water molecules which increases the miscibility of the lipids and the water. The increased temperature causes the fats and oils to become more soluble in the water as its temperature rises under hydrothermal conditions. The fats and oils eventually become completely miscible in water when the water reaches its supercritical state (Peterson *et al.,* 2008: 44).

Fats and oils are present in biological systems as triacylglycerides, which consist of three fatty acids bound to a glycerol backbone. The triacylglycerides/water system is reactive and water hydrolyzes the triacylglycerides to form fatty acids (Peterson *et al.,* 2008: 44). The latter hydrolysis reactions occur mainly in the oil phase and proceed to an increasing equilibrium level with increasing water-to-oil ratios. According to Peterson and co-workers (2008: 44) the equilibrium level is, however, independent of temperature (Peterson *et al.,* 2008: 44). Although it is believed that the reaction is of first order within the oil phase, an induction period is usually observed in practice. The induction period is probably related to the relatively low solubility of water in the triacylglycerides as compared to the fatty acids (Peterson *et al.,* 2008: 44). More fatty acids are formed as the reaction proceeds, which increases the solubility of the water in the oil phase as well as the observed reaction rate. Free fatty acids degrade in hydrothermal systems to produce long-chained hydrocarbons (Peterson *et al.,* 2008: 44).

2.4.5 Liquefaction in subcritical water

Liquefaction in subcritical water produces a viscous crude oil replacement. This crude oil product differs from conventional crude oil in the oxygen content of the oil. The crude oil replacement contains approximately 10 to 20% oxygen, whereas

conventional petroleum contains less than 1% oxygen (Peterson *et al.,* 2008: 45). The high oxygen content results in certain undesirable properties of the oil, such as lower energy content, poor thermal stability, lower volatility, higher corrosivity and a tendency to polymerize. These undesirable properties are the reason why bio-crudes cannot be processed with current petroleum feedstocks (Peterson *et al.,* 2008: 45).

Bio-crudes must therefore be burned directly as fuel oils or be processed through a deoxygenation process. The primary chemical goal of liquefaction is, however, to remove oxygen heteroatoms. The oxygen is preferably removed as CO_2 and H_2O (Peterson *et al.,* 2008: 46), because in this way a large percentage of the feedstock's heating value is conserved. Removing oxygen in the form of CO_2 is more advantageous than removing it as H_2O because it increases the H/C ratio and results in a more desirable fuel (Peterson *et al.,* 2008: 46).

2.4.6 Influence of operating conditions on the thermochemical liquefaction process

This section describes the influence of the various operating conditions on the thermochemical liquefaction process. Section 2.4.6.1 discusses the influence of operating temperature on thermochemical liquefaction, whereas section 2.4.6.2 describes the influence of the atmosphere of the process.

In Section 2.4.6.3 the influence of the operating pressure is discussed and section 2.4.6.4 discusses the effect of the holding time on the thermochemical liquefaction process.

Section 2.4.6.5 further states the influence of the solvent on the thermochemical liquefaction process, while section 2.4.6.6 discusses the influence of the catalyst load on thermochemical liquefaction.

2.4.6.1 Influence of operating temperature on the thermochemical liquefaction process

Studies (Yokoyama *et al.,* 1987: 1153; Karaca & Bolat, 2000: 50; Xu & Etcheverry, 2008: 339) have been conducted on various feedstocks in order to determine the

influence of the operating temperature on thermochemical liquefaction. These studies have shown that the oil yield increases with an increase in the operating temperature. The oil yield may, however, decline or level off at certain temperatures. Table 2.11 depicts the influence of a rise in operating temperature on thermochemical liquefaction for various feedstocks.

Table 2.11: Influence of an increase in operating temperature on thermochemical liquefaction.

Feedstock	Temperature (°C)	Observations	Comments	Reference
Sewage sludge	250 – 340	Increased oil yield.	Temperatures above 300 °C assist in the separation of the oily and aqueous phases.	Yokoyama *et al.,* 1987: 1153.
Lignite and sawdust mixture	300 – 400	Increase in oil yield.	-	Karaca & Bolat, 2000: 50.
Woody biomass	200 – 260	Increase in oil yield.	Oil yield levelled off above 300 °C due to the condensation and cyclization reactions of the liquid products as well as the cracking reactions of the hydrocarbon gases.	Xu & Etcheverry, 2008: 339.
Ethanol stillage	250 – 340	Increase in the gas yield, decrease in the residue and the aqueous soluble yields.	-	Minowa *et al.,* 1994: 581.
Rye straw	350 – 400	Decreased oil yield with red mud, CoO-MoO_3 and CoO-MoO_3-sulphur catalysts. Increased oil yield with red mud – sulphur catalyst.	Higher temperatures eliminate oxygen from pyrolysis products by hydrodeoxygenation reactions, which are accompanied by hydrocracking.	Klopries *et al.,* 1990: 449.
Pine wood	300 – 400	High temperatures produce permanent gas and water.	Thermal-cracking reactions are enhanced at high temperatures.	Rezzoug & Capart, 2002: 640.
Sawdust	250 – 450	Rise in the oil yield with rise in temperature.	Rise in oil yield due to decomposition of asphaltenes and preasphaltenes. High temperature results in increased formation of free radicals, which requires more active hydrogen in order to prevent polymerization.	Yan *et al.,* 1999: 138.

Table 2.11 continued

Feedstock	Temperature (°C)	Observations	Comments	Reference
Sawdust	200 – 350	Increase in oil yield.	Increased temperature promotes the pyrolysis of the biomass to preasphaltenes and asphaltenes, which decomposes to oil.	Wang *et al.,* 2007a: 1592.
Spirulina sp.	300 – 425	Increased oil yield.	-	Matsui *et al.,* 1997: 1045.
Dunaliella tertiolecta	250 – 340	Increase in calorific value of oil and a decrease in the viscosity.	Increased calorific value due to increased carbon and hydrogen content of the oil.	Minowa *et al.,* 1995b: 1737.
Cellulose	271 – 407	Increase in oil yield and calorific value	Optimum oil yield may be at temperatures higher than the maximum oil yield.	Donovan *et al.,* 1981: 901.
Garbage	250 – 340	Increased oil yield.	-	Minowa *et al.,* 1995a: 119.
Silver birch	280 – 420	Oil yield increased up to a maximum and decreased again.	The oil yield increased to 53.3 wt% at 380 °C and decreased again at temperatures higher than 380 °C. The decrease is due to competition between the hydrolysis and repolimerization reactions during liquefaction.	Qian *et al.,* 2007: 201.
Wood (*Cunninghamia lanceolata*)	280 – 360	The oil yield increases from 280 to 320 °C and then decreases up to 360 °C. Higher heating value increases.	The oil yield decreases at higher temperatures due to the competition between hydrolysis and repolymerization. Higher heating value increases due to increased carbon content and decreased oxygen content.	Qu *et al.,* 2003: 600.

2.4.6.2 Influence of the reaction atmosphere on the thermochemical liquefaction process

The atmosphere in which thermochemical liquefaction is conducted influences the reaction pathway that is followed in order to produce the oil. The presence of a reduction gas favours the abstraction process, whereas the absence of a reduction gas favours pyrolytic evolution.

The atmosphere required for thermochemical liquefaction is also dependent on the hydrogen content of the biomass. Biomass with sufficient hydrogen content does not require the use of a reducing agent due to the stabilization of the free radicals, which are formed during the thermochemical liquefaction process by internal hydrogen-shuttling within the raw material (Björnbom *et al.,* 1986: 1053). Björnbom and co-workers (1986: 1053) conducted thermochemical liquefaction experiments with raw peat in a reducing (CO) and an inert (N_2) atmosphere and found that carbon monoxide is not necessary to convert the peat to oil due to the high hydrogen content of the raw material. Their results indicate that internal H-shuttling in the raw peat is sufficient to stabilize the free radicals formed during thermochemical liquefaction.

Xu and Lancaster (2008: 1581), however, found that a reducing atmosphere (H_2 gas) improved the yield of oil in the thermochemical liquefaction of pulp/paper sludge. The pulp/paper sludge studied by Xu and Lancaster (2008: 1581) contained 5.2 wt% hydrogen, whereas the peat studied by Björnbom and co-workers (1986: 1051) contained 7 wt% hydrogen. The smaller amount of hydrogen in the pulp/paper sludge may therefore result in less H-shuttling and create the need for a reducing atmosphere in order to improve liquefaction, whereas the peat contains sufficient hydrogen in order to sustain the liquefaction process.

Matsui and co-workers (1997: 1044) conducted thermochemical liquefaction experiments on *Spirulina* sp. in a nitrogen and hydrogen atmosphere. The *Spirulina* sp. contained 7.4 wt% hydrogen. The atmosphere of the liquefaction experiments did not affect the oil yield. This may also be ascribed to the internal hydrogen-shuttling that occurs in the *Spirulina* sp. (Matsui *et al.,* 1997: 1044).

Boocock and co-workers (1980: 468) also showed that liquefaction of poplar wood in an inert nitrogen atmosphere produces oil with approximately the same composition as oil obtained from liquefaction reactions which was conducted with a hydrogen

atmosphere. The oil obtained in the inert atmosphere only had a small amount of hydrogen less than the oil obtained in a hydrogen atmosphere, but it was less viscous and flowed at room temperature (Boocock *et al.,* 1980: 468).

The reaction atmosphere required for liquefaction is therefore dependent on the hydrogen content of the biomass. Biomass with sufficient hydrogen content for internal hydrogen-shuttling does not require a reducing atmosphere, whereas biomass with insufficient hydrogen content requires a reducing atmosphere for optimum liquefaction yields.

2.4.6.3 Influence of operating pressure on the thermochemical liquefaction process

Various studies (Yokoyama *et al.,* 1987: 1153; Björnbom *et al.,* 1981: 9; Wang *et al.,* 2007a: 1593) conducted on the liquefaction of biomass encompassed an investigation of the influence of operating pressure on the thermochemical liquefaction process.

These studies generally showed that the operating pressure does not significantly influence the thermochemical liquefaction process. Yokoyama et al. (1987: 1153) discovered that changes in the operating pressure of the thermochemical liquefaction process of sewage sludge had little effect on the conversion yields of heavy oils. No significant changes in the calorific values of the heavy oils were observed with a change in the operating pressure (Yokoyama *et al.,* 1987: 1153).

In their study on the thermochemical liquefaction of peat, Björnbom and co-workers (1981: 9) found that a ten-fold reduction in the initial CO pressure only produced a two-fold reduction in the conversion of the peat. This finding confirms the low sensitivity of conversion to the initial CO pressure (Björnbom *et al.,* 1981: 9).

Wang *et al.* (2007a: 1593) also discovered that the initial cold pressure of the atmosphere does not significantly affect the conversion and oil yield for the thermochemical liquefaction of sawdust. The experiments conducted by Yan and co-workers (1999: 139) on the thermochemical liquefaction of sawdust, however, produced an increased oil yield with an increase in the initial hydrogen pressure when the holding time of the reaction is particularly long (30 minutes). During shorter holding times (10 minutes) the initial operating pressure does, however, not

significantly affect the liquefaction (Yan *et al.,* 1999: 139). This phenomenon may be explained from the mechanism of liquefaction. The rate of pyrolysis to form preasphaltene and asphaltene is so high that the first step in the liquefaction process may be completed within the allocated 10 minute reaction time. The following step in the liquefaction process requires hydrogenation of the formed preasphaltene and asphaltene to oil of smaller size molecules. This step requires more hydrogen and is therefore dependent on the hydrogen pressure. The dependency of the early stage of pyrolysis on hydrogen is weak, whereas the latter stage demands more active hydrogen in order to decompose the preasphaltene and asphaltene to oil (Yan *et al.,* 1999: 142).

Xu and Etcheverry (2008: 340) discovered that an increase in the initial H_2 pressure resulted in an increase in the oil yield for the liquefaction woody biomass. They attributed this to the ability of the H_2 to break down the woody biomass and to stabilize the intermediate free radicals formed in the process (Xu & Etcheverry, 2008: 339 – 340).

The atmosphere in which liquefaction is conducted therefore influences the liquefaction process. The experiments conducted by Xu and Etcheverry (2008: 340) as well as Yan and co-workers (1999: 139) indicate that the use of a reducing atmosphere may lead to an increase in the oil yield obtained by thermochemical liquefaction due to ability of the reducing atmosphere to break down the biomass by abstraction.

The effect of the initial operating pressure is dependent on the hydrogen content of the biomass as well as the type of atmosphere used for liquefaction. An inert atmosphere (N_2) is not affected by changes in the initial operating pressure.

2.4.6.4 Influence of holding time on the thermochemical liquefaction process

Studies on the influence of the holding time on thermochemical liquefaction have been conducted by various persons (Yokoyama *et al.,* 1987: 1153; Björnbom *et al.,* 1981: 8; Yan *et al.,* 1999: 139; Wang *et al.,* 2007a: 1593).

Thermochemical liquefaction of sewage sludge showed Yokoyama and co-workers (1987: 1153) that an increase in the holding time does not result in a significant

difference in the yields of the heavy oil. Björnbom and co-workers (1981: 8) discovered the same result for the liquefaction of Swedish peats when they reduced the holding time from 120 to 15 min. This produced no difference in the yield or total raw material conversion of the peats. Björnbom and co-workers (1981: 8) discovered that a slow heating rate compensates for a short holding time and therefore produces approximately the same yield of oil as well as the same conversion of the raw material.

In contrast to the previous results, the oil yield obtained from the thermochemical liquefaction of sawdust increased with an increase in the holding time (Yan *et al.,* 1999: 139). Experiments conducted by Wang and co-workers (2007a: 1593) on sawdust showed that the conversion and oil yield increased with an increase in the holding time up to a maximum time. The thermochemical liquefaction of the sawdust provides a constant oil yield and conversion after a holding time of 30 min (Wang *et al.,* 2007a: 1593). Dote and co-workers (1996: 493) also observed an increase in the oil yield with an increase in the holding time for the liquefaction of albumin.

The holding time can influence the properties of the oil obtained from thermochemical liquefaction. Minowa and co-workers (1995b: 1737) observed a decrease in the viscosity of oil obtained from thermochemical liquefaction of algae with an increase in the holding time.

The thermochemical liquefaction of garbage led Minowa and co-workers (1995a: 119) to the conclusion that the effect of the holding time is dependent on the reaction temperature and that a high reaction temperature may be accompanied by a shorter holding time (Minowa *et al.,* 1995a: 119). Qu and co-workers (2003: 600 – 603) discovered that a prolonged holding time during the liquefaction of wood (*Cunninghamia lanceolata*) decreases the heavy oil yield due to condensation and repolymerization of the intermediates to form solid residues.

The various observations stated above were obtained from different types of biomass and liquefaction atmospheres. The influence of the holding time may therefore not be generalized and varies in collaboration with the type of biomass, the atmosphere of liquefaction and the operating temperature.

2.4.6.5 Influence of solvent on the thermochemical liquefaction process

In this instance the solvent that is referred to is the media that is used for the thermochemical liquefaction process. The solvent that is used during thermochemical liquefaction affects the liquefaction process. Wang and co-workers (2007a: 1589) found that the composition of the oil obtained from thermochemical liquefaction of sawdust differed with the use of different solvents. They observed that the contribution of the type of solvent influences the liquefaction stronger than the type of atmosphere. Wang and co-workers (2007a: 1591) identified two types of solvent:

- Solvent with the ability to donate hydrogen and
- Solvent without the ability to donate hydrogen.

The solvent acts as a hydrogen-donor and also promotes the destruction of the molecular structure of the biomass feed (Yan *et al.,* 1999: 142). Wang and co-workers (2007a: 1589) found that the presence of a solvent favours the molecular rearrangement and stabilization of the free radicals by a hydrogen donor. This was especially the case for a hydrogen donating solvent (Wang *et al.,* 2007a: 1589). The presence of a solvent also promotes the hydrocracking of heavier molecules to light ones due to its ability to penetrate the molecules as well as their supply of hydrogen (Wang *et al.,* 2007a: 1589).

A solvent which has the ability to donate and transport hydrogen improves the hydrogenation and hydrocracking reactions with the inhibition of polycondensation (Wang *et al.,* 2007b: 190). Water may also be a preferred solvent in certain cases. Matsui and co-workers (1997: 1046) conducted studies on the thermochemical liquefaction of algae (*Spirulina*) and observed an increase in the oil yield when water was used as a solvent. Water is therefore suggested as the solvent of choice for the liquefaction of micro-algae (Matsui *et al.,* 1997: 1046).

Vanasse and co-workers (1988: 118) observed that a solvent with a similar Hildebrand parameter as the constituents of wood, results in good solvent-polymer interaction during thermochemical liquefaction of the wood. This was illustrated by the lower oil yield that was obtained when ethylene glycol (a solvent with an almost identical Hildebrand parameter as the polymers of the wood) was used as solvent (Vanasse *et al.,* 1988: 118). The ethylene glycol solvent interacts with the wood polymers, which stabilize the polymer chains and eliminate the chance for cross

linking and charification reactions. A creosote solvent does not interact with the polymers in the wood and therefore results in a higher oil yield (Vanasse *et al.,* 1988: 118).

The properties of the solvent used during thermochemical liquefaction affects the liquefaction process and the preferred solvent for liquefaction of algae was found to be water (Matsui *et al.,* 1997: 1046).

2.4.6.6 Influence of catalyst load on thermochemical liquefaction of biomass

The amount of catalyst and the type of catalyst used during liquefaction influences the liquefaction process. The catalyst has the ability to improve the oil yield obtained from thermochemical liquefaction. Yokoyama and co-workers (1987: 1152) hypothesized that catalysts such as alkali metal salts enhance the hydrolytic degradation of organic materials into smaller fractions. The degradation is then followed by condensation, deoxygenation, isomerisation and cyclization (Yokoyama *et al.,* 1987: 1152).

The catalyst may also have various other effects on the thermochemical liquefaction process. It may, for instance, influence the properties of the product oil or even help control the pH of the aqueous phase. Table 2.12 lists the work done by various researchers and the influence the catalyst had on their thermochemical liquefaction process.

Table 2.12: Influence of the catalyst on the thermochemical liquefaction process.

Biomass	Catalyst	Observation	Comment	Reference
Sewage sludge	Sodium carbonate	At 300 °C and 12.0 MPa a 5 wt% (based on dry solid) catalyst load increased the oil yield from 19.5 wt% (based on volatile solid in sewage) to 50 wt%.	Catalyst helped control the aqueous phase pH to near neutrality and assisted the separation of the oily materials and the aqueous phase.	Yokoyama *et al.,* 1987: 1152.
Peat	Potassium carbonate	Catalyst increases peat conversion.	-	Björnbom *et al.,* 1981: 9; Panayotova-Björnbom *et al.,* 1979: 165.
Albumin	Sodium carbonate	Catalyst prevented distribution of nitrogen to product oil.	-	Dote *et al.,* 1996: 496.
Wood	Potassium carbonate	Catalyst increased conversion and total oil yield.	Catalyst caused shift in composition of oil from n-C_7 and n-C_8 to n-C_{11} hydrocarbons.	Bhaskar *et al.,* 2008: 2240.
Microcystic viridis	Sodium carbonate	Addition of 5wt% catalyst produced an increased oil yield.	-	Yang *et al.,* 2004: 23.
Botryococcus braunii	Sodium carbonate	No effect.	-	Dote *et al.,* 1994: 1857.
Dunaliella tertiolecta	Sodium carbonate	Catalyst addition affected the product oil properties.	-	Minowa *et al.,* 1995b: 1737.
Spirulina sp.	$Fe(CO)_5$-S	Increased catalyst load resulted in increased oil yield.	Catalyst load did not affect the conversion and gas yield.	Matsui *et al.,* 1997:1045.

Table 2.12 continued

Biomass	Catalyst	Observation	Comment	Reference
Wood	$FeSO_4$ or FeS	Catalyst addition increased oil production.	Catalyst addition suppresses the formation of gases, water and char.	Xu & Etcheverry, 2008: 340.
Garbage	Sodium carbonate	Catalyst addition increases oil yield.	Catalyst contributes to liquefaction of garbage.	Minowa *et al.,* 1995a: 119.

2.5 References

Amin, S. 2009. Review on biofuel oil and gas production processes from microalgae. Energy Conversion and Management, 50(7): 1 – 7.

Bhaskar, T., Sera, A., Muto, A. & Sakato, Y. 2008. Hydrothermal upgrading of wood biomass: Influence of the addition of K_2CO_3 and cellulose/lignin ratio. Fuel, 87: 2236 – 2242.

Biofuels Industrial Strategy of the Republic of South Africa. 2007. http://www.fanrpan.org/documents/d00472/Biofuels industry RSA Dec2007.pdf. Date of access: 18 March 2007.

Björnbom, E., Olsson, B. & Karlsson, O. 1986. Thermochemical refining of raw peat prior to liquefaction. Fuel, 65: 1051 – 1056.

Björnbom, P., Granath, L., Kannel, A., Karlsson, G., Lindström, L. & P-Björnbom, E. 1981. Liquefaction of Swedish peats. Fuel, 60: 7 – 13.

Bold, H.C. & Wynne, M.J. 1978. Introduction to the Algae: Structure and Reproduction. New Jersey: Prentice-Hall, Inc. 706 p.

Boocock, D.G.B., Mackay, D., McPherson, M., Nadeau, S.& Thurier, R. 1979. Direct hydrogenation of hybrid poplar wood to liquid and gaseous fuels. The Canadian Journal of Chemical Engineering, 57: 98 – 101.

Boocock, D.G.B., Mackay, D., Franco, H. & Lee, P. 1980. The production of synthetic organic liquids from wood using a modified nickel catalyst. The Canadian Journal of Chemical Engineering, 58: 466 – 469.

Boocock, D.G.B., Konar, S.K., Leung, A. & Ly, L.D. 1992. Fuels and chemicals from sewage sludge 1: The solvent extraction and composition of a lipid from a raw sewage sludge. Fuel, 71: 1283 – 1289.

Carter, D., Darby, D., Hallé, J. & Hunt, P. 2005. How to make biodiesel. Great Britian. 111 p.

Chisti, Y. 2007. Biodiesel from microalgae. Biotechnology Advances, 25: 294 – 306.

Chornet, E. & Overend, R.P. 1985. Biomass Liquefaction: An Overview. (In Overend, R.P., Milne, T.A. & Mudge, L.K., ed. Fundamentals of Thermochemical Biomass Conversion. New York: Elsevier Applied Science Publishers. p. 967 – 1001).

Chornet, E., Eugène, D. & Overend, R.P. 1985. Fluidodynamic Effects in Fractional Solubilization of Biomass Leading to Liquefaction. (In Overend, R.P., Milne, T.A. & Mudge, L.K., ed. Fundamentals of Thermochemical Biomass Conversion. New York: Elsevier Applied Science Publishers. p. 839 – 849).

Collyer, D.M. & Fogg, G.E. 1955. Studies on Fat Accumulation by Algae. Journal of experimental botany, 6(2): 256 – 275.

Donovan, J.M., Molton, P.M. & Demmitt, T.F. 1981. Effect of pressure, temperature, pH, and carbon monoxide on oil yields from cellulose liquefaction. Fuel, 60(10): 898 – 902.

Dote, Y., Inoue, S., Ogi, T. & Yokoyama, S. 1996. Studies on the direct liquefaction of protein-contained biomass: The distribution of nitrogen in the products. Biomass and Bioenergy, 11(6): 491 – 498.

Dote, Y., Sawayama, S., Inoue, S., Minowa, T. & Yokoyama, S. 1994. Recovery of liquid fuel from hydrocarbon-rich microalgae by thermochemical liquefaction. Fuel, 73(12): 1855 – 1857.

Eager, R.L., Mathews, J.F. & Pepper, J.M. 1982. Liquefaction of Aspen Poplar Wood. The Canadian Journal of Chemical Engineering, 60: 289 – 294.

Eager, R.L., Mathews, J.F. & Pepper, J.M. 1985. Liquefaction of Aspen Poplar to Produce an Oil and Chemicals. (In Overend, R.P., Milne, T.A. and Mudge, L.K., ed. Fundamentals of Thermochemical Biomass Conversion. New York: Elsevier Applied Science Publishers. p. 1051 – 1071).

Erzengin, M. & Küçük, M.M. 1998. Liquefaction of sunflower stalk by using supercritical extraction. Energy Conversion Management, 39(11): 1203 – 1206.

Fukuda, H., Kondo, A. & Noda, H. 2001. Biodiesel fuel production by transesterification of oils. Journal of Bioscience and Bioengineering, 92(5): 405 – 416.

Ginzburg, B. 1993. Liquid fuel (oil) from halophilic algae: A renewable source of non-polluting energy. Renewable Energy, 3(2-3): 249 – 252.

Goudriaan, F., Van de Beld, B., Boerefijn, F.R., Bos, G.M., Naber, J.E., Van der Wal., S. & Zeevalkink, J.A. 2001. Thermal efficiency of the HTU® process for biomass liquefaction. (In Bridgwater, A.V., ed. Progress in Thermochemical Biomass Conversion. Oxford: Blackwell Science Ltd. p. 1312 – 1325).

Gressel, J. 2007. Transgenics are imperative for biofuel crops. Plant Science, 174(3): 246 – 263.

Herro, A. 2008. Better than corn? Algae Set to Beat Out Other Biofuel Feedstocks. World Watch, 21(1): 4.

Hu, Q., Sommerfeld, M., Jarvis, E., Ghirardi, M., Posewitz, M., Seibert, M. & Darzins, A. 2008. Microalgal triacylglycerols as feedstocks for biofuel production: perspectives and advances. The Plant Journal, 54: 621 – 639.

Inoue, S., Dote, Y., Sawayama, S., Minowa, T., Ogi, T. & Yokoyama, S. 1994. Analysis of oil derived from liquefaction of Botryococcus Braunii. Biomass and Bioenergy, 6(4): 269 – 274.

Inoue, S., Minowa, T., Sawayama, S. & Ogi, T. 2001. Organic composition of liquidized model kitchen garbage. (In Bridgwater, A.V., ed. Progress in Thermochemical Biomass Conversion. Oxford: Blackwell Science Ltd. p. 1219 – 1225).

Karaca, F. & Bolat, E. 2000. Coprocessing of a Turkish lignite with a cellulosic waste material 1. The effect of coprocessing on liquefaction yields at different reaction temperatures. Fuel Processing Technology, 64: 47 – 55.

Karaca, F. & Bolat, E. 2002. Coprocessing of a Turkish lignite with a cellulosic waste material 2. The effect of coprocessing on liquefaction yields at different reaction pressures and sawdust/lignite ratios. Fuel Processing Technology, 75: 109 – 116.

Karlsson, O. 1990. The composition of peat liquids 2: Functional group analysis of peat liquefaction products. Fuel, 69: 613 – 616.

Klopries, B., Hodek, W. & Bandermann, F. 1990. Catalytic hydroliquefaction of biomass with red mud and CoO-MoO_3 catalysts. Fuel, 69: 448 – 455.

Kondili, E.M. & Kaldellis, J.K. 2007. Biofuel implementation in East Europe: Current status and future prospects. Renewable and Sustainable Energy Reviews, 11: 2137 – 2151.

Lédé, J. 1999. Solar thermochemical conversion of biomass. Solar Energy, 65(1): 3 – 13.

Li, J., Wu, L. & Yang, Z. 2008. Analysis and upgrading of bio-petroleum from biomass by direct deoxy-liquefaction. Journal of Analytical and Applied Pyrolysis, 81: 199 – 204.

Lin, C. & Li, R. 2009. Fuel properties of biodiesel produced from the crude fish oil from the soapstock of marine fish. Fuel Processing Technology, 90: 130 – 136.

Matsui, T., Nishihara, A., Ueda, C., Ohtsuki, M., Ikenaga, N. & Suzuki, T. 1997. Liquefaction of micro-algae with iron catalyst. Fuel, 76(11): 1043 – 1048.

Matsumura, Y., Minowa, T., Potic, B., Kersten, S.R.A., Prins, W., Van Swaaij, W.P.M., Van de Beld, B., Elliot, D.C., Neuenschwander, G.G., Kruse, A. & Antal, M.J. 2005. Biomass gasification in near- and super-critical water: Status and prospects. Biomass and Bioenergy, 29: 269 – 292.

McKeough, P.J. 1983. Oxygen removal during the direct liquefaction of low-rank materials. Fuel, 62: 445 – 449.

Meier, D., Larimer, D.R. & Faix, O. 1986. Direct liquefaction of different lignocellulosics and their constituents 1: Fractionation, elemental composition. Fuel, 65: 910 – 915.

Miller, J.D.A. 1962. Fats and Steroids. (In Lewin, R.A., ed. Physiology and Biochemistry of Algae. New York: Academic Press. p. 357 – 370.)
Minowa, T., Kondo, T. & Sudirjo, T. 1998. Thermochemical liquefaction of Indonesian biomass residues. Biomass and Bioenergy, 14(5-6): 517 – 524.

Minowa, T., Murakami, M., Dote, Y., Ogi, T. & Yokoyama, S. 1994. Effect of operating conditions on thermochemical liquefaction of ethanol fermentation stillage. Fuel, 73(4): 579 – 582.

Minowa, T., Murakami, M., Dote, Y., Ogi, T. & Yokoyama, S. 1995a. Oil production from garbage by thermochemical liquefaction. Biomass and Bioenergy, 8(2): 117 – 120.

Minowa, T., Yokoyama, S., Kishimoto, M. & Okakura, T. 1995b. Oil production from algal cells of Dunaliella tertiolecta by direct thermochemical liquefaction. Fuel, 74(12): 1735 – 1738.

National Renewable Energy Laboratory. 1998. www.**nrel**.gov/docs/legosti/fy98/24190.pdf. Date of access: 22 May 2008.

Qian, Y., Zuo, C., Tan, J. & He, J. 2007. Structural analysis of bio-oils from sub-and supercritical water liquefaction of woody biomass. Energy, 32: 196 – 202.

Qu, Y., Wei, X. & Zhong, C. 2003. Experimental study on the direct liquefaction of *Cunninghamia lanceolata* in water. Energy, 28: 597 – 606.

Panayotova-Björnbom, E., Björnbom, P., Cavalier, J.C. & Chornet, E. 1979. The combined dewatering and liquid phase hydrogenolysis of raw peat using carbon monoxide. Fuel Processing Technology, 2: 161 – 169.

Peacocke, G.V.C. & Bridgwater, A.V. 2001. Transport, Handling and Storage of Biomass Derived Fast Pyrolysis Liquid. (In Bridgwater, A.V., ed. Progress in

Thermochemical Biomass Conversion. Oxford: Blackwell Science Ltd. p. 1482 – 1499).

Peterson, A.A., Vogel., F., Lachance, R.P., Fröling, M., Antal., M.J. & Tester, J.W. 2008. Thermochemical biofuel production in hydrothermal media: A review of sub- and supercritical water technologies. Energy and Environmental Science, 1: 32 – 65.

Prescott, G.W. 1969. The Algae: A Review. London: Thomas Nelson and Sons Ltd. 436 p.

Rezzoug, S. & Capart, R. 2002. Liquefaction of wood in two successive steps: solvolysis in ethylene-glycol and catalytic hydrotreatment. Applied Energy, 72: 631 – 644.

Rezzoug, S. & Capart, R. 2003. Assessment of wood liquefaction in acidified ethylene glycol using experimental design methodology. Energy Conversion and Management, 44: 781 – 792.

Rocha, J.D., Brown, S.D., Love, G.D. & Snape, C.E. 1997. Hydropyrolysis: a versatile technique for solid fuel liquefaction, sulphur speciation and biomarker release. Journal of Analytical and Applied Pyrolysis, 40 – 41: 91 – 103.

Sawayama, S., Inoue, S., Dote, Y. & Yokoyama, S. 1995. CO_2 fixation and oil production through microalga. Energy Conversion Management, 36(6-9): 729 – 731.

Sawayama, S., Minowa, T. & Yokoyama, S. 1999. Possibility of renewable energy production and CO_2 mitigation by thermochemical liquefaction of microalgae. Biomass and Bioenergy, 17: 33 – 39.

Schuchardt, U. & De Assis Pereira Matos, F. 1982. Liquefaction of sugar cane bagasse with formate and water. Fuel, 61(2): 106 – 110.

Soetaert, W. 2008. Second generation biofuels. http://www.ef4.be/documents/evenements/biocarburants/041_gent.pdf. Date of access: 8 April 2008.

Tiffany, L.H. 1958. Algae: The Grass of Many Waters. Springfield: Charles C Thomas. 199 p.

Vanasse, C., Chornet, E. & Overend, R.P. 1988. Liquefaction of Lignocellulosics in Model Solvents: Creosote Oil and Ethylene Glycol. The Canadian Journal of Chemical Engineering, 66: 112 – 120.

Van den Hoek, C., Mann, D.G. & Jahns, H.M. 1995. Algae: An introduction to phycology. Cambridge: University Press. 627 p.

Vasilakos, N.P. & Austgen, D.M. 1985. Hydrogen-Donor Solvents in Biomass Liquefaction. Industrial and Engineering Chemistry Process Design and Development, 24(2): 304 – 311.

Walton, T.E. & Paudler, W.W. 1981. Conversion of cellulose to hydrocarbons. Fuel, 60: 650 – 654.

Wang, G., Li, W., Li, B. & Chen, H. 2007a. Direct liquefaction of sawdust under syngas. Fuel, 86: 1587 – 1593.

Wang, G., Li, W., Li, B., Chen, H. & Bai, J. 2007b. Direct liquefaction of sawdust under syngas with and without catalyst. Chemical Engineering and Processing, 46: 187 – 192.

Wang, C., Pan, J., Li, J & Yang, Z. 2008. Comparative studies of products produced from four different biomass samples via deoxy-liquefaction. Bioresource Tecnology, 99: 2778 – 2786.

Williams, J.P. 1979. Glycerolipids and fatty acids of algae. (In Hellebust, J.A. & Craigie, J.S., ed. Handbook of phycological methods: Physiological and biochemical methods. Cambridge: Cambridge University Press. p. 99 – 107.)

Xu, C. & Etcheverry, T. 2008. Hydro-liquefaction of woody biomass in sub- and super-critical ethanol with iron-based catalysts. Fuel, 87: 335 – 345.

Xu, C. & Lancaster, J. 2008. Conversion of secondary pulp/paper sludge powder to liquid oil products for energy recovery by direct liquefaction in hot-compressed water. Water Research, 42: 1571 – 1582.

Yan, Y., Xu, J., Li, T. & Ren, Z. 1999. Liquefaction of sawdust for liquid fuel. Fuel Processing Technology, 60: 135 – 143.

Yang, Y.F., Feng, C.P., Inamori, Y. & Maekawa, T. 2004. Analysis of energy conversion characteristics in liquefaction of algae. Resources, Conservation and Recycling, 43: 21 – 33.

Yokoyama, S., Ogi, T., Koguchi, K. & Nakamura, E. 1984. Direct liquefaction of wood by catalyst and water. Liquid fuels technology, 2(2): 155 – 163.

Yokoyama, S., Suzuki, A., Murakami, M., Ogi, T., Koguchi, K. & Nakamura, E. 1987. Liquid fuel production from sewage sludge by catalytic conversion using sodium carbonate. Fuel, 66: 1150 – 1155.

Yuan, X.Z., Li, H., Zeng, G.M., Tong, J.Y. & Xie, W. 2007. Sub- and supercritical liquefaction of rice straw in the presence of ethanol-water and 2-propanol-water mixture. Energy, 32: 2081 – 2088.

Zhong, C. & Wei, X. 2004. A comparative experimental study on the liquefaction of wood. Energy, 29: 1731 – 1741.

Chapter 3. - Experimental

Chapter 3 provides a description of the experimental work conducted. Section 3.1 discusses the materials that were used during the study. In Section 3.2 the cultivation and preparation of the algae is discussed. Section 3.3 provides a description of the thermochemical liquefaction experiments, whereas Section 3.4 describes the analytical equipment used in the study and the methodology for the use of the analytical equipment.

3.1 Materials

The materials used in this study are divided into two categories. These categories are the chemicals that were used (discussed in Section 3.1.1) and the algae that were used (described in Section 3.1.2).

3.1.1 Chemicals used

Table 3.1 shows the information regarding the chemicals used in this study. The chemicals were used as received from the supplier without any prior purification.

In this study chloroform was used as oil extractant. A detailed description of the selection process followed to identify chloroform as solvent is given in Appendix A.

Table 3.1: Information on chemicals used.

Component	Purity (%)	Supplier	CAS no.	Purpose
Boric acid	98.0	Merck	10043-35-3	Preparation of algal medium.
Calcium chloride dihydrate	99.0	Merck	10035-04-8	Preparation of algal medium.
Chloroform	99.0	Merck	67-66-3	Solvent for oil extraction.
Citric acid	99.0	Merck	77-92-09	Preparation of algal medium.
Cobalt (II) nitrate hexahydrate	99.0 – 102.0	Merck	10026-22-9	Preparation of algal medium.
Copper sulphate pentahydrate	99.0 – 100.5	Merck	7758-99-8	Preparation of algal medium.
Dipotassium hydrogen orthophosphate	98.0 – 101.0	Merck	7758-11-4	Preparation of algal medium.
EDTA (disodium magnesium salt)	99.0 – 101.0	Merck	60-00-4	Preparation of algal medium.
Iron sulphate heptahydrate	98.0 – 105.0	Merck	7720-78-7	Preparation of algal medium.
Magnesium sulphate heptahydrate	99.0	Merck	10034-99-8	Preparation of algal medium.
Manganese chloride tetrahydrate	98.0	Sigma Aldrich	7773-01-5	Preparation of algal medium.
Sodium carbonate	99.5	Merck	497-19-8	Preparation of algal medium; catalyst for thermochemical liquefaction.
Sodium metasilicate nonahydrate	98.0	Sigma-Aldrich	13517-24-3	Preparation of algal medium.
Sodium molybdate dehydrate	99.5	Merck	10102-40-6	Preparation of algal medium.
Sodium nitrate	98.5	Merck	7631-99-4	Preparation of algal medium.
Trimethyl sulfonium hydroxide	0.25 M in methanol	Sigma Aldrich	17287-03-5	Derivitization agent for analysis of oil composition.
Zinc sulphate heptahydrate	99.5 – 103.0	Merck	7446-20-0	Preparation of algal medium.

3.1.2 Algae used

In this study, different algae were used to conduct the experiments. Section 3.1.2.1 discusses *Microcystis aeruginosa*, while sections 3.1.2.2 and 3.1.2.3 provide brief descriptions of *Cyclotella meneghinia* and *Nitzschia pusilla*, respectively.

3.1.2.1 *Microcystis aeruginosa* collected from the Hartebeespoort dam

Algae were collected on the 8th of January 2009 from Hartebeespoort dam, which is situated approximately 55 km from Johannesburg in the North-West province. The Hartebeespoort dam is a 20 km^2 water reservoir (Department of Water Affairs and Forestry, 2005: 2). The location of the North-West Province (Anon., 2009a) and the Hartebeespoort dam (Anon., 2009b) is shown in Figures 3.1 and 3.2, respectively.

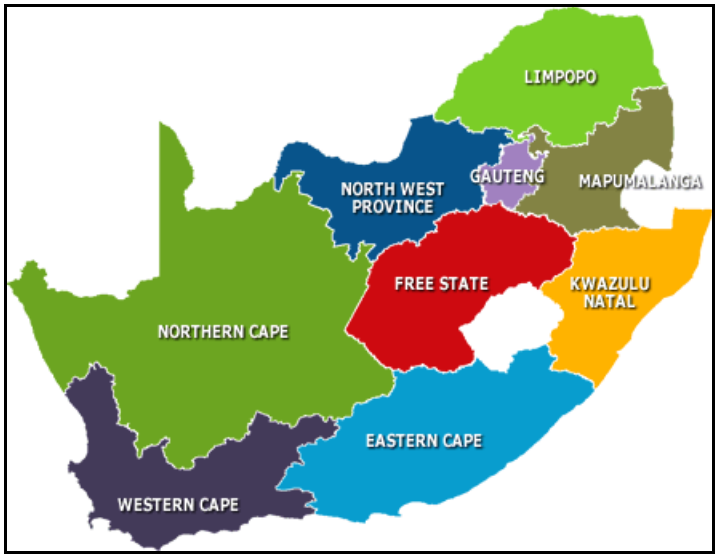

Figure 3.1: Map of South Africa.

Figure 3.2: Map of North-West Province.

The Hartebeespoort dam is in a state of eutrophication, i.e. the water is enriched with nutrients, especially phosphates and nitrates. This results in algal blooms in the dam. A study conducted on the algal cultures in the Hartebeespoort dam found that *M. aeruginosa* constitutes more than 90% of the algal biomass in the dam during late summer (NSPU, 1985). Figure 3.3 shows a photo of such a microalgal bloom in the Hartebeespoort dam, while Figure 3.4 shows a closer view of the microalgal bloom.

Figure 3.3: Microalgal bloom in Hartebeespoort dam.

Figure 3.4: Closer view of microalgal bloom in Hartebeespoort dam.

M. aeruginosa is classified as cyanobacteria and occur in South African catchments during summer to autumn periods. Figure 3.5 shows a scanning electron microscope (SEM) microphotograph of *M. aeruginosa* cells. The picture was taken at 3000 times magnification.

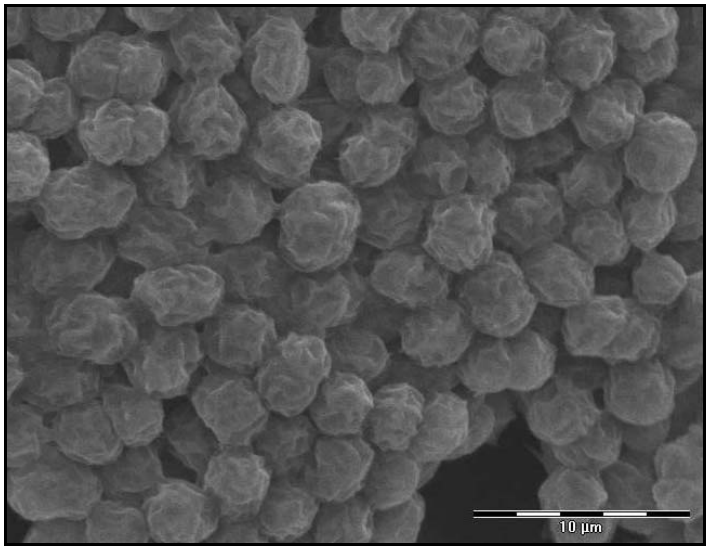

Figure 3.5: Scanning electron microscope microphotograph of *Microcystis aeruginosa*.

3.1.2.2 Cyclotella meneghinia

Cyclotella meneghinia is classified as a diatom, consisting of centric cells with a diameter of 3 – 5 µm. The *C. meneghinia* was cultured in vitro for this study. Figure 3.6 shows a light microscope microphotograph taken at 280 times magnification of the *C. meneghinia* culture.

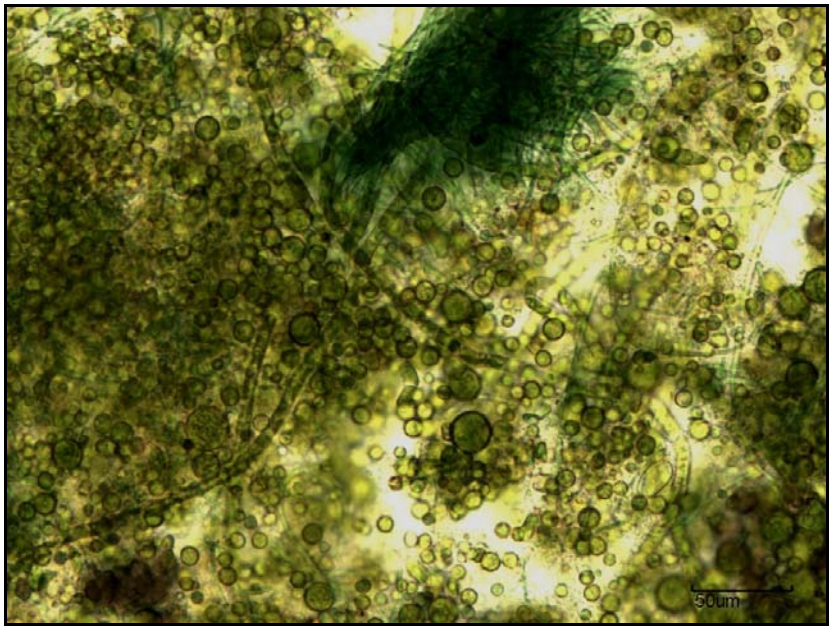

Figure 3.6: Light microscope microphotograph picture of *Cyclotella meneghinia* culture.

3.1.2.3 Nitzschia pusilla

Cells of *Nitzschia pusilla* occur apart from each other and are usually highly elongated, have rounded poles and are symmetrical. Figure 3.7 shows a light microscope microphotograph of the *N. pusilla* culture taken at 280 times magnification.

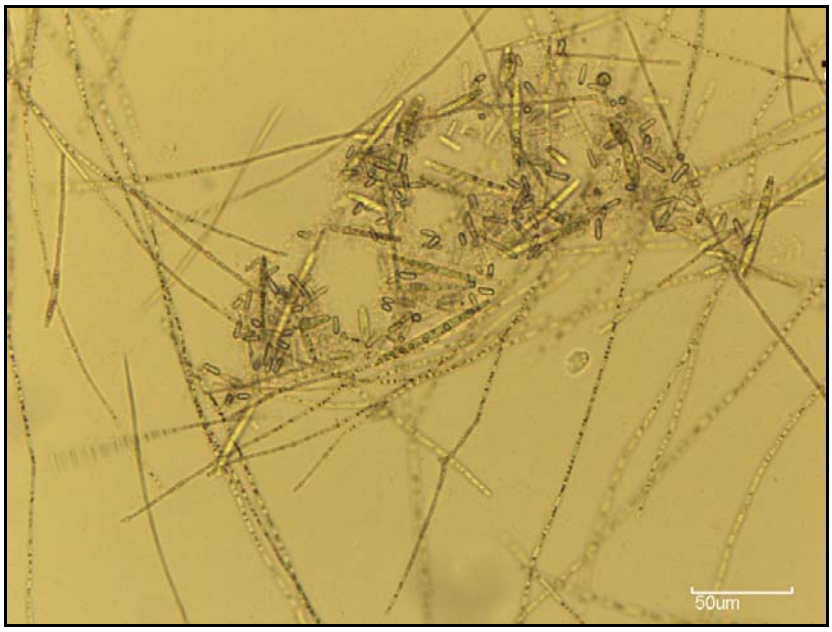

Figure 3.7: Light microscope microphotograph of *Nitzschia pusilla* culture.

3.2 Cultivation and preparation of algae

In this section the cultivation and preparation of the algae is discussed. In Section 3.2.1 the procedure that was followed to cultivate the *C. meneghinia* and *N. pusilla* is discussed, whereas Section 3.2.2 describes the sample preparation carried out prior to the thermochemical liquefaction experiments.

3.2.1 Cultivation

A modified BG-11 medium was used to cultivate the *C. meneghinia* and *N. pusilla*. The medium was aerated by using aquarium air pumps in order to introduce the carbon dioxide required by the algae for reproduction. Table 3.2 gives the composition of the modified BG-11 medium (Krüger, 1978: 7).

Table 3.2: Composition of modified BG-11 medium.

Compound	**Concentration (g.L^{-1})**
$NaNO_3$	1.5
K_2HPO_4	0.04
Na_2CO_3	0.02
$MgSO_4.7H_2O$	0.075
$CaCl_2.2H_2O$	0.036
$Na_2SiO_3.9H_2O$	0.058
EDTA (disodium magnesium salt)	0.001
Citric acid	0.012
$FeSO_4$	0.006
Trace-metal mix (1 mL.L^{-1})	
H_3BO_3	2.86
$MnCl_2.4H_2O$	1.81
$ZnSO_4.7H_2O$	0.022
$Na_2MoO_4.2H_2O$	0.391
$CuSO_4.5H_2O$	0.079
$Co(NO_3)_2.6H_2O$	0.0494

The *C. meneghinia* and *N. pusilla* were obtained from the School of Environmental Sciences and Development at the Potchefstroom campus of the North-West University. Prior to inoculation of the algae in the various Erlenmeyer flasks, the

flasks were sterilized for 2 hours at 139 °C in a vertical steam sterilizer to ensure that the Erlenmeyer flasks contained no contaminants.

The algae were inoculated in 1L Erlenmeyer flasks with 500 mL medium and left to grow for 2 weeks in order to obtain sufficient amounts of algae for the inoculation of the 5L Erlenmeyer flasks. The 1L Erlenmeyer flasks were also aerated. After the 2 week period, the cultures in the 1L Erlenmeyer flasks were used as inoculum for the 5L Erlenmeyer flasks. The 5L Erlenmeyer flasks contained 4L medium for the cultivation of the algae. During the cultivation of the algae, the Erlenmeyer flasks were kept in the same room. This room did not receive any direct sunlight in order to prevent the temperature of the medium to become too hot, which hinders the cultivation of the algae. The algae were cultivated for at least 2 months in the 5L Erlenmeyer flasks. In order to illustrate the increase in biomass as the cultivation process continued, Figure 3.8 shows a photo of *C. meneghinia* after it was inoculated and Figure 3.9 shows a photo of the *C. meneghinia* after 9 days of cultivation.

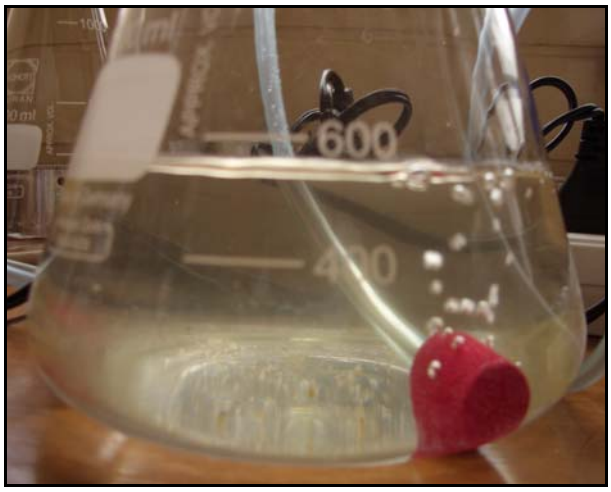

Figure 3.8: *Cyclotella meneghinia* after inoculation.

Figure 3.9: *Cyclotella meneghinia* after 9 days of cultivation.

3.2.2 Sample preparation

It is necessary to prepare the algae for the experiments. The preparation includes drying, milling and sampling of the algae. The algae were dried at 100 °C for approximately 12 hours prior to use. The dried algae were ground in a porcelain pestle and mortar to obtain an even size distribution. In order to obtain a representative sample for the thermochemical liquefaction experiments, the method of coning and quartering was used as described by Patnaik (2004: 19 – 20). Figure 3.10 shows how the process of coning and quartering is done.

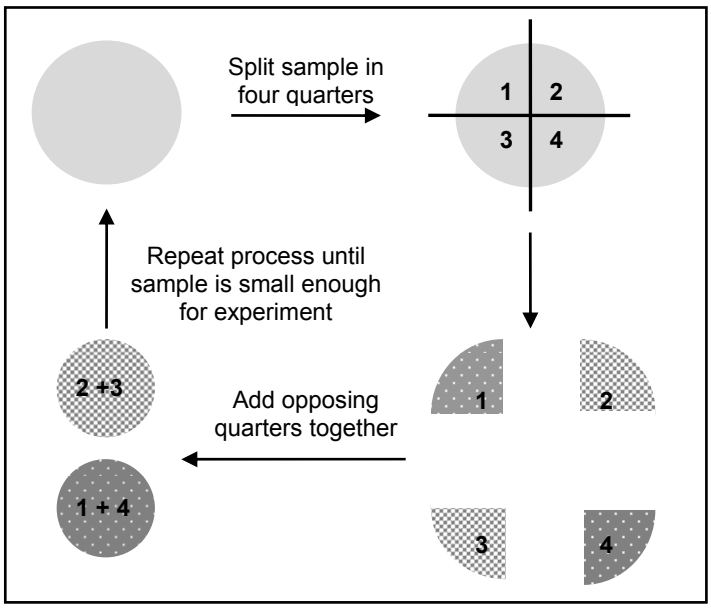

Figure 3.10: Coning and quartering process.

The algae is poured into a cone and flattened. The circular layer of material is then quartered and the alternate quarters are added together to form a new cone. The process is continued until a small enough sample size is obtained.

3.3 Thermochemical liquefaction experiments

In this section the procedure that was followed to conduct the thermochemical liquefaction experiments are discussed as well as the equipment that was used. In Section 3.3.1 the apparatus that was used, is described and a description of the experimental procedure is given. Section 3.3.2 describes the purification steps that were followed to purify the algal oil. In Section 3.3.3 the evaluation of the energy aspects of thermochemical liquefaction is discussed.

3.3.1 Apparatus and description

The thermochemical liquefaction experiments were conducted in a standard high pressure autoclave (Sawayama *et al.,* 1995: 731; Dote *et al.,* 1996: 492; Yang *et al.,* 2004: 24; Dote *et al.,* 1991: 56). The autoclave is constructed from grade 316 stainless steel. A detailed description of the mechanical design of the autoclave is given in Appendix C. Figures 3.11 and 3.12 show three-dimensional representations of the closed and expanded autoclave, respectively. In Table 3.3 the dimensions of the autoclave chamber are given.

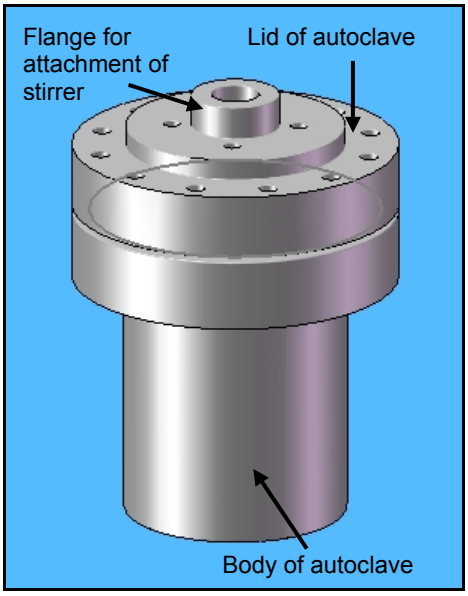

Figure 3.11: Three-dimensional representation of closed autoclave.

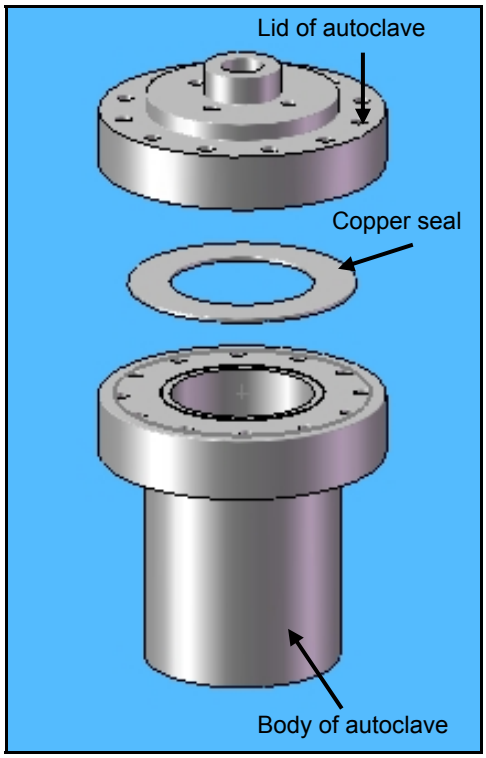

Figure 3.12: Three-dimensional representation of expanded autoclave.

Table 3.3: Dimensions of autoclave chamber.

Dimension	Value
Inside diameter (mm)	90
Length (mm)	150
Volume (mm^3)	954
Volume (L)	0.954

A schematic representation of the experimental setup can be seen in Figure 3.13 as well as a photo of the experimental setup in Figure 3.14.

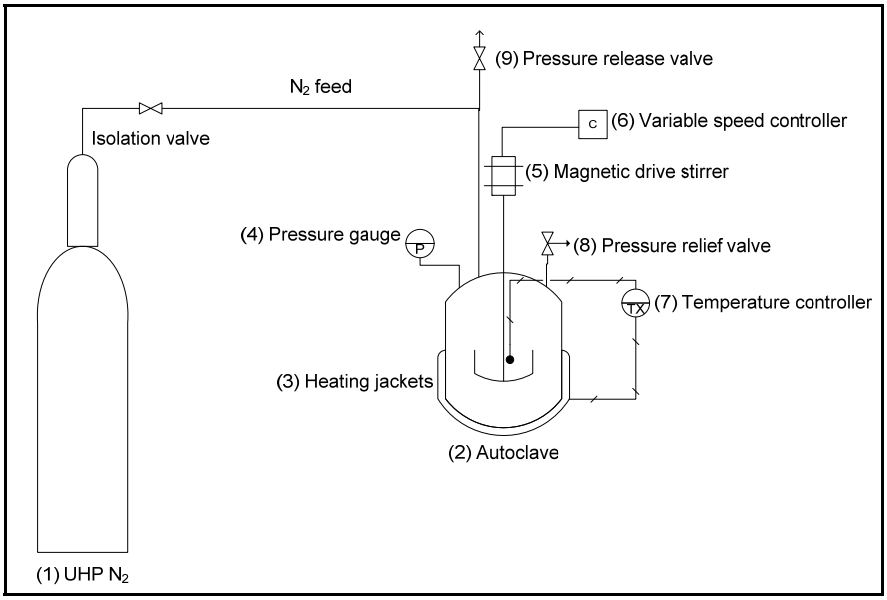

Figure 3.13: Schematic representation of the experimental setup.

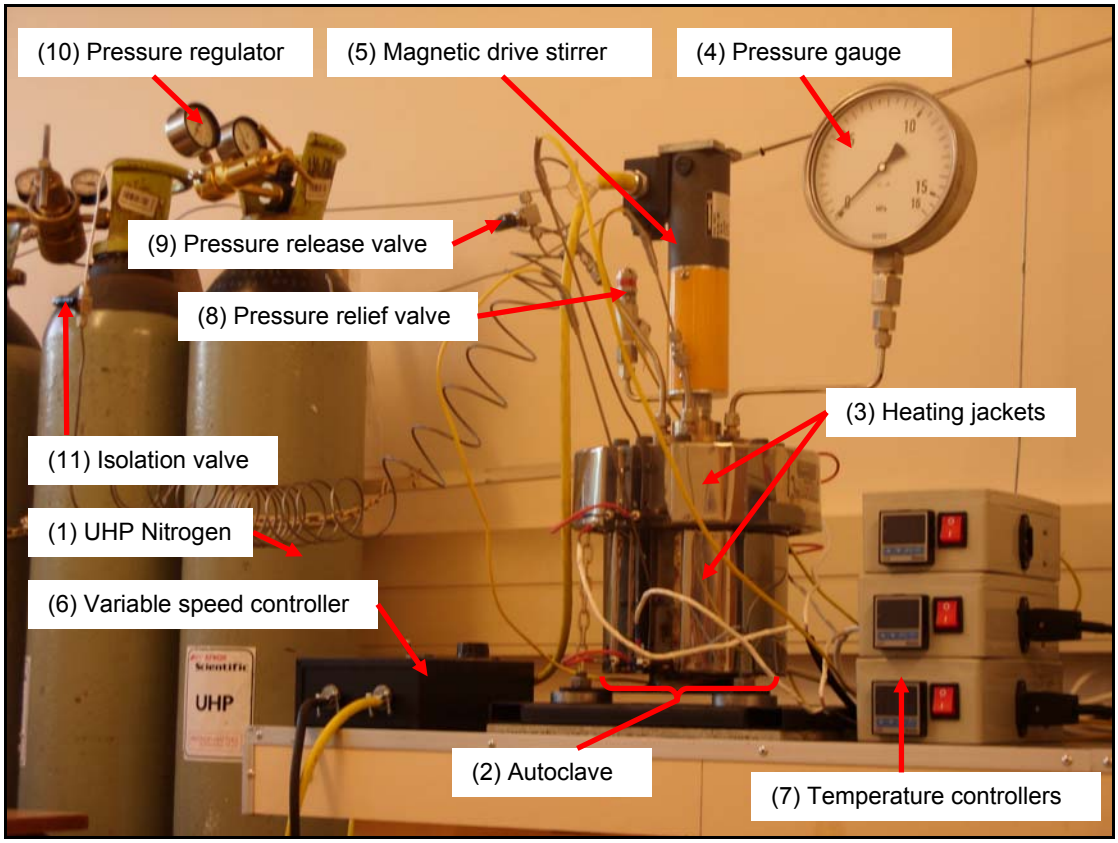

Figure 3.14: Experimental setup.

The autoclave (2) was charged with 3 grams algae, 500 mL water and varying amounts of sodium carbonate as catalyst. The removable top plate of the autoclave was fastened in place and the residual air was purged from the autoclave by ultra

high purity (UHP) nitrogen (1) for 10 minutes. The pressure release valve (9) and isolation valve (11) were closed before the experiment was started.

The temperature of the autoclave was increased up to the required operating temperature by the heating jackets (3) (one for the main body of the autoclave and another for the end plate of the autoclave) which were controlled by temperature controllers (7). The reaction temperature was held constant for the duration of the chosen reaction time and the heating time of the autoclave was kept constant at 2 hours. At the initiation of the experiment, the magnetic drive stirrer (5) was switched on and set to 750 rpm (30% of its maximum speed) by the variable speed controller (6).

The pressure in the autoclave is obtained by the vaporization of the water according to the vapour-liquid equilibrium and is therefore dependent on the reaction temperature. The pressure inside the autoclave was measured with a pressure gauge (4). A pressure relief valve (8) was also fitted to the autoclave to ensure that the pressure of the autoclave stayed within the design limits.

After the experiment was completed, the heating jackets (3) were removed from the autoclave (2) and the autoclave was allowed to cool down to room temperature. An electrical fan was used to assist in the cooling of the autoclave. The pressure release valve (9) was opened to release the pressure in the autoclave (2), which builds up due to gas formation after an experiment was completed. Chloroform (100 mL) was added to the reaction mixture after it had cooled down to room temperature and stirred inside the autoclave for 10 minutes to ensure that any oil that may be fixed to the inside of the autoclave was dissolved. The mixture was then filtered under a vacuum with Whatman No. 31 filter paper to remove any solid residue. The filtrate was then poured into a separation funnel to allow the mixture to settle out into an aqueous and an organic layer, which contains the algal oil. The aqueous and organic layers obtained for a typical experiment can be seen in Figure 3.15.

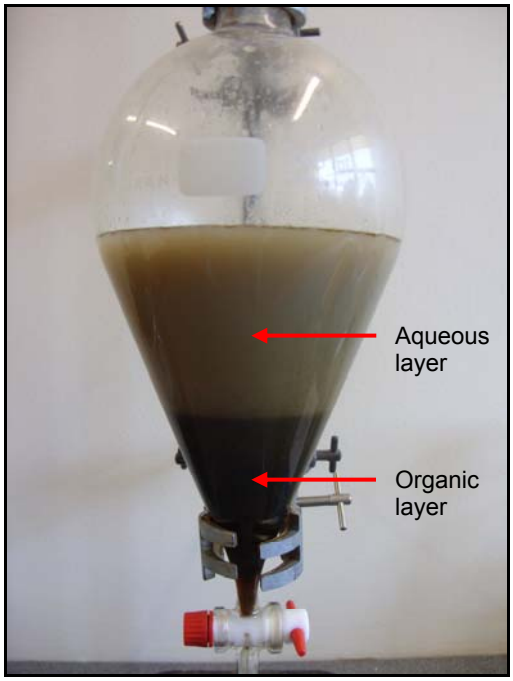

Figure 3.15: Aqueous and organic layers.

In order to identify the most significant operating conditions that influence the process of thermochemical liquefaction, a literature study was conducted. Section 2.4.6 provides a full account of the literature study. The literature study identified the reaction temperature, residence time, catalyst load and the liquefaction solvent as the operating conditions which have the largest influence on thermochemical liquefaction. Matsui and co-workers (1997: 1046), however, identified water to be the best liquefaction solvent for micro-algae. Therefore the effect of the reaction temperature, residence time and catalyst load on thermochemical liquefaction were studied.

In order to determine the range of the each of the operating conditions an in depth literature study, as given in Section 2.4.6, was conducted to study the theoretical effect of these conditions on the process of thermochemical liquefaction. Previous studies conducted on the thermochemical liquefaction of algae showed that the optimum reaction temperature for the liquefaction of *Botryococcus braunii* was 300 °C (Dote *et al.,* 1994: 1855), whereas the liquefaction of *Microcystis viridis* was at an optimum at 340 °C (Yang *et al.,* 2004: 32). These respective maxima were obtained with a sodium carbonate catalyst load of 5 wt% (Dote *et al.,* 1994: 1855; Yang *et al.,* 2004: 32). Therefore, the influence of the catalyst load was studied around the centre point of 5 wt%, whereas the reaction temperature was studied around the

centre point of 300 °C. The studies conducted previously on the thermochemical liquefaction of algae varied the residence time from 5 min to a maximum of 2 hours (Dote *et al.,* 1994: 1855; Minowa *et al.,* 1995: 1737; Matsui *et al.,* 1997: 1045; Yang *et al.,* 2004: 26). Yang and co-workers (2004: 26), however, found that thermochemical liquefaction of *M. viridis* was almost complete within a reaction time of 30 min. Due to these findings, the influence of residence time on the thermochemical liquefaction process was evaluated around the centre point of 30 min.

A central composite design (CCD) was used to determine the influence of these parameters on the thermochemical liquefaction process. In Appendix B the CCD is discussed in depth. A CCD has the ability to evaluate the influence of the parameters individually as well as the influence of their interaction with each other. Design-Expert® Version 7.1.5, a powerful statistical software package, was used in the configuration and evaluation of the CCD. Table 3.4 states the limits of the operating conditions used in the CCD and Table 3.5 lists the CCD experiments.

Table 3.4: Limits of operating conditions used in the CCD.

Operating condition	**Lower limit**	**Centre point**	**Upper limit**
Operating Temperature (°C)	260	300	340
Residence Time (min)	15	30	45
Catalyst load (wt%)	0	5	10

Table 3.5: CCD experiments.

Run	Operating Temperature (°C)	Catalyst load (wt%)	Residence Time (min)
1	260	10	45
2	340	10	45
3	260	0	15
4	300	5	30
5	260	10	15
6	340	0	45
7	260	0	45
8	300	5	30
9	300	5	30
10	340	10	15
11	340	5	30
12	300	5	30
13	300	5	45
14	300	10	30
15	300	5	30
16	260	5	30
17	300	0	30
18	340	0	15
19	300	5	30
20	300	5	15

3.3.2 Purification of algal oil

The organic layer, which contained the dissolved algal oil, obtained from decantation was subjected to vacuum distillation in order to obtain the pure algal oil. The vacuum distillation was carried out at a temperature of 70 °C to ensure total evaporation of the chloroform (see Figure 3.16).

The vacuum distillation was carried out in an oil bath (1), with a magnetic stirrer hotplate (2). A vacuum trap (3) was used to protect the vacuum pump (4) from any liquids that may enter. The temperature of the oil bath was monitored by a thermocouple (5) and controlled at 70 °C by a temperature controller (6). A cold trap (7) filled with ice water was used to ensure condensation of the chloroform. Figure 3.16 shows a picture of the vacuum distillation setup.

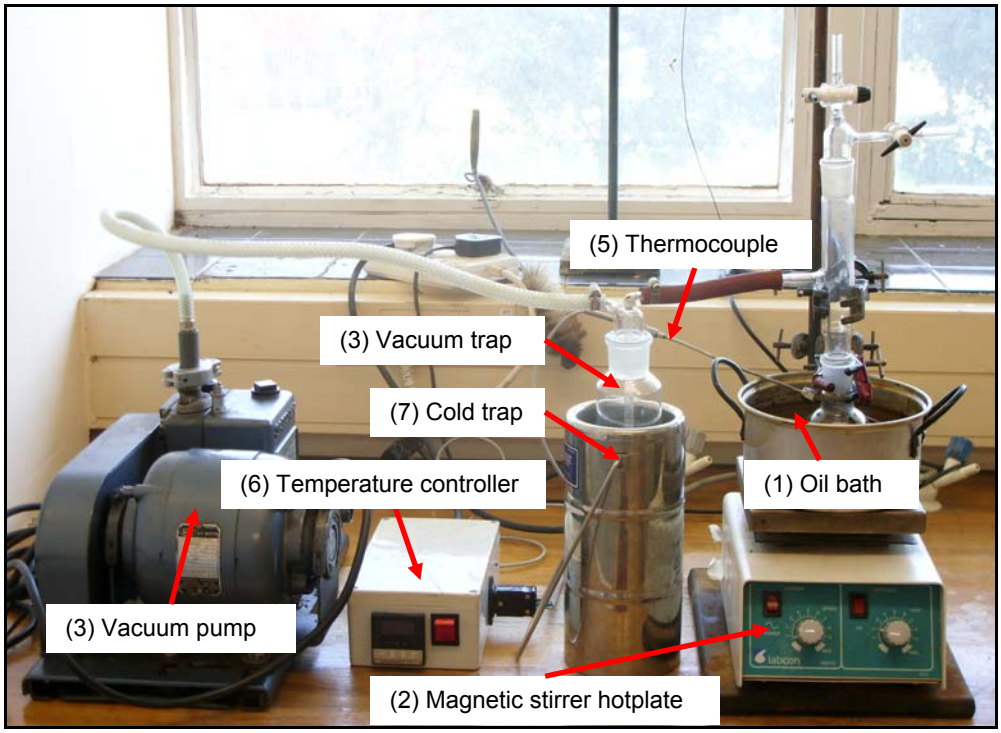

Figure 3.16: Picture of vacuum distillation setup.

3.3.3 Evaluation of energy aspects of thermochemical liquefaction

In order to determine the energy requirements for thermochemical liquefaction, a device was used to determine the amount of the current used during the experiment. The energy requirements of the thermochemical liquefaction process was determined at a reaction temperature of 300 °C, a catalyst load of 5 wt%, residence time of 30 minutes and 3 grams of *M. aeruginosa* algae. Figure 3.17 depicts the apparatus that was used to determine the current, while Figure 3.18 shows a photo of the instrument used to obtain a digital output.

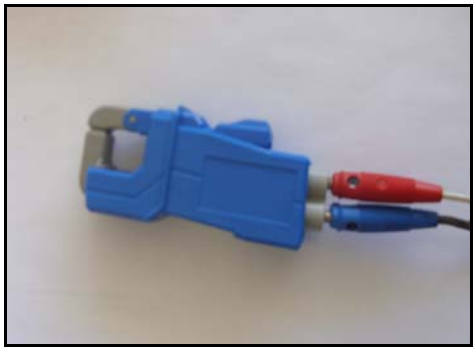

Figure 3.17: Ampere meter.

Figure 3.18: Multimeter used to obtain digital output.

In order to evaluate the energy efficiency of the process, the energy consumption ratio was used. The ECR (energy consumption ratio) is defined as follows:

$$ECR = \frac{Energy\ required\ to\ maintain\ the\ reaction\ temperature}{Available\ energy\ \ from\ the\ oil\ \ produced}$$

3.4 Analytical equipment and methodology

In this section a description is given regarding the analytical equipment that was used in this study. In Section 3.4.1 a discussion is given about the bomb calorimeter. Section 3.4.2 describes the use of the elemental analyzer, whereas Section 3.4.3 provides a description of the gas chromatograph and the procedure that was followed to obtain the results.

3.4.1 Bomb Calorimeter

The calorific value of the algae was determined with a MC-1000, Mk 2 Modular Calorimeter. The calorimeter ignites the loaded sample under an oxygen atmosphere. After ignition of the sample, the temperature increase is measured and converted by the relevant computer software into the energy content (MJ) per kilogram of sample. In order to determine the calorific value of the dried algae, a representative sample of the algae was loaded into the bomb calorimeter. The sample weight ranged between 0.5 and 1 gram. Figure 3.19 shows the bomb calorimeter.

Figure 3.19: Bomb calorimeter.

3.4.2 Elemental analysis

A sample was taken of the algal oil obtained from vacuum distillation. The mass of the sample varied between 50 and 100 mg. The sample was used for the determination of the carbon, hydrogen, nitrogen, sulphur and oxygen content of the algal oil. The elemental analysis was conducted with an elemental analyzer. Section 3.4.2.1 describes the elemental analyzer that was used to determine the elemental analysis.

3.4.2.1 Elemental analyzer

The samples were analyzed by a FLASH 2000 Organic Elemental Analyzer. The elemental analyzer determined the weight percentage of carbon, nitrogen, hydrogen and sulphur in the oil. The oxygen content of the oil was determined by difference. Figure 3.20 shows a picture of the elemental analyzer.

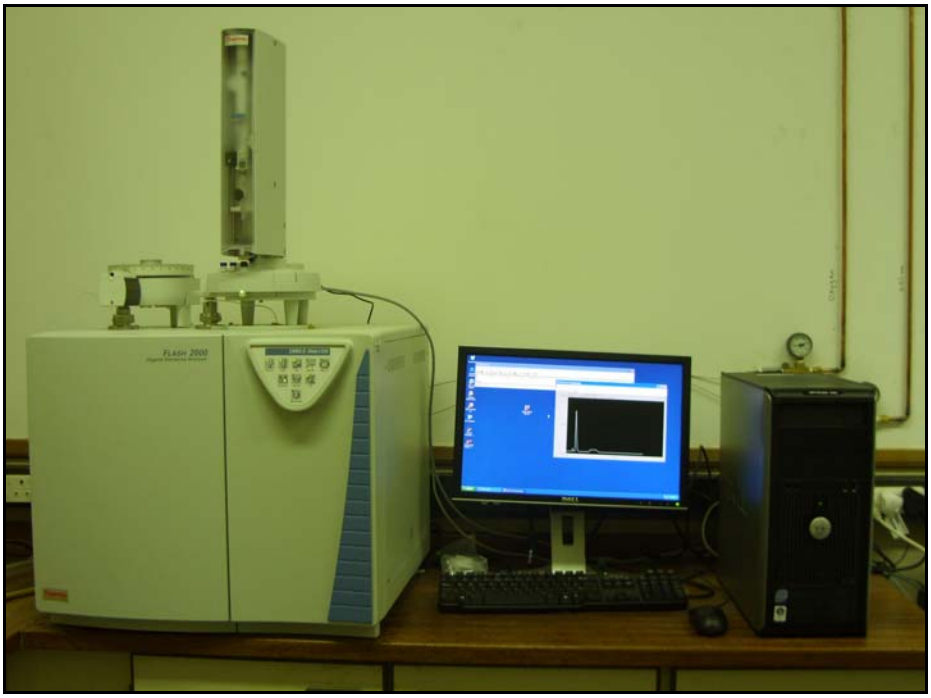

Figure 3.20: Elemental analyzer.

3.4.3 Gas chromatography

Gas chromatography is an analytical technique used to determine the composition of the algal oil. In section 3.4.3.1 a description of the gas chromatograph, the apparatus used to perform gas chromatography, is given. Section 3.4.3.2 discusses the procedure that was followed in order to prepare the sample for injection on the gas chromatograph.

3.4.3.1 Gas chromatograph

The samples were analyzed by an Agilent 7890 gas chromatograph (GC), equipped with an Agilent 7683B autoinjector, HP-5 capillary column (30m x 320 µm x 0.25 µm) and a flame ionization detector (FID). Gas chromatography enabled the determination of the composition of the oil. The gas chromatograph (1) with the autoinjector (2) is shown in Figure 3.21.

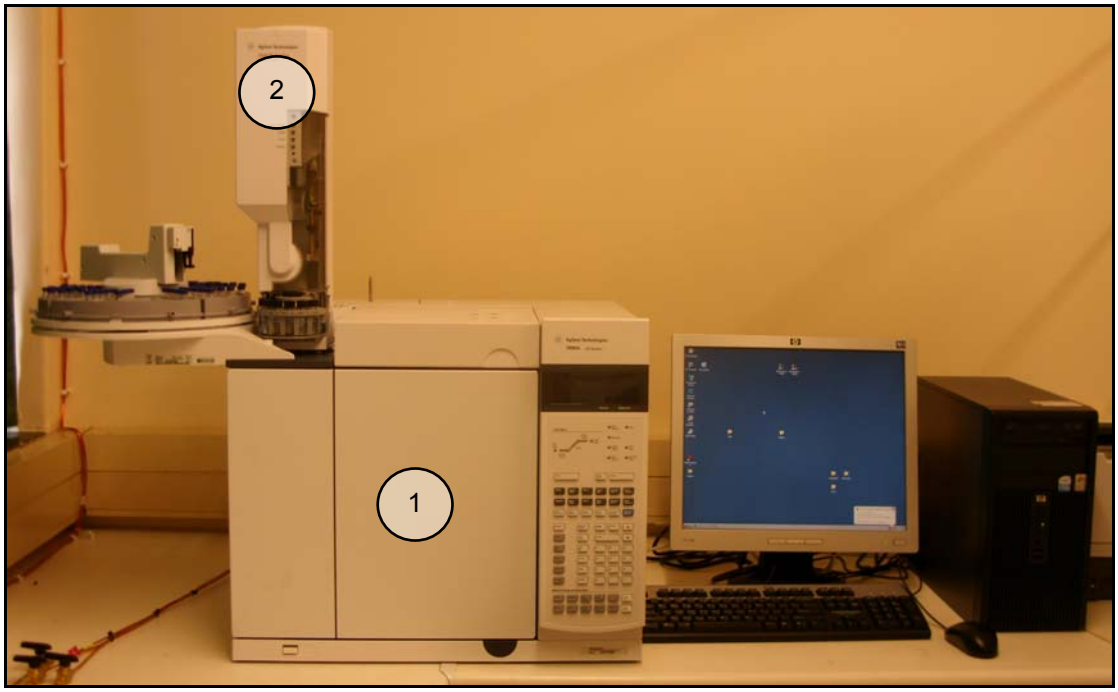

Figure 3.21: Gas chromatograph with auto-injector.

The GC analysis conditions were: inlet temperature of 275 °C; injection volume of 0.2 µL (auto injection); oven programming of 90 °C for 4 min, 90 to 300 °C at 10 °C.min^{-1}, 300 °C for 20 min; FID detector at 350 °C; H_2 flow rate of 40 mL.min^{-1}, make-up He flow rate of 10 mL.min^{-1} and air flow rate of 400 mL.min^{-1}.

3.4.3.2 Sample preparation for gas chromatography

For analysis on the GC, the oil must be dissolved in a suitable solvent. In Appendix A chloroform was identified as the best solvent for the dissolution of the algal oil. In order to quantify the components of the algal oil, an external standard is required. For the purpose of this study, decanoic acid was chosen. The calibration of the gas chromatograph and choice of external standard is discussed in Appendix D.

A standard solution of 5 g.L^{-1} decanoic acid in chloroform was prepared. The oil obtained from vacuum distillation was dissolved in 10 mL of the standard solution. In order for the GC to detect the components of the algal oils, the fatty acids must be methylated to their associate methyl esters. Trimethyl Sulfonium Hydroxide (TMSH) was identified as derivatization agent due to its ability to methylate the fatty acids in a single step.

The derivatization process was completed in a 1 mL micro centrifuge tube. 100 µL of the dissolved oil was introduced into the micro centrifuge tube and 100 µL of the TMSH was added. The resulting mixture was vortexed at room temperature for 5 min. The content of the micro centrifuge tube was transferred to a GC vial and then injected onto the GC for analysis.

3.5 References

Anonymous. 2009a. http://www.familytravelsa.co.za/. Date of access: 7 April 2009.

Anonymous. 2009b. http://www.stayinsouthafrica.co.za/northwest.htm. Date of access: 7 April 2009.

Department of Water Affairs and Forestry ***see*** South Africa. Department of Water Affairs and Forestry.

Dote, Y., Sawayama, S., Inoue, S., Minowa, T. & Yokoyama, S. 1994. Recovery of liquid fuel from hydrocarbon-rich microalgae by thermochemical liquefaction. Fuel, 73(12): 1855 – 1857.

Dote, Y., Inoue, S., Ogi, T. & Yokoyama, S. 1996. Studies on the direct liquefaction of protein-contained biomass: The distribution of nitrogen in the products. Biomass and Bioenergy, 11(6): 491 – 498.

Dote, Y., Yokoyama, S., Ogi, T., Minowa, T. & Murakami, M. 1991. Liquefaction of barley stillage and upgrading of primary oil. Biomass and Bioenergy, 1(1): 55 – 60.

Krüger, G.H.J. 1978. The effect of physico-chemical factors on growth relevant to the mass culture of mycrocystis under sterile conditions. Bloemfontein: UFS. (Thesis – Ph.D). 134 p.

Matsui, T., Nishihara, A., Ueda, C., Ohtsuki, M., Ikenaga, N. & Suzuki, T. 1997. Liquefaction of micro-algae with iron catalyst. Fuel, 76(11): 1043 – 1048.

Minowa, T., Yokoyama, S., Kishimoto, M. & Okakura, T. 1995. Oil production from algal cells of Dunaliella tertiolecta by direct thermochemical liquefaction. Fuel, 74(12): 1735 – 1738.

NSPU (National Scientific Programmes Unit, South Africa). 1985. The Limnology of Hartbeespoort Dam. Report 110. 279 p.

Patnaik, P. 2004. Dean's analytical chemistry handbook. 2nd edition. New York: McGraw-Hill. 1193 p.

Sawayama, S., Inoue, S., Dote, Y. & Yokoyama, S. 1995. CO_2 fixation and oil production through microalga. Energy Conversion Management, 36(6-9): 729 – 731.

South-Africa. Department of Water Affairs and Forestry. 2005. Dam remediation: Hartbeespoort Dam. 16p.

Yang, Y.F., Feng, C.P., Inamori, Y. & Maekawa, T. 2004. Analysis of energy conversion characteristics in liquefaction of algae. Resources, Conservation and Recycling, 43: 21 – 33.

Chapter 4. – Results and Discussion

This chapter provides a detailed description of all the results obtained from the cultivation of *Cyclotella meneghinia* and *Nitzschia pusilla* as well as thermochemical liquefaction experiments conducted on *Microcystis aeruginosa, C. meneghinia* and *N. pusilla*. The cultivation of the algae is discussed in Section 4.1. In Section 4.2 the results that were obtained from the thermochemical liquefaction experiments are discussed.

4.1 Cultivation of algae

In this section the results that were obtained from the cultivation of *C. meneghinia* (Section 4.1.1) and the cultivation of *N. pusilla* (Section 4.1.2) microalgae are discussed. The *M. aeruginosa* was collected from the Hartebeespoort dam as discussed in Section 3.1.2.1.

4.1.1 Cultivation of *Cyclotella meneghinia*

The *Cyclotella meneghinia* was cultivated for a period of two months before it was harvested. On average the *C. meneghinia* produced 0.45 grams of dried algal biomass per liter of algal medium. The culture could, however, not be kept homogenous and some contamination occurred. The *C. meneghinia* was contaminated with the blue-green algae *Phormidium* sp. and *Cylindrospermopsis* sp. The culture also contained the cyanobacterium *Synechocystis* sp. and some zooplankton. Figure 4.1 shows a light microscope microphotograph of the *C. meneghinia* culture at 280 times magnification that was obtained after culturing. In Figure 4.1 it is clearly visible that *C. meneghinia* is not the only algal culture in the medium.

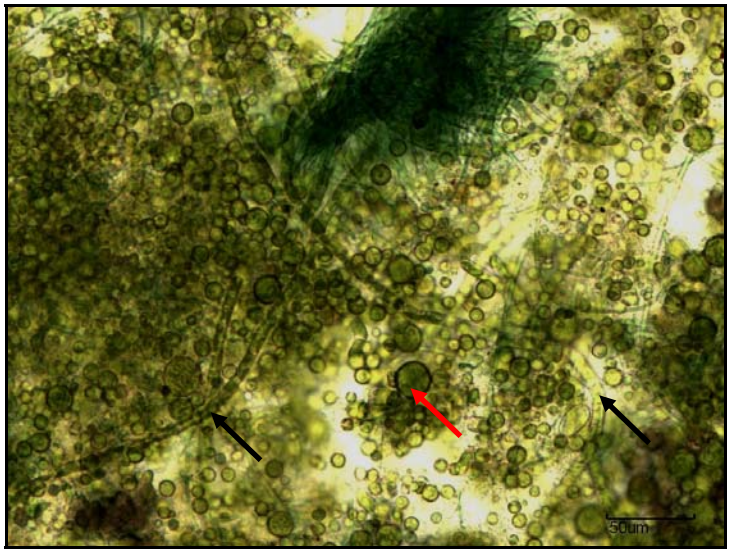

Figure 4.1: Light microscope microphotograph of *Cyclotella meneghinia* culture.

(→ Cyclotella meneghinia cells, → Intruder cells)

4.1.2 Cultivation of *Nitzschia pusilla*

The *Nitzschia pusilla* was cultivated for a period of three months before it was harvested. On average the *N. pusilla* produced 0.56 grams of dried algal biomass per liter of algal medium. As was the case for the *C. meneghinia,* the culture could not be kept homogenous and some contamination occurred. The *N. pusilla* was contaminated with the blue-green algae *Phormidium* sp. and *Cylindrospermopsis* sp. The culture also contained the cyanobacterium *Synechocystis* sp. Figure 4.2 shows a light microscope microphotograph of the *N. pusilla* culture at 280 times magnification that was obtained after culturing. Figure 4.2 shows that *N. pusilla* is not the only algal culture in the medium.

Figure 4.2: Light microscope microphotograph of *Nitzschia pusilla* culture.

(→ Nitzschia pusilla cells, → Intruder cells)

4.2 Thermochemical liquefaction

In this section the results that were obtained from the thermochemical liquefaction experiments that were conducted on *M. aeruginosa, C. meneghinia* and *N. pusilla* are discussed. Section 4.2.1 evaluates the experimental error of the thermochemical liquefaction process.

In Sections 4.2.2, 4.2.3 and 4.2.4 the influence of the reaction temperature, catalyst load and residence time on the process of thermochemical liquefaction is discussed. Section 4.2.5 describes the influence of the interaction that occurs between the manipulated variables on thermochemical liquefaction. The elemental analyses of the extracted oils are discussed in Section 4.2.6 and the energy aspects of thermochemical liquefaction are evaluated in Section 4.2.7. In Section 4.2.8 a summary is given of the results that were obtained from the thermochemical liquefaction experiments.

4.2.1 Experimental error

In order to determine the experimental error for the thermochemical liquefaction process, an experiment was repeated six times with identical operating conditions. Table 4.1 gives the operating conditions for the experiments that were used to determine the experimental error.

Table 4.1: Operating conditions for experimental error experiments.

Operating condition	Value
Reaction Temperature (°C)	300
Catalyst Load (wt%)	5
Residence time (min)	30

The experimental error was determined for a 95% confidence interval (assuming a normal distribution of yield values). Appendix E provides a detailed description of the calculations of the experimental error. The experimental error was calculated to be 8.1% for the oil yield and 28.8% for the determination of the oil composition. The experimental error obtained for the determination of the oil yield suggests the process produces consistent yields of oil. The error observed for the determination of the oil composition may be attributed to the heterogeneity of the algae. No reference has been made to the experimental error of previous studies conducted on the thermochemical liquefaction of algae.

The experimental errors were also determined for the bomb calorimeter and the elemental analyzer. The experimental error of the bomb calorimeter was determined by analyzing a sample 3 times, whereas for the elemental analyzer a sample was analyzed 5 times. Appendix E provides a detailed description of the experimental error calculations of the bomb calorimeter and experimental analyzer. The bomb calorimeter produced an error of 0.094%, while the elemental analyzer produced an error of 3.03%.

4.2.2 The influence of reaction temperature on thermochemical liquefaction

The influence of the reaction temperature on thermochemical liquefaction was studied for the liquefaction of *M. aeruginosa, C. meneghinia and N. pusilla*. The effect of reaction temperature on the liquefaction of *M. aeruginosa, C. meneghinia and N. pusilla* is given in Figure 4.3.

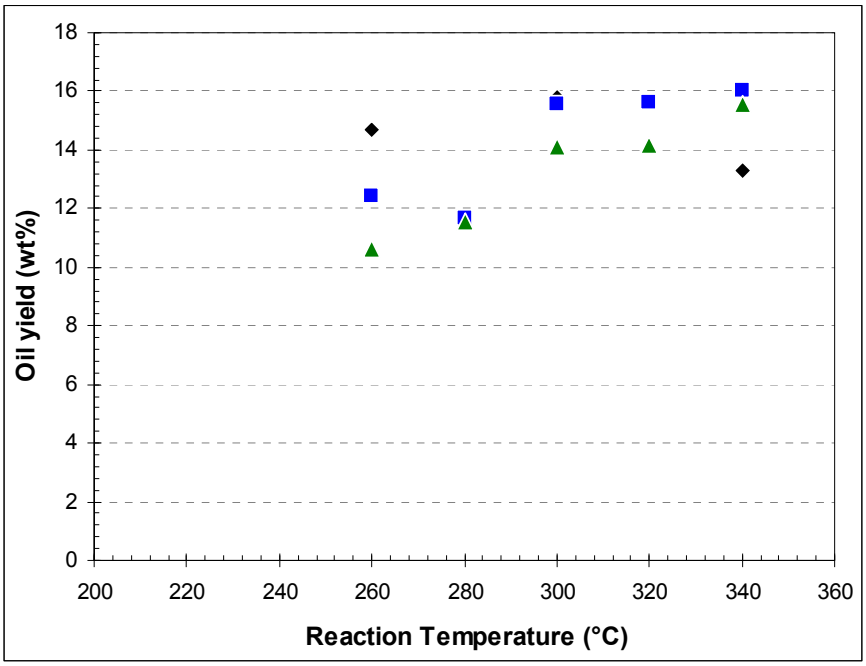

Figure 4.3: Influence of reaction temperature on oil yield by thermochemical liquefaction.
(♦ *Microcystis aeruginosa*; ▲ *Nitzschia pusilla*; ■ *Cyclotella meneghinia*)
(Catalyst load = 5 wt%; Residence Time = 30 minutes)

Figure 4.3 shows an increase in the oil yield with a corresponding increase in the reaction temperature. Thermochemical liquefaction occurs due to free radical formation as discussed in Section 2.4.4. The reaction temperature influences the rate of free radical formation. At high reaction temperatures, free radicals are formed more rapidly; which, in the absence of sufficient hydrogen-shuttling, results in repolymerization reactions.

The elemental analysis of the algal biomass indicated that *M. aeruginosa* (6.47 wt%) had a smaller hydrogen content than *C. meneghinia* (6.54 wt%) and *N. pusilla* (6.71 wt%). Although the difference in the hydrogen content is relatively small, it remains significant in comparison with the oil yield obtained. The higher hydrogen content of *C. meneghinia* and *N. pusilla* provides an explanation for the trend that was observed for these algae. These algae contain sufficient hydrogen to stabilize the free radicals that are formed at high temperatures thereby preventing repolimerization and thus a continued increase in oil yield is observed with an increase in reaction temperature. Yang and co-workers (2004: 26) observed the same trend for the liquefaction of *Microcystis viridis*.

Figure 4.3 indicates that the liquefaction of *M. aeruginosa* produces maximal oil yield at 300 °C. An increase in the reaction temperature to 340 °C produces a decrease in the oil yield. The lower hydrogen content of *M. aeruginosa* provides an explanation for this phenomenon. The hydrogen content of the *M. aeruginosa* is not sufficient for hydrogen-shuttling to stabilize the free radicals that form at 340 °C, which results in repolymerization reactions and a corresponding decrease in the oil yield. Studies conducted on the thermochemical liquefaction of *Botryococcus braunii* produced the same trend as was observed for the *M. aeruginosa* and produced a maximum oil yield at 300 °C (Dote *et al.,* 1994: 1856; Sawayama *et al.,* 1995: 730).

The hypothesis of the hydrogen shuttling is confirmed by previous work conducted on the thermochemical liquefaction of microalgae (Qu *et al.,* 2003: 600; Yan *et al.,* 1999: 139). Qu and co-workers (2003: 600) attributed the decrease of the oil yield at high reaction temperatures to the competition between hydrolysis and repolymerization reactions. Higher reaction temperatures benefit the repolymerization reactions and accelerate repolymerization, which decreases the oil yield (Qu *et al.,* 2003: 600). The repolymerization occurs in the presence of free radicals. Therefore Yan *et al.* (1999: 139) attributed the decrease in the oil yield at high reaction temperatures to the formation of free radicals. Yan and co-workers (1999: 139) found that higher reaction temperatures result in an increased rate of free radical formation. When a significant amount of free radicals are formed, more active hydrogen is required to stabilize them. If there is a deficiency in the active hydrogen, these free radicals undergo repolymerization, which in turn results in a decrease in the oil yield (Yan *et al.,* 1999: 139).

The influence of the reaction temperature on the composition of the extracted oil was also evaluated. Figure 4.4 shows the influence of the reaction temperature on the composition of the oil obtained from the liquefaction of *M. aeruginosa, C. meneghinia and N. pusilla*.

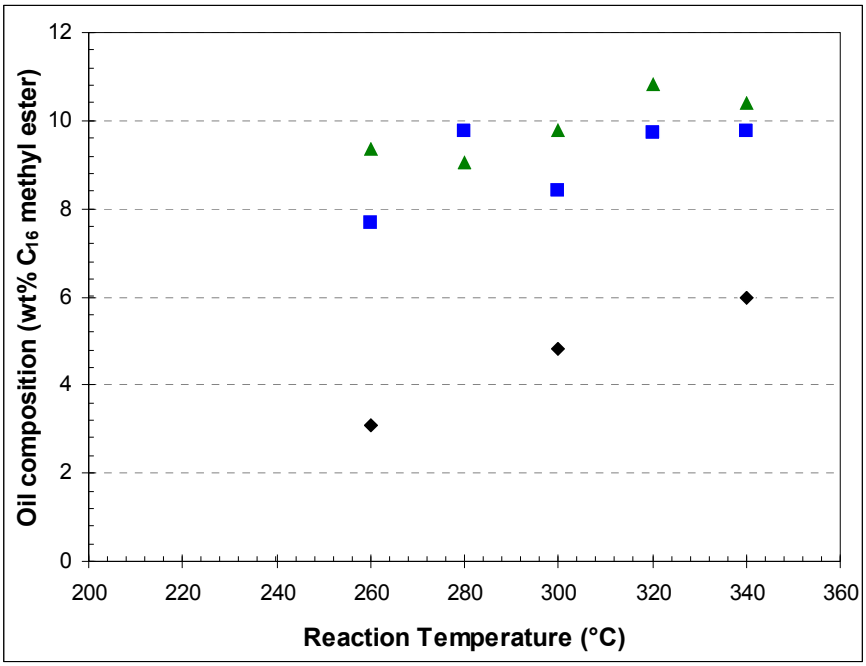

Figure 4.4: Influence of reaction temperature on oil composition by thermochemical liquefaction.

(♦ *Microcystis aeruginosa*; ▲ *Nitzschia pusilla*; ■ *Cyclotella meneghinia*)

(Catalyst load = 5 wt%; Residence Time = 30 minutes)

The experimental error obtained for the oil composition prevents any conclusions from being made on the influence of the reaction temperature on the composition of the oil. The trend of the data obtained from the thermochemical liquefaction experiments, however, indicates that an increase in the reaction temperature produces a higher C_{16} methyl ester content due to an increased rate of hydrolysis. These C_{16} esters are obtained prior to the exhaustion of the hydrogen and the formation of excess free radicals, which results in repolymerization reactions.

The trend observed in Figure 4.4 is confirmed by the data obtained from the central composite design, which is discussed in detail in Appendix B.2. The analysis of variance (ANOVA) of the oil composition indicated that the reaction temperature is statistically significant at a 99% probability level and that an increase in the reaction temperature produces an increase in the C_{16} methyl ester content of the extracted oil.

4.2.3 The influence of catalyst load on thermochemical liquefaction

The literature study showed that sodium carbonate was the preferred catalyst for the thermochemical liquefaction of algae (Dote *et al.,* 1994 1855; Yang *et al.,* 2004: 21).

Therefore the influence of a sodium carbonate catalyst was evaluated in this study. Figure 4.5 shows the effect of the catalyst load on the oil yield at a reaction temperature of 300 °C and a residence time of 30 min for the liquefaction of *M. aeruginosa, C. meneghinia and N. pusilla*.

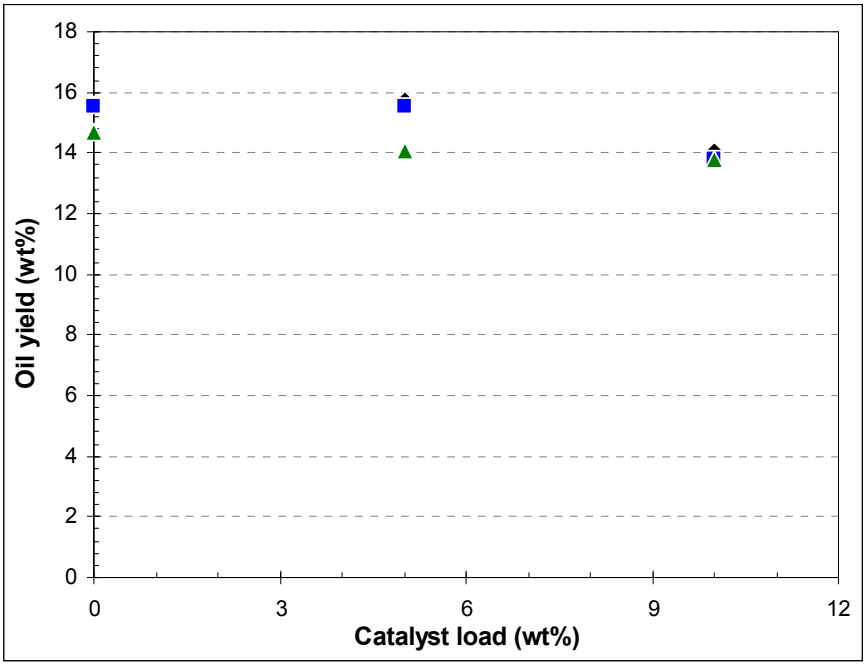

Figure 4.5: Influence of catalyst load on oil yield by thermochemical liquefaction.
(♦ *Microcystis aeruginosa*; ▲ *Nitzschia pusilla*; ■ *Cyclotella meneghinia*)
(Reaction Temperature = 300 °C; Residence Time = 30 minutes)

The trend of the data depicted in Figure 4.5 shows that the addition of a sodium carbonate catalyst has a negative effect on the oil yield for the liquefaction of *M. aeruginosa, C. meneghinia and N. pusilla*. The data obtained from the central composite design confirms the trend shown in Figure 4.5. The ANOVA of the oil yield, discussed in detail in Appendix B.2, indicates that the influence of the catalyst load on the oil yield is statistically significant at a 99% probability level. The oil yield ANOVA shows that an increase in the catalyst load produces a decrease in the oil yield.

The addition of a Na_2CO_3 catalyst produced an increase in the production of C_{16} esters in the oil. Figure 4.6 depicts the influence of the catalyst load on the oil composition at a reaction temperature of 300 °C and a residence time of 30 min for the liquefaction of *M. aeruginosa, C. meneghinia and N. pusilla*.

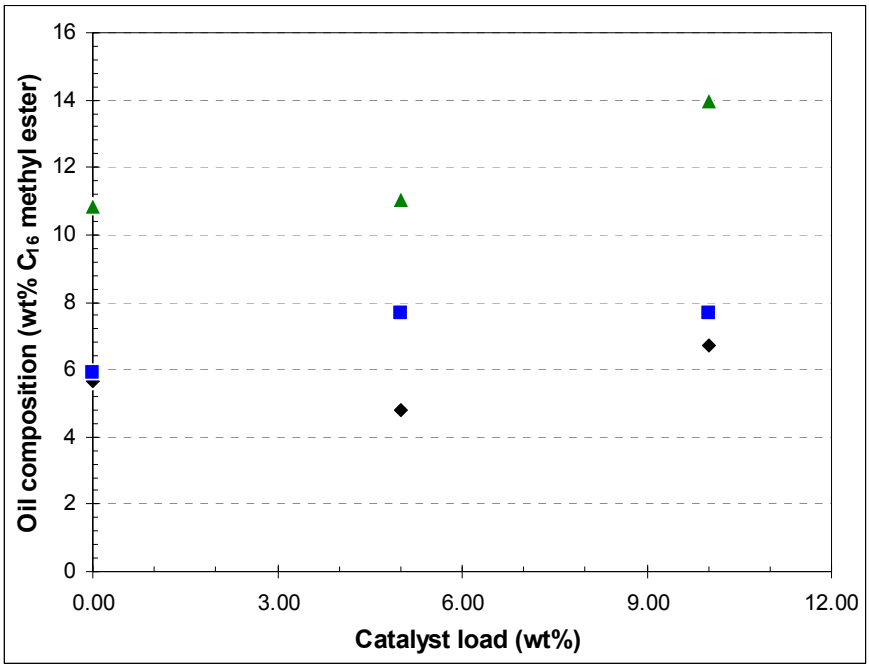

Figure 4.6: Influence of catalyst load on oil composition by thermochemical liquefaction.
(♦ *Microcystis aeruginosa*; ▲ *Nitzschia pusilla*; ■ *Cyclotella meneghinia*)
(Reaction Temperature = 300 °C; Residence Time = 30 minutes)

The experimental error for the oil composition prevents any conclusive remarks to be made on the influence of the catalyst load on the composition of the oil. In Figure 4.6 a trend can be observed with the increase of the catalyst load. The trend in Figure 4.6 shows that the addition of catalyst produces an increase in the C_{16} content of the oil obtained from the liquefaction of *M. aeruginosa, C. meneghinia and N. pusilla*. The ANOVA of the oil composition, discussed in detail in Appendix B.2, confirms the trend observed in Figure 4.6 and indicates that the influence of the catalyst load on the oil composition is statistically significant at a 95% probability level. The ANOVA also indicates that an increase in the catalyst load produces a corresponding increase in the C_{16} methyl ester content of the extracted oil.

The influence of Na_2CO_3 on the oil yield and oil composition may be explained in the light of the lipid content of the algae. The lipid composition of plant cells are dominated by three characteristic glyceroglycolipids and one phospholipid. These lipids comprise the main polar lipid component of plant cells and are enriched in monogalactosyl-diacylglycerol (MGDG) and digalactosyl-diacylglycerol (DGDG), which are responsible for 50 and 30% of the total membrane lipids (Vieler *et al.,* 2007: 143 – 144). Figure 4.7 shows the most important lipids that are found in algae.

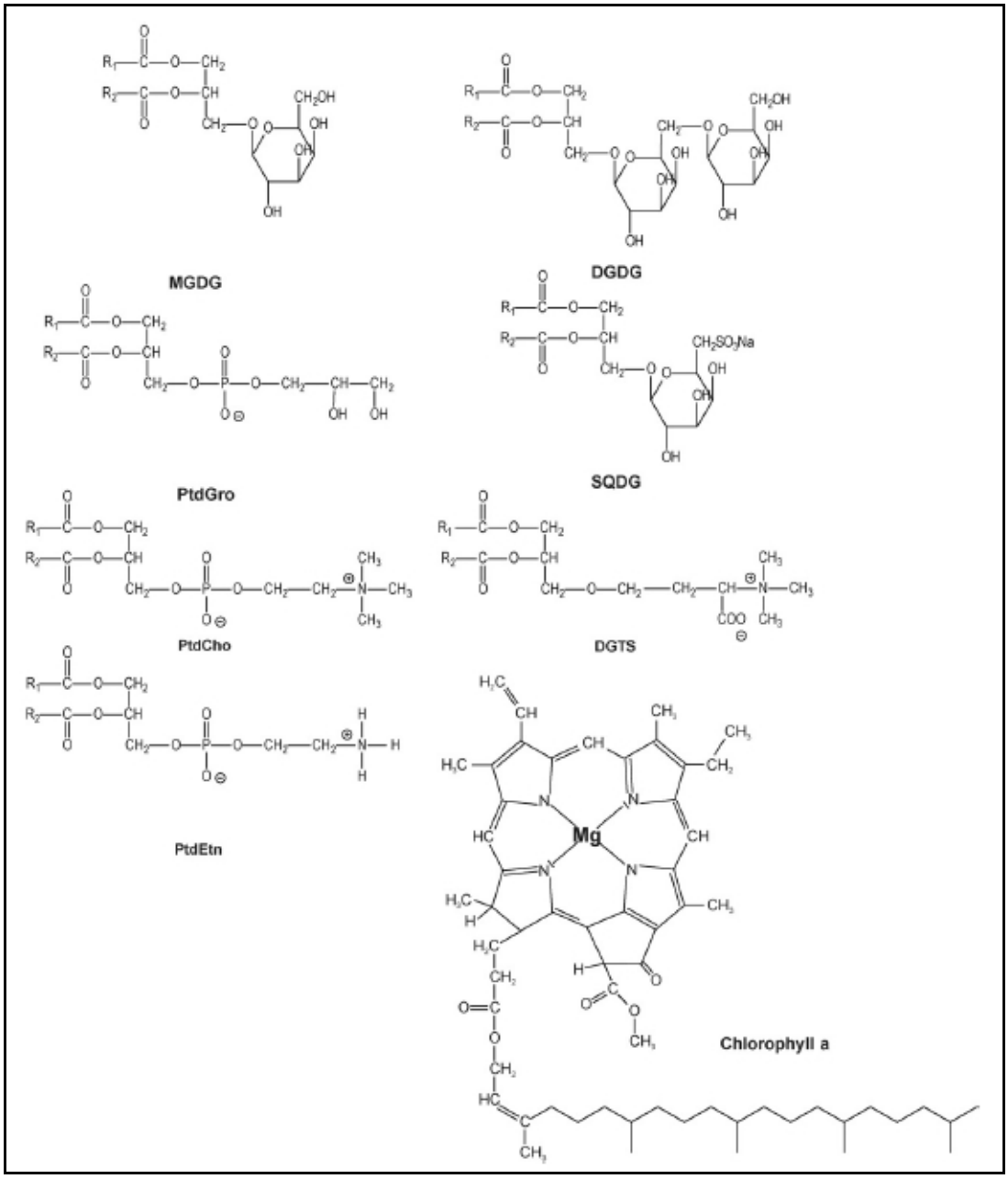

Figure 4.7: Most important lipids found in algae (Vieler *et al.,* 2007: 145).

MGDG is formed by the addition of galactose to a diglyceride in a process called galactosylation, whereas DGDG is formed by the galactosylation of MGDG (Lem & Williams, 1981: 944). Sulfoquinovosyl-diacylglycerol (SQDG) contained in the algal cells contains $C_{16:0}$ and $C_{18:1}$ lipids (Gushina & Harwood, 2006: 165), whereas $C_{16:0}$ is the major fatty acid in MGDG and DGDG (Gushina & Harwood, 2006: 169; Zepke *et al.,* 1978: 160). Figure 4.6 indicates that the addition of Na_2CO_3 liberates more C_{16} from the membrane lipids.

Na_2CO_3 is a base, whereas the C_{16} fatty acid is an acid. The Na_2CO_3 dissociates in water according to the following equation (Kotz and Treichel, 2003: 695):

$$Na_2CO_3 \rightarrow 2Na^+ + CO_3^{2-}$$

The decrease in the oil yield observed in Figure 4.5 can therefore be attributed to an acid-base reaction between the C_{16} fatty acid and the Na_2CO_3, which produces a water-soluble sodium salt. Therefore the total oil content is decreased by a loss of the C_{16} fatty acid through a saponification reaction with Na_2CO_3.

4.2.4 The influence of residence time on thermochemical liquefaction

The influence of residence time on thermochemical liquefaction of *M. aeruginosa* was investigated. In order to evaluate the influence of residence time on the liquefaction of *M. aeruginosa*, experiments were conducted at an operating temperature of 300 °C and a catalyst load of 5 wt%. Table 4.2 shows the results obtained for the various residence times.

Table 4.2: Results of residence time evaluation for liquefaction of *Microcystis aeruginosa*.

Residence Time (min)	Oil Yield (wt%)	Wt% C_{16} esters in oil
0	11.30%	3.42%
15	13.33%	6.50%
30	15.07%	7.38%
45	15.40%	7.40%
60	13.07%	6.30%

From Table 4.2 it may be seen that the oil yield reaches a maximum at a residence time of 45 min. The dependence of the oil yield on the residence time is depicted in Figure 4.8.

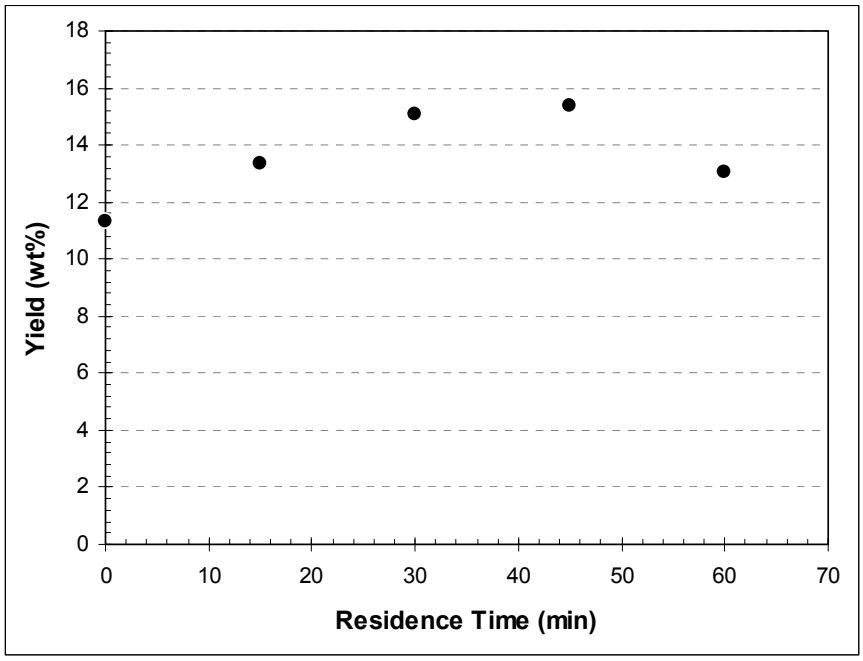

Figure 4.8: Oil yield versus residence time for liquefaction of *Microcystis aeruginosa.* (Reaction Temperature = 300 °C, Catalyst Load = 5 wt%)

Section 2.4.4. states that the production of oil from thermochemical liquefaction occurs through the formation of free radicals. From Figure 4.8 it is deduced that the process of thermochemical liquefaction is almost complete after a residence time of 30 min. Yang and co-workers (2004: 26) conducted thermochemical liquefaction experiments of *Microcystis viridis* with residence times of 30 and 60 minutes, respectively. They determined that the liquefaction was almost complete within a reaction time of 30 min and observed a decrease in the oil yield at a reaction time of 60 min due to decomposition of the oil (Yang *et al.,* 2004: 26). The maximum oil yield is obtained at a residence time of 45 min, which indicates that the liquefaction of the *M. aeruginosa* reaches completion after 45 min. An increase in the residence time to 60 min produced a decrease in the oil yield.

The decrease in oil yield with an increase in the residence time is attributed to condensation and repolymerization reactions that occur with prolonged residence time (Qu *et al.,* 2003: 603). Section 2.4.4.2 states that free radicals are formed during thermochemical liquefaction. These free radicals are responsible for thermal decompositions (Chornet & Overend, 1985: 981). Björnbom and co-workers (1986: 1053) stated that a raw material with sufficient hydrogen content has the ability to stabilize the free radicals that are formed during liquefaction due to internal hydrogen shuttling within the raw material. This explains the reduction in the oil content with an increase in the residence time. The hydrogen content of the algae is not sufficient to

stabilize all the free radicals that are formed as the reaction progresses. This deficiency in a reducing agent results in condensation and repolymerization reactions.

The decrease in the C_{16} esters with an increase in the residence time is also attributed to the condensation and repolymerization reactions that occur. Figure 4.9 depicts the dependence of the C_{16} esters on the residence time.

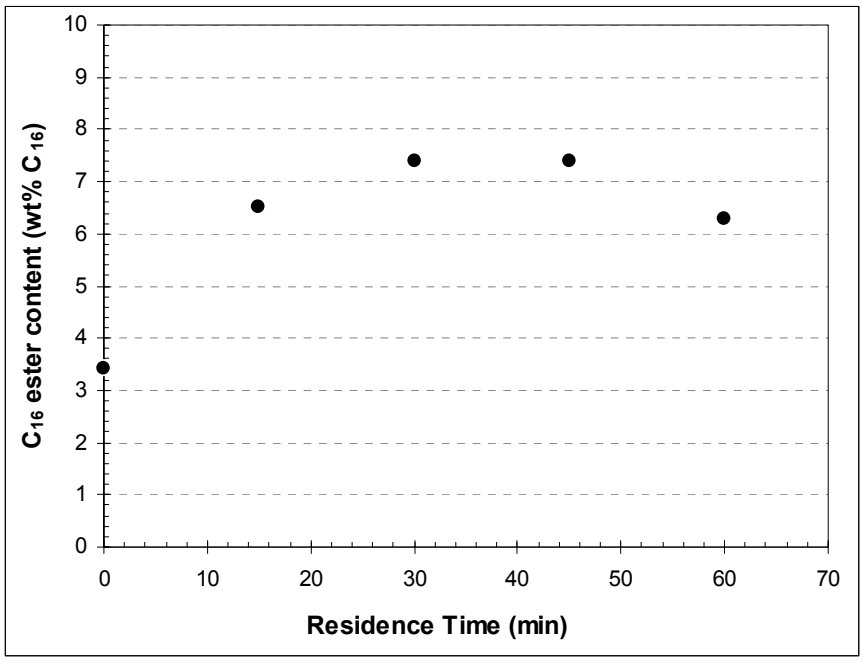

Figure 4.9: C_{16} ester content of oil versus residence time for liquefaction of *Microcystis aeruginosa*.

(Residence Time = 300 °C, Catalyst Load = 5 wt%)

4.2.5 The coupled influence of the manipulated variables on thermochemical liquefaction

In Sections 4.2.2 to 4.2.4 the influence of the each individually manipulated variable in the process of thermochemical liquefaction was discussed. There is, however, a possibility that these manipulated variables are dependent on each other. Therefore the interaction of the manipulated variables was studied in this section in order to determine the dependence of the manipulated variables on each other. This is done by using an ANOVA for the response variables, which is described in detail in Appendix B. The oil yield ANOVA evaluates the influence of the interaction of the manipulated variables on the oil yield, whereas the ANOVA for the oil composition

evaluates the influence of the interaction of the manipulated variables on the composition of the oil. Table 4.3 provides a summary of the ANOVA results for the interaction of the manipulated variables.

Table 4.3: ANOVA results for interaction of manipulated variables.

Interaction	Sum of Squares	Mean Square	F Value	p-value Prob > F
Oil yield ANOVA				
Reaction Temperature·Catalyst Load	2.599	2.599	3.981	0.074
Reaction Temperature·Residence Time	0.018	0.018	0.028	0.871
Catalyst Load·Residence Time	0.696	0.696	1.066	0.326
Oil composition ANOVA				
Reaction Temperature·Catalyst Load	0.097	0.097	0.074	0.791
Reaction Temperature·Residence Time	1.110	1.110	0.853	0.378
Catalyst Load·Residence Time	2.464	2.464	1.893	0.199

Evaluation of the p-values in Table 4.3 enables the significance of the interaction terms to be determined. The p-values in Table 4.3 indicate that the only interaction of any significance that occured between the manipulated variables was the interaction between the reaction temperature and the catalyst load. The interaction between the reaction temperature and the catalyst load was statistically significant at a 90% probability level for the oil yield. The interaction that occurred between the residence time and the reaction temperature as well as between the residence time and the catalyst load is negligible for both the oil yield and the composition of the oil.

Graphical representation of the oil yield ANOVA results for the interaction between the reaction temperature and the catalyst load confirms the significance of this interaction on the oil yield. Figure 4.10 shows the influence of the interaction between the reaction temperature and catalyst load on the oil yield.

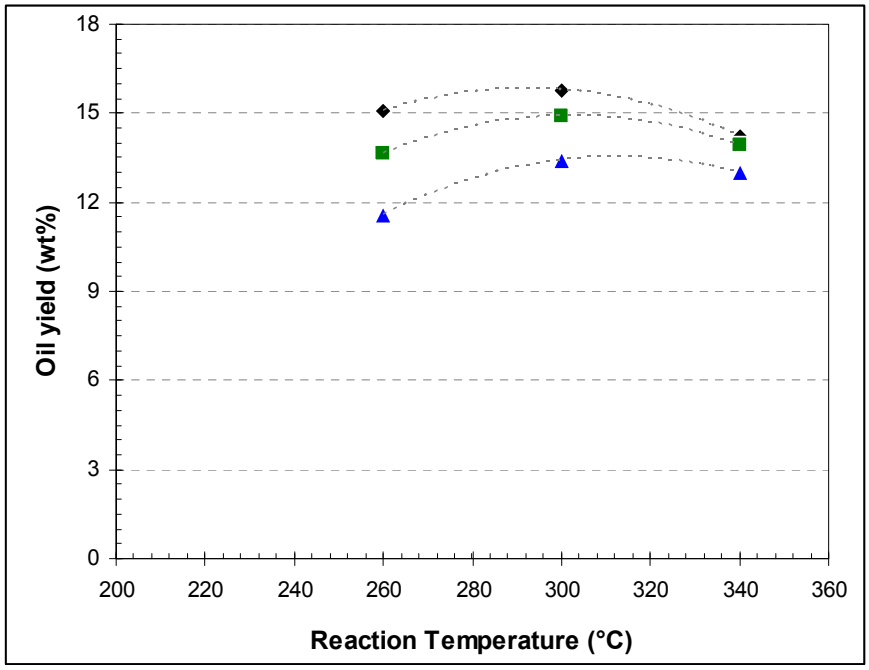

Figure 4.10: Influence of reaction temperature on oil yield for liquefaction of *Microcystis aeruginosa* at various catalyst loads.

(♦ 0 wt% Catalyst Load; ■ 5 wt% Catalyst Load; ▲ 10 wt% Catalyst Load)

Figure 4.10 indicates that the influence of the reaction temperature on the oil yield differed at various catalyst loads. This confirms the significance of the interaction between the reaction temperature and the catalyst load. At high temperatures the difference between the catalyst loads was smaller than at low temperatures. This phenomenon can be explained by the hypothesis of the free radical formation. At low temperatures the free radicals are produced slower than at high reaction temperatures, which allow the fatty acids more time to form salt complexes with the sodium carbonate catalyst. High reaction temperatures increase the rate of free radical formation. The catalyst and fatty acids combine quickly until all the catalyst is exhausted. The remaining free radicals result in repolimerization reactions, which decrease the oil yield further. At high temperatures the quantity of the free radicals that were produced were very high in comparison with the available quantity of catalyst and therefore the influence of the catalyst load was less significant than at lower temperatures.

4.2.6 Elemental analysis

Elemental analysis of the algal biomass and the extracted oil was conducted in order to determine the efficiency of the thermochemical liquefaction process to deoxygenate the biomass. The elemental analysis of the extracted algal oil was also necessary to determine the heating value of the oil. The experimental conditions did not have an influence on the elemental composition of the oil obtained from thermochemical liquefaction and therefore the experimental conditions did not affect the degree of deoxygenation that occurred during thermochemical liquefaction. Appendix F.3 contains the relevant elemental analyzes to substantiate the independent nature of the elemental composition on the experimental conditions. Table 4.4 shows the elemental analysis of the algal biomass, whereas Table 4.5 lists the elemental analysis of the algal oils that were obtained.

Table 4.4: Elemental analysis of algal biomass.

Element composition	***Microcystis aeruginosa***	***Cyclotella meneghinia***	***Nitzschia pusilla***
Wt% C	42.05	44.86	45.04
Wt% N	7.96	6.54	6.50
Wt% H	6.47	7.19	6.71
Wt% S	0.24	1.36	0.47
Wt% O*	43.29	40.04	41.28

* Calculated by difference.

Table 4.5: Elemental analysis of thermochemical liquefaction oil.

Element composition	***Microcystis aeruginosa***	***Cyclotella meneghinia***	***Nitzschia pusilla***
Wt% C	66.23	67.78	75.14
Wt% N	4.92	4.59	5.50
Wt% H	7.85	8.10	8.58
Wt% S	0.29	0.34	0.29
Wt% O*	20.72	19.19	10.49

* Calculated by difference.

The elemental analysis of the oil obtained from thermochemical liquefaction was used to estimate the higher heating value of the oil. Beckman and co-workers

(quoted by Channiwala *et al.,* 2002: 1053) provided the following equation to calculate the higher heating value of biomass derived oils within a 5% tolerance:

$$HHV\,(MJ.kg^{-1}) = 0.352C + 0.944H + 0.105(S - O)$$

where C, H, S and O represent the carbon, hydrogen, sulphur and oxygen content of the material in weight percentage on a dry basis, respectively. Table 4.6 shows the higher heating values of the algal biomass and the thermochemical liquefaction oil.

Table 4.6: Higher heating values of algal biomass and liquefaction oil.

Higher heating value (MJ.kg^{-1})	***Microcystis aeruginosa***	***Cyclotella meneghinia***	***Nitzschia pusilla***
Algal biomass	20.717 ± 0.019	18.872 ± 0.420	17.402 ± 0.564
Liquefaction oil	28.57 ± 1.22	29.53 ± 1.51	33.48 ± 0.61

The results obtained from the elemental analysis were in good correlation with results obtained from previous studies (Minowa *et al.,* 1995b: 1736 – 1737; Matsui *et al.,* 1997: 1047; Yang *et al.,* 2004: 27) as summarized in Table 4.7. Table 4.7 also lists the calorific values of the oils that were obtained from previous studies.

Table 4.7: Elemental analysis from previous studies.

Property	***Dunaliella tertiolecta*** [a]		***Spirulina* sp.** [b]		***Microcystis viridis***	
	Algae	**Oil**	**Algae**	**Oil**	**Algae**	**Oil**
Wt% C	53.3	73.72	46.1	66.6	46.0	60.4
Wt% N	9.8	6.89	4.8	7.8	9.5	6.3
Wt% H	5.2	8.69	7.4	8.5	7.3	7.4
Wt% O	31.7	10.70	41.3	17.0	37.2	23.7
Wt% S	-	-	0.4	-		2.2
Calorific value (MJ.kg^{-1})	-	35.53		31.9		29.1

a. Minowa *et al*., 1995b: 1736 – 1737.

b. Matsui *et al.,* 1997: 1047.

c. Yang *et al.,* 2004: 27.

Table 4.6 indicates that there was a significant increase in the energy content between the algal biomass and the oil obtained from thermochemical liquefaction. This is due to the reduction of the oxygen content of algal biomass, which produces oil with the desired properties for combustion.

4.2.7 Energy aspects of thermochemical liquefaction

In order to evaluate energy efficiency of the process, the energy consumption ratio is used. The ECR (energy consumption ratio) is defined as follows:

$$ECR = \frac{Energy\ required\ to\ maintain\ the\ reaction\ temperature}{Available\ energy\ \ from\ the\ oil\ \ produced}$$

The ECR was evaluated at a reaction temperature of 300 °C, a catalyst load of 5 wt%, residence time of 30 min and 3 grams of *M. aeruginosa*. The calculation of the ECR is discussed in detail in Appendix G. These conditions produced an ECR of 424, which indicates that much more energy is required to extract the oil from the algae than is produced from combustion of the algal oil.

Studies conducted by Minowa and co-workers (1995b: 1738) on the thermochemical liquefaction of *Dunaliella tertiolecta* algae produced an ECR of 0.75 at 300°C. They used an autoclave that was 10 times smaller than the one used in this study, which requires a lot less energy to be heated (Minowa *et al.,* 1995b: 1736). Assuming that the thermochemical liquefaction experiments were conducted in the same size autoclave as was used by Minowa and co-workers (1995b: 1736), the ECR can be calculated for the thermochemical liquefaction of *M. aeruginosa, C. meneghinia and N. pusilla* algae at 300 °C as summarized in Table 4.8.

Table 4.8: Energy consumption ratio for smaller autoclave size.

	Microcystis aeruginosa	***Cyclotella meneghinia***	***Nitzschia pusilla***
Mass of oil (gram)	0.4428	0.4659	0.423
Calorific value ($MJ.kg^{-1}$)	28.42	28.89	34.14
Energy required to heat autoclave(kJ)	30.566	30.566	30.566
Energy from oil produced (kJ)	12.584	13.460	14.441
ECR	2.429	2.271	2.117

Table 4.8 indicates that by lowering the energy requirements of the heating process, a more favourable ECR can be obtained. An increase in the algal load to the autoclave will result in even lower ECR values. Therefore an ECR value of less than unity is attainable, which indicates that the process of thermochemical liquefaction can be a net energy producer.

4.2.8 Summary

In this study the influence of the reaction temperature, catalyst load and residence time on the process of thermochemical liquefaction was investigated. The reaction temperature and catalyst load was identified as the two manipulated variables which influence the oil yield obtained from thermochemical liquefaction of algae. The interaction between the reaction temperature and the catalyst load also has a significant influence on the oil yield obtained from thermochemical liquefaction of algae. The residence time had a negligible influence on the oil yield and the composition of the oil. The interaction of the residence time with the reaction temperature and catalyst load also had no signifant influence on the process of thermochemical liquefaction.

Thermochemical liquefaction of *M. aeruginosa* produced an average oil yield of 14.07 wt% ± 1.19 wt%. Piorreck and co-workers (1984: 209) found that *M. aeruginosa* contains 12 to 18 wt% (of the dry weight) lipids, whereas Piorreck and Pohl determined (1984: 220) that the fatty acid content of *M. aeruginosa* amounts to 12 – 18 wt% of the total lipids, with C_{16} fatty acids being the major constituent of the fatty acids. The bulk of the lipids extracted from *M. aeruginosa* are the polar membrane lipids (Piorreck *et al.,* 1984: 210). The low C_{16} methyl ester content detected in this study therefore correlates with the previous studies (Piorreck & Pohl*,* 1984: 220; Piorreck *et al.,* 1984: 210). The oil yield obtained from the thermochemical liquefaction of *M. aeruginosa* was a maximum (15.60 wt%) at a reaction temperature of 300 °C, catalyst load of 0 wt% Na_2CO_3 and a residence time of 30 min.

Studies conducted on the influence of environmental conditions on the lipid content of *M. aeruginosa* indicated that the nitrogen concentrations of the growth medium did not affect the lipid content of *M. aeruginosa* (Piorreck *et al.,* 1984: 209). The significance of this observation is that *M. aeruginosa* can be harvested from the Hartebeespoort dam and does not require specific culturing conditions in order to optimize the oil production.

Thermochemical liquefaction of *N. pusilla* produced an average oil yield of 13.21 wt% ± 1.19 wt%. This correlates with studies conducted on the lipid content of various species of *Nitzschia*, which found that the lipid content of the *Nitzschia* species can vary from 9.63 wt% for *Nitzschia sp.* (Ben-Amotz & Tornabene, 1983: 123) to 17.5 wt% for *Nitzschia closterium* and 15 wt% for *Nitzschia paleacea*, respectively

(Renaud *et al.,* 1995: 600). Previous studies also showed that C_{16} fatty acids are the major component of the neutral lipids in the *Nitzschia* species (Falk-Petersen *et al.,* 1998: 44; Pratoomyot *et al.,* 2005: 1183). As is the case with *M. Aeruginosa,* the polar lipids constitute the bulk of the oil extracted from the *Nitzschia* specie (Ben-Amotz & Tornabene, 1983: 123). The maximum oil yield, 15.33 wt%, obtained from thermochemical liquefaction of *N. pusilla,* at 340 °C, is therefore in correspondence with the literature. This yield was obtained with 5 wt% catalyst.

Thermochemical liquefaction of *C. meneghinia* produced an average oil yield of 13.78 wt% ± 1.19 wt%. Sicko-Goad and Andresen (1991: 713) found that the total extractable lipid content of *C. meneghinia* is 17.8 wt% (Sicko-Goad & Andresen, 1991: 713), which compares with the oil yield obtained from this study. The discrepancy in the oil yield may be ascribed to the culturing conditions of the algae. The results obtained from the composition of the oil extracted from *C. meneghinia* correlates with worked conducted by Sriharan and co-workers (1991: 322 – 324) on other strains of *Cyclotella* algae. They observed that *Cyclotella cryptica* contained 9.96 wt% neutral lipids, with C_{16} fatty acid being the major constituent of the algal oil. Vieler and co-workers (2007: 153) showed that the membrane lipids such as MGDG are the prevalent lipids in *C. meneghinia*. This confirms the results obtained from the thermochemical liquefaction of *C. meneghinia*. The thermochemical liquefaction of *C. meneghinia* delivered a maximum oil yield of 16.03 wt% at 340 °C, 30 minutes residence time and 5 wt% catalyst load.

The evaluation of the oil yields and composition of the oils obtained from the thermochemical liquefaction of the *M. aeruginosa, C. meneghinia* and *N. pusilla* algae show that thermochemical liquefaction extracts the maximum amount of oil from the algal cells.

Evaluation of the elemental analysis of the various thermochemical liquefaction oils verifies that deoxygenation of the biomass occurred during the process of thermochemical liquefaction. The deoxygenation of the algae proceeds through dehydration or decarboxylation (Matsui *et al.,* 1997: 1046). Table 4.9 shows the evaluation of the elemental analysis.

Table 4.9: Evaluation of elemental analysis.

Property	*Microcystis aeruginosa*		*Cyclotella meneghinia*		*Nitzschia pusilla*	
	Algae	**Oil**	**Algae**	**Oil**	**Algae**	**Oil**
Hydrogen/Carbon (H/C ratio)	0.154	0.119	0.148	0.120	0.145	0.114
Oxygen/Carbon (O/C ratio)	1.031	0.315	0.927	0.284	0.924	0.140

The decrease in the O/C ratio from the biomass to the liquefaction oil verifies that deoxygenation of the algae occurred. A comparison of the H/C and O/C ratios of the liquefaction oils to the elemental content of coal, petroleum and wood shows that the liquefaction oil contains large amounts of unsaturated membrane lipids due to its low H/C ratio. Table 4.9 indicates that the H/C ratio of *M. aeruginosa* was lower than that of *C. meneghinia* and *N. pusilla* algae. This indicates that *M. aeruginosa* contains more unsaturated membrane lipids than *C. meneghinia* and *N. pusilla*. This is also evident from the higher C_{16} methyl ester content of the *C. meneghinia* and *N. pusilla* algae.

Evaluation of the calorific values of the oils obtained from thermochemical liquefaction of *M. aeruginosa* (28.57 ± 1.22), *C. meneghinia* (29.53 ± 1.51) and *N. pusilla* (33.48 ± 0.61) shows that the oil obtained from thermochemical liquefaction of algae had similar heating values that that of South African coals. Barker (1999) reported that the average calorific value for South African coals is 27.31 $MJ.kg^{-1}$ (Barker, 1999). The oil contained more saturated compounds than the South African coals and less sulphur (Barker, 1999). The oil obtained from thermochemical liquefaction of algae will therefore burn cleaner than any of the coals that are available in South Africa.

The oil obtained from thermochemical liquefaction of algae did, however, not contain acceptable amounts of saturated fatty acids in order to justify the processing of the oil for biodiesel production. The oil can be used in its crude form in simple gasification processes as an alternative to coal combustion. In order to use the oil with other petroleum products it needs to be processed further to deoxygenate it even more.

4.3 References

BARKER, O.B. 1999. A techno-economic and historical overview of the South African coal industry in the 19th and 20th centuries, in Bulletin 113. ed. Pinheiro, H.J. (South African Bureau of Standards), pp. 1-63

Ben-Amotz, A. & Tornabene, T.G. 1983. Chemical profile of algae with emphasis on lipids of microalgae. (*In* SERI (Solar Energy Research Institute). Aquatic Species Program Review. San Diego, Calif. p. 123 – 133.)

Björnbom, E., Olsson, B. & Karlsson, O. 1986. Thermochemical refining of raw peat prior to liquefaction. Fuel, 65: 1051 – 1056.

Channiwala, S.A. & Parikh, P.P. 2002. A unified correlation for estimating HHV of solid, liquid and gaseous fuels. Fuel, 81: 1051 – 1063.

Chornet, E. & Overend, R.P. 1985. Biomass Liquefaction: An Overview. (In Overend, R.P., Milne, T.A. and Mudge, L.K., ed. Fundamentals of Thermochemical Biomass Conversion. New York: Elsevier Applied Science Publishers. p. 967 – 1001).

Dote, Y., Sawayama, S., Inoue, S., Minowa, T. & Yokoyama, S. 1994. Recovery of liquid fuel from hydrocarbon-rich microalgae by thermochemical liquefaction. Fuel, 73(12): 1855 – 1857.

Dote, Y., Inoue, S., Ogi, T. & Yokoyama, S. 1996. Studies on the direct liquefaction of protein-contained biomass: The distribution of nitrogen in the products. Biomass and Bioenergy, 11(6): 491 – 498.

Falk-Petersen, S., Sargent, J.R, Henderson, J., Hegseth, E.N., Hop, H. & Okolodkov, Y.B. 1998. Lipids and fatty acids in ice algae and phytoplankton from the marginal ice zone in the Barents Sea. Polar Biology, 20: 41 – 47.

Gushina, I.A. & Harwood, J.L. 2006. Lipids and lipid metabolism in eukaryotic algae. Progress in Lipid Research, 45: 160 – 186.

Kotz, J.C. & Treichel, P.M. 2003. Chemistry and Chemical Reactivity. 5th ed. United States of America: Thomson Brooks/Cole. 997 p.

Lem, N.W. & Williams, J.P. 1981. Desaturation of fatty acids associated with monogalatosyl diacylglycerol: The effects of San 6706 and San 9785. Plant Physiology, 68: 944 – 949.

Matsui, T., Nishihara, A., Ueda, C., Ohtsuki, M., Ikenaga, N. & Suzuki, T. 1997. Liquefaction of micro-algae with iron catalyst. Fuel, 76(11): 1043 – 1048.

Minowa, T., Murakami, M., Dote, Y., Ogi, T. & Yokoyama, S. 1995a. Oil production from garbage by thermochemical liquefaction. Biomass and Bioenergy, 8(2): 117 – 120.

Minowa, T., Yokoyama, S., Kishimoto, M. & Okakura, T. 1995b. Oil production from algal cells of Dunaliella tertiolecta by direct thermochemical liquefaction. Fuel, 74(12): 1735 – 1738.

Piorreck, M., Baasch, K. & Pohl, P. 1984. Biomass production, total protein, chlorophylls, lipids and fatty acids of freshwater green and blue-green algae under different nitrogen regimes. Phytochemistry, 23(2): 207 – 216.

Piorreck, M. & Pohl, P. 1984. Formation of biomass, total protein, chlorophylls, lipids, and fatty acids in green and blue-green algae during one growth phase. Phytochemistry, 23(2): 217 – 223.

Pratoomyot, J., Srivilas, P. & Noiraksar, T. 2005. Fatty acids composition of 10 microalgal species. Songklanakarin Journal Science and Technology, 27(6): 1179 – 1187.

Qu, Y., Wei, X. & Zhong, C. 2003. Experimental study on the direct liquefaction of *Cunninghamia lanceolata* in water. Energy, 28: 597 – 606.

Renaud, S.M., Zhou, H.C., Parry, D.L., Thinh, L. & Woo, K.C. 1995. Effect of temperature on the growth, total lipid content and fatty acid composition of recently isolated tropical microalgae *Isochrysis sp., Nitzschia closterium, Nitzschia paleacea,*

and commercial species *Isochrysis sp.* (clone T.ISO). Journal of Applied Phycology, 7: 595 – 602.

Sawayama, S., Inoue, S., Dote, Y. & Yokoyama, S. 1995. CO_2 fixation and oil production through microalga. Energy Conversion Management, 36 (6 – 9): 729 – 731.

Sicko-Goad, L. & Andresen, N.A. 1991. Effect of growth and light/dark cycles on diatom lipid content and composition. Journal of Phycology, 27: 710 – 718.

Sriharan, S., Bagga, D. & Mohamad, N. 1991. The effects of nutrients and temperature on biomass, growth, lipid production, and fatty acid composition of Cyclotella cryptica Reimann, Lewin, and Guillard. Applied biochemistry and biotechnology, 28 – 29(1): 317 – 326.

Vieler, A., Wilhelm, C., Goss, R., Süß, R. & Schiller, J. 2007. The lipid composition of the unicellular green alga *Chlamydomonas reinhardtii* and the diatom *Cyclotella meneghiniana* investigated by MALDI-TOF MS and TLC. Chemistry and Physics of Lipids, 150: 143 – 155.

Yan, Y., Xu, J., Li, T. & Ren, Z. 1999. Liquefaction of sawdust for liquid fuel. Fuel Processing Technology, 60: 135 – 143.

Yang, Y.F., Feng, C.P., Inamori, Y. & Maekawa, T. 2004. Analysis of energy conversion characteristics in liquefaction of algae. Resources, Conservation and Recycling, 43: 21 – 33.

Zepke, H.D., Heinz, E., Radunz, A., Linscheid, M. & Pesch, R. 1978. Combination and positional distribution of fatty acids in lipids from blue-green algae. Archives of Microbiology, 119: 157 – 162.

Chapter 5. – Conclusions and Recommendations

In this study the extraction of oil from *Microcystis aeruginosa, Cyclotella meneghinia* and *Nitzschia pusilla* by thermochemical liquefaction was investigated. The thermochemical liquefaction was conducted in a high pressure autoclave under an inert atmosphere. The study entailed investigating the effect of process conditions such as reaction temperature, catalyst load and residence time on the yield and the composition of the liquefaction oil.

5.1 Influence of biomass used during thermochemical liquefaction

The thermochemical liquefaction of *M. aeruginosa, C. meneghinia* and *N. pusilla* produced maximal oil yields of 15.60 wt%, 15.33 wt% and 16.03 wt%, respectively. The difference in oil yield obtained from the various algae was very small. This suggests that the algae from the Hartebeespoort dam can be used for the extraction of oil and it is not necessary to cultivate alge especially for this purpose.

A comparison of heating values of the oil extracted from *M. aeruginosa* (28.57 ± 1.22 $MJ.kg^{-1}$), *C. meneghinia* (29.53 ± 1.51 $MJ.kg^{-1}$) and *N. pusilla* (33.48 ± 0.61 $MJ.kg^{-1}$) indicates that the oil extracted from *N. pusilla* has the most favourable heating value. *N. pusilla*, therefore, has a slight advantage over *M. aeruginosa* and *C. meneghinia* when the energy content is evaluated.

M. aeruginosa is readily available from the Hartebeespoort dam and no cost of cultivation is, therefore, associated with it. *C. meneghinia* and *N. pusilla* have to be cultivated especially for the oil extraction. Taking all these aspects into consideration, it is more economically feasible to use *M. aeruginosa* algae for oil extraction. In the process the algal blooms in the Hartebeespoort dam can also be controlled.

5.2 Influence of reaction conditions

The type of algae used during thermochemical liquefaction determined the effect of the reaction temperature on thermochemical liquefaction. The thermochemical liquefaction of *M. aeruginosa* produced a maximum oil yield at 300 °C, whereas the

thermochemical liquefaction of *C. meneghinia and N. pusilla* produced maximum yields at 340 °C. An increase in the reaction temperature, however, produced a more favourable oil composition.

The influence of the residence time on thermochemical liquefaction of algae was negligible. The catalyst load affected thermochemical liquefaction of all the algae in a similar manner and reduced the oil yield. In contrast to this, the addition of catalyst produced a more favourable oil composition. The reaction conditions had no effect on the elemental composition of thermochemical liquefaction oil or on the calorific value of the liquefaction oil.

5.3 Energy considerations of thermochemical liquefaction

The oil produced by thermochemical liquefaction of *M. aeruginosa* (28.57 ± 1.22), *C. meneghinia* (29.53 ± 1.51) and *N. pusilla* (33.48 ± 0.61) had calorific values comparable to those of South African coals (27.31 $MJ.kg^{-1}$) (Barker, 1999). Therefore, the oil may be used in combustion processes as an alternative to coal. In order to use the oil with petroleum products it must be processed further to remove more oxgygen.

The evaluation of the energy consumption ratio showed that, under the conditions evaluated in this study, the process of thermochemical liquefaction used more energy than is available from the liquefaction oil. It is, however, possible to adjust the thermochemical liquefaction process in order to obtain more energy from the extracted oil than is used for the process to be carried out. This can be done by using a smaller autoclave or larger biomass content in the thermochemical liquefaction experiments.

5.4 Recommendations

5.4.1 Catalyst for thermochemical liquefaction

It is recommended that the type of catalyst that is used during thermochemical liquefaction be varied. Matsui and co-workers (1997: 1048) showed that the addition of iron catalysts to the thermochemical liquefaction of *Spirulina* sp. produced an increased oil yield. Therefore, it is recommended that the influence of catalysts other

than alkali salts, such as Na_2CO_3, on the thermochemical liquefaction of algae be studied.

5.4.2 Atmosphere for thermochemical liquefaction

It is recommended that experiments be conducted in a reducing atmosphere to determine the effect of the reaction atmosphere on the thermochemical liquefaction of algae. Matsui and co-workers (1997: 1044) conducted thermochemical liquefaction experiments on *Spirulina* sp. in a nitrogen and hydrogen atmosphere and observed that the reaction atmosphere does not affect the oil yield.

This may not be the case for the microalgae used in this study. The reaction atmosphere does affect the thermochemical liquefaction of biomass. Björnbom and co-workers (1986: 1053) conducted thermochemical liquefaction experiments with raw peat in a reducing (CO) and an inert (N_2) atmosphere and found that carbon monoxide is not necessary to convert the peat to oil due to the high hydrogen content of the raw material.

5.4.3 Solvent for thermochemical liquefaction

Matsui and co-workers (1997: 1048) studied the influence of the solvent that was used during thermochemical liquefaction of *Spirulina* sp.. They found that water produced a higher oil yield, but that thermochemical liquefaction of *Spirulina* sp. in toluene produced oil with a higher energy content.

Yan *et al.* (1999: 142) postulated that a hydrogen-donor solvent promotes the destruction of the molecular structure of the biomass feed for the hydrothermal liquefaction of sawdust.

It is therefore recommended that the influence of the solvent on the thermochemical liquefaction of the algae be studied.

5.4.4 Biomass load for thermochemical liquefaction

Karagöz and co-workers (2006: 92) observed that the biomass load influenced the thermochemical liquefaction of wood biomass. Therefore it is recommended that the influence of the biomass load on the thermochemical liquefaction of algae be studied in order to determine a suitable experimental configuration to make the thermochemical liquefaction of algae a net energy producer.

5.5 References

BARKER, O.B. 1999. A techno-economic and historical overview of the South African coal industry in the 19th and 20th centuries, in Bulletin 113. ed. Pinheiro, H.J. (South African Bureau of Standards), pp. 1-63

Björnbom, E., Olsson, B. & Karlsson, O. 1986. Thermochemical refining of raw peat prior to liquefaction. Fuel, 65: 1051 – 1056.

Karagöz, S., Bhaskar, T., Muto, A. & Sakata, Y. 2006. Hydrothermal upgrading of biomass: Effect of K_2CO_3 concentration and biomass/water ratio on products distribution. Bioresource Technology, 97: 90 – 98.

Matsui, T., Nishihara, A., Ueda, C., Ohtsuki, M., Ikenaga, N. & Suzuki, T. 1997. Liquefaction of micro-algae with iron catalyst. Fuel, 76(11): 1043 – 1048.

Yan, Y., Xu, J., Li, T. & Ren, Z. 1999. Liquefaction of sawdust for liquid fuel. Fuel Processing Technology, 60: 135 – 143.

Appendix A. – Choice of solvent

The choice of solvent is dependent on the properties of the algal lipids. Lipids may be divided into two groups. The first group consists of open-chain compounds with polar head groups and long non-polar tails, whereas the second group consists of fused-ring compounds. Algal lipids are categorized in group one, which includes fatty acids, triacylglycerols, sphingolipids, phosphoacylglycerols and glycolipids (Campbell & Farrell, 2003: 191).

The lipids contained in the algal cells consist of glycerine and fatty acids. Figure A.1 shows an example of a fatty acid and Figure A.2 shows the glycerol molecule. In Figure A.3 the combination of the fatty acid and glycerol to form a triacylglycerol is depicted (Campbell & Farrell, 2003: 193).

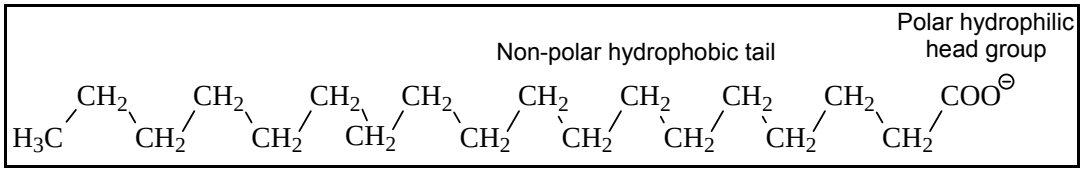

Figure A. 1: Stearic acid.

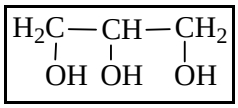

Figure A. 2: Glycerol molecule.

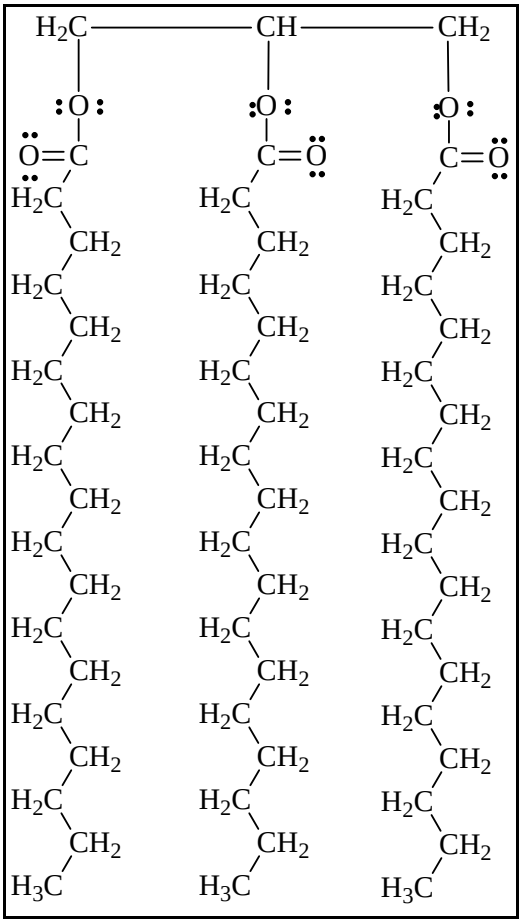

Figure A. 3: Tristearin (Campbell and Farrell, 2003: 193).

The three ester groups of the triacylglycerol are polar, whereas the tails of the fatty acids are nonpolar. This phenomenon results in the triacylglycerol being termed as amphipathic (Campbell & Farrell, 2003: 193). This unique property must be kept in mind in order to choose a suitable solvent. The occurrence of the polar group brings about a solubilizing effect on a paraffin-chain compound, especially in a polar solvent (Ralston *et al.,* 1944: 320).

A literature study on thermochemical liquefaction showed that various solvents have been used during thermochemical liquefaction experiments for the extraction of the product oil. Table A.1 lists the various solvents that have been used as well as the properties of the solvents.

Table A. 1: Solvents used for extraction of liquefaction product oil.

Solvent	**Dielectric constant at 25 °C[a]**	**Dipole moment (D)[a]**	**Solubility in water ($g.L^{-1}$) at 20 °C[b]**	**Boiling Point (°C)[a]**	**Hildebrand solubility parameter ($MPa^{1/2}$)[c]**	**Previous studies**
Acetone	21.01	2.88	Miscible	56.05	20.2	Eager *et al.,* 1982: 289 – 294; Rezzoug & Capart, 2002: 631 – 644; Li *et al.,* 2008: 199 – 204; Bhaskar *et al.,* 2008: 2236 – 2242; Xu & Lancaster, 2008: 1571 – 1582; Xu & Etcheverry, 2008: 335 – 345.
Benzene	2.2825	0	1.78	80.09	18.8	Erzengin & Kücük, 1998: 1203 – 1206.
Chloroform	4.8069	1.04	8	61.17	19.0	Boocock *et al.,* 1992: 1283 – 1289; Schuchardt & De Assis Pereira Matos, 1982: 106 – 110; Boocock *et al.,* 1979: 98 – 101; Yokoyama *et al.,* 1984: 155 – 163; Yang *et al.,* 2004: 21 – 33.
Dichloromethane	8.93	1.60	17.6	40	19.8	Dote *et al.,* 1996: 491 – 498; Minowa *et al.,* 1994: 579 – 582; Rocha *et al.,* 1997: 91 – 103; Pütün *et al.,* 2008: 815 – 824; Meier *et al.,* 1986: 910 – 915; Inoue *et al.,* 1994: 269 – 274.
n-Hexane	1.8865	0	0.011	68.73	14.9	Karaca & Bolat, 2002: 109 – 116; Li *et al.,* 2008: 389 – 394; Wang *et al.,* 2007a: 1587 – 1593; Yan *et al.,* 1999: 135 – 143; Wang et al., 2007b: 187 – 192.

a. Lide, 2006: 15-13 – 15-21.

b. Lide, 2006: 8-87 – 8-96.

c. Barton, 1983: 142 – 149.

Table A.1 indicates that solvents with various polarities have been used to extract the liquefaction product oil. In order to evaluate the effectiveness of the various solvents, the Hansen solubility parameters of the solvents are considered. Hansen (2007: 4) found that materials with similar Hansen solubility parameters have a high affinity for each other (Hansen, 2007: 4). Table A.2 gives the Hansen solubility parameters for the various solvents as well as some fatty acids.

Table A. 2: Hansen solubility parameters (Barton, 1983: 153 – 157).

	Hansen solubility parameters ($MPa^{1/2}$)			
Compound	δ_d	δ_p	δ_h	δ_t
Acetone	15.5	10.4	7.0	20.0
Benzene	18.4	0.0	2.0	18.6
Chloroform	17.8	3.1	5.7	19.0
Dichloromethane	18.2	6.3	6.1	20.3
n-Hexane	14.9	0.0	0.0	14.9
Oleic acid	14.3	3.1	5.5	15.6
Stearic acid	16.4	3.3	5.5	17.6

Hansen's total cohesion parameter, δ_t is an approximation of the Hildebrand parameter, δ, as given in Table A.1. Hansen's total cohesion parameter is determined by the following equation:

$$\delta_t^2 = \delta_d^2 + \delta_p^2 + \delta_h^2$$

where δ_d is the dispersion bonding parameter, δ_p is the polar bonding parameter and δ_h is the hydrogen bonding parameter (Barton, 1983: 141). From Table A.2 it can be seen that the Hansen solubility parameters of chloroform correlates best with that of the fatty acids. Therefore chloroform is the most suitable solvent for the fatty acid system.

Studies have been conducted to evaluate the solubility of various fatty acids in a variety of organic solvents (Ralston & Hoerr, 1942; Hoerr & Ralston, 1944; Skau & Bailey, 1959; Hoerr & Harwood, 1951). Ralston and Hoerr (1942: 550 – 552) investigated the solubility of saturated fatty acids in benzene and acetone. Tables A.3 and A.4 list the solubilities of the fatty acids in acetone and benzene, respectively (Ralston and Hoerr, 1942: 550 – 552).

Table A. 3: Solubilities of fatty acids in acetone (Ralston & Hoerr, 1942: 550 – 552).

	Grams acid per 100 grams acetone					
Fatty acid	**0 °C**	**10 °C**	**20 °C**	**30 °C**	**40 °C**	**56.5 °C**
Caprylic acid	221	975	∞	∞	∞	∞
Nonylic acid	356	3740	∞	∞	∞	∞
Capric acid	45.3	112	407	4660	∞	∞
Undecylic acid	50.2	149	706	∞	∞	∞
Lauric acid	8.95	21.9	60.5	218	1590	∞
Tridecylic acid	7.52	20.2	78.6	316	8230	∞
Myristic acid	2.75	6.50	15.9	42.5	149	∞
Pentadecylic acid	2.20	5.27	13.8	49.3	183	∞
Palmitic acid	0.60	1.94	5.38	15.6	58.0	880
Heptadecylic acid	0.40	1.50	4.28	14.6	67.5	1330
Stearic acid	0.21	0.80	1.54	4.93	17.0	220

Table A. 4: Solubilities of fatty acids in benzene (Ralston & Hoerr, 1942: 550 – 552).

	Grams acid per 100 grams benzene					
Fatty acid	**10 °C**	**20 °C**	**30 °C**	**40 °C**	**50 °C**	**60 °C**
Caprylic acid	770	∞	∞	∞	∞	∞
Nonylic acid	2680	∞	∞	∞	∞	∞
Capric acid	145	398	8230	∞	∞	∞
Undecylic acid	208	663	∞	∞	∞	∞
Lauric acid	32.3	93.6	260	1390	∞	∞
Tridecylic acid	42.4	117	354	7600	∞	∞
Myristic acid	6.95	29.2	87.4	239	1290	∞
Pentadecylic acid	8.84	36.2	103	295	2280	∞
Palmitic acid	1.04	7.30	34.8	105	306	2170
Heptadecylic acid	1.52	9.23	42.1	121	369	5450
Stearic acid	0.24	2.46	12.4	51.0	145	468

Hoerr and Ralston (1944: 332) investigated the solubilities of normal saturated fatty acids in chloroform, whereas Hoerr and Harwood (1951: 781) investigated the solubilities of normal saturated fatty acids in n-Hexane. Tables A.5 and A.6 list the solubility data obtained for normal saturated fatty acids in chloroform (Hoerr & Ralston, 1944: 332) and n-Hexane (Hoerr & Harwood, 1951: 781), respectively.

Table A. 5: Solubilities of fatty acids in chloroform (Hoerr & Ralston, 1944: 332).

	Grams acid per 100 grams chloroform						
Fatty acid	**0 °C**	**10 °C**	**20 °C**	**30 °C**	**40 °C**	**50 °C**	**60 °C**
Caprylic acid	213	720	∞	∞	∞	∞	∞
Nonylic acid	336	2340	∞	∞	∞	∞	∞
Capric acid	61	122	326	6550	∞	∞	∞
Undecylic acid	74	161	485	∞	∞	∞	∞
Lauric acid	22.4	39.1	83	207	2120	∞	∞
Tridecylic acid	28.4	53	116	315	6550	∞	∞
Myristic acid	8.1	15.1	32.5	78	205	1000	∞
Pentadecylic acid	9.5	17.7	38.1	91	246	1750	∞
Palmitic acid	2.9	6.0	15.1	36.4	91	250	1820
Heptadecylic acid	3.6	7.5	17.8	42.6	106	297	5000
Stearic acid	0.4	2.0	6.0	17.5	48.7	124	365

Table A. 6: Solubilities of fatty acids in n-Hexane (Hoerr & Harwood, 1951: 781).

No. of C	**Grams acid per 100 grams n-Hexane**						
atoms	**0 °C**	**10 °C**	**20 °C**	**30 °C**	**40 °C**	**50 °C**	**60 °C**
Caprylic acid	136	2600	∞	∞	∞	∞	∞
Nonylic acid	249	640	∞	∞	∞	∞	∞
Capric acid	23.8	81.2	290	5150	∞	∞	∞
Lauric acid	4.9	14.7	47.7	193	1440	∞	∞
Myristic acid	1.2	4.1	11.9	41.8	198	1650	∞
Pentadecylic acid	0.5	2.9	14.0	60.2	289	2950	∞
Palmitic acid	-	0.5	3.1	14.5	62.4	239	2280
Heptadecylic acid	-	0.2	2.9	17.4	73.0	300	7600
Stearic acid	-	-	0.5	4.3	19.0	79.2	303

Table A.7 shows a summary of the solubilities of the normal fatty acids in the various solvents at 20 and 30 °C.

Table A. 7: Solubilities of normal fatty acids in various solvents at 20 and 30 °C.

	Grams acid per 100 grams solvent							
	Chloroform[a]		Acetone[b]		Benzene[b]		n-Hexane[c]	
Fatty acid	**20 °C**	**30 °C**	**20 °C**	**30 °C**	**20 °C**	**30 °C**	**20 °C**	**30 °C**
Caprylic acid	∞	∞	∞	∞	∞	∞	∞	∞
Nonylic acid	∞	∞	∞	∞	∞	∞	∞	∞
Capric acid	326	6550	**407***	4660	398	**8230#**	290	5150
Undecylic acid	485	∞	**706***	∞	663	∞	-	-
Lauric acid	83	207	60.5	218	**93.6**	**260#**	47.7	193
Tridecylic acid	**116***	315	78.6	316	117	**354#**	-	-
Myristic acid	**32.5***	78	15.9	42.5	29.2	**87.4#**	11.9	41.8
Pentadecylic acid	**38.1***	91	13.8	49.3	36.2	**103#**	14.0	60.2
Palmitic acid	**15.1***	**36.4#**	5.38	15.6	7.30	34.8	3.1	14.5
Heptadecylic acid	**17.8***	**42.6#**	4.28	14.6	9.23	42.1	2.9	17.4
Stearic acid	**6.0***	**17.5#**	1.54	4.93	2.46	12.4	0.5	4.3

* Bold values indicate the solvent with the best solubility at 20 °C for the specific fatty acid.

\# Bold and underlined values indicate the solvent with the best solubility at 30 °C for the fatty acid .

a. Hoerr & Ralston, 1944: 332.

b. Ralston & Hoerr, 1942: 550 – 552.

c. Hoerr & Harwood, 1951: 781.

From Table A.7 it is clear that the longer chain fatty acids are more soluble in chloroform. The Hansen solubility parameters also identified chloroform to be the best solvent, which is in agreement with the trend viewed in Table A.7.

The difference between dichloromethane and chloroform (trichloromethane) is the addition of an extra chloride atom. This chloride atom increases the polarizability of the chloroform molecule. Chloroform therefore has highly active electron acceptor atoms (Ralston & Hoerr, 1945: 172). These highly active electron acceptor atoms have the ability of forming hydrogen bonds with the fatty acid molecules (Sedgwick *et al.,* 1952: 335), which increases the solubility of the fatty acids in chloroform. Due to dichloromethane's smaller polarizability the formation of hydrogen bonds between the dichloromethane and the fatty acid molecules do not occur as freely as for the chloroform molecules. Gunstone (1967: 76) also identified chloroform as the most suitable solvent for the solvation of fatty acids.

A.1 References

Barton, A.F.M. 1983. CRC Handbook of Solubility Parameters and Other Cohesion Parameters. Boca Raton: CRC Press. 594 p.

Bhaskar, T., Sera, A., Muto, A. & Sakato, Y. 2008. Hydrothermal upgrading of wood biomass: Influence of the addition of K_2CO_3 and cellulose/lignin ratio. Fuel, 87: 2236 – 2242.

Boocock, D.G.B., Mackay, D., McPherson, M., Nadeau, S. & Thurier, R. 1979. Direct hydrogenation of hybrid poplar wood to liquid and gaseous fuels. The Canadian Journal of Chemical Engineering, 57: 98 – 101.

Boocock, D.G.B., Konar, S.K., Leung, A. & Ly, L.D. 1992. Fuels and chemicals from sewage sludge 1: The solvent extraction and composition of a lipid from a raw sewage sludge. Fuel, 71: 1283 – 1289.

Campbell, M.K. & Farrell, S.O. 2003. Biochemistry. 4th ed. United States of America: Thomson. 725 p.

Dote, Y., Inoue, S., Ogi, T. & Yokoyama, S. 1996. Studies on the direct liquefaction of protein-contained biomass: The distribution of nitrogen in the products. Biomass and Bioenergy, 11(6): 491 – 498.

Eager, R.L., Mathews, J.F. & Pepper, J.M. 1982. Liquefaction of Aspen Poplar Wood. The Canadian Journal of Chemical Engineering, 60: 289 – 294.

Erzengin, M. & Küçük, M.M. 1998. Liquefaction of sunflower stalk by using supercritical extraction. Energy Conversion Management, 39(11): 1203 – 1206.

Gunstone, F.D. 1967. An introduction to the chemistry and biochemistry of fatty acids and their glycerides. Bungay: Chapman and Hall. 209 p.

Hansen, C.M. 2007. Hansen solubility parameters: a user's handbook. 2nd ed. Boca Raton: CRC Press. 519 p.

Hoerr, C.W. & Harwood, H.J. 1951. Solubilities of high molecular weight aliphatic compounds in n-Hexane. Journal of Organic Chemistry, 16: 779 – 791.

Hoerr, C.W. & Ralston, A.W. 1944. The solubilities of the normal saturated fatty acids. II. Journal of Organic Chemistry, 9: 329 – 337.

Inoue, S., Dote, Y., Sawayama, S., Minowa, T., Ogi, T. & Yokoyama, S. 1994. Analysis of oil derived from liquefaction of Botryococcus Braunii. Biomass and Bioenergy, 6(4): 269 – 274.

Karaca F. & Bolat, E. 2002. Coprocessing of a Turkish lignite with a cellulosic waste material 2. The effect of coporcessing on liquefaction yields at different reaction pressures and sawdust/lignite ratios. Fuel Processing Technology, 75: 109 – 116.

Li, J., Wu, L. & Yang, Z. 2008. Analysis and upgrading of bio-petroleum from biomass by direct deoxy-liquefaction. Journal of Analytical and Applied Pyrolysis, 81: 199 – 204.

Li, J., Yang, J. & Liu, Z. 2008. Hydro-treatment of a direct coal liquefaction residue and its components. Catalysis Today, 130: 389 – 394.

Lide, D.R. 2006. CRC handbook of Chemistry and Physics: a ready-reference book of chemical and physical data. 87th edition. Boca Raton: Taylor & Francis.

Meier, D., Larimer, D.R. & Faix, O. 1986. Direct liquefaction of different lignocellulosics and their constituents 1: Fractionation, elemental composition. Fuel, 65: 910 – 915.

Minowa, T., Murakami, M., Dote, Y., Ogi, T. & Yokoyama, S. 1994. Effect of operating conditions on thermochemical liquefaction of ethanol fermentation stillage. Fuel, 73(4): 579 – 582.

Pütün, E., Ateş, F. & Pütün, A.E. 2008. Catalytic pyrolysis of biomass in inert and steam atmospheres. Fuel, 87: 815 – 824.

Ralston, A.W. & Hoerr, C.W. 1942. The solubilities of the normal saturated fatty acids. Journal of Organic Chemistry, 7: 546 – 555.

Ralston, A.W. & Hoerr, C.W. 1945. Solubilities of binary mixtures of the saturated fatty acids. Journal of Organic Chemistry, 10(2): 170 – 174.

Ralston, A.W., Hoerr, C.W. & Crews, L.T. 1944. Solubilities of some normal saturated aliphatic hydrocarbons. Journal of Organic Chemistry, 9(4): 319 – 328.

Rezzoug, S. & Capart, R. 2002. Liquefaction of wood in two successive steps: solvolysis in ethylene-glycol and catalytic hydrotreatment. Applied Energy, 72: 631 – 644.

Rocha, J.D., Brown, S.D., Love, G.D. & Snape, C.E. 1997. Hydropyrolysis: a versatile technique for solid fuel liquefaction, sulphur speciation and biomarker release. Journal of Analytical and Applied Pyrolysis, 40 – 41: 91 – 103.

Schuchardt, U. & De Assis Pereira Matos, F. 1982. Liquefaction of sugar cane bagasse with formate and water. Fuel, 61: 106 – 110.

Sedgwick, R.S., Hoerr, C.W. & Harwood, H.J. 1952. Solubilities of saturated fatty acid esters. Journal of Organic Chemistry, 17(2): 327 – 337.

Skau, E.L. & Bailey, A.V. 1959. Correlation of solubility data for long chain compounds. II. The isopleth method of predicting solubilities of missing members of homologous series. Journal of Physical Chemistry, 63: 2047 – 2054.

Wang, G., Li, W., Li, B. & Chen, H. 2007a. Direct liquefaction of sawdust under syngas. Fuel, 86: 1587 – 1593.

Wang, G., Li, W., Li, B., Chen, H. & Bai, J. 2007b. Direct liquefaction of sawdust under syngas with and without catalyst. Chemical Engineering and Processing, 46: 187 – 192.

Xu, C. & Etcheverry, T. 2008. Hydro-liquefaction of woody biomass in sub- and super-critical ethanol with iron-based catalysts. Fuel, 87: 335 – 345.

Xu, C. & Lancaster, J. 2008. Conversion of secondary pulp/paper sludge powder to liquid oil products for energy recovery by direct liquefaction in hot-compressed water. Water Research, 42: 1571 – 1582.

Yan, Y., Xu, J., Li, T. & Ren, Z. 1999. Liquefaction of sawdust for liquid fuel. Fuel Processing Technology, 60: 135 – 143.

Yang, Y.F., Feng, C.P., Inamori, Y. & Maekawa, T. 2004. Analysis of energy conversion characteristics in liquefaction of algae. Resources, Conservation and Recycling, 43: 21 – 33.

Yokoyama, S., Ogi, T., Koguchi, K. & Nakamura, E. 1984. Direct liquefaction of wood by catalyst and water. Liquid fuels technology, 2(2): 155 – 163.

Appendix B. – Central composite design

B.1 Theoretical Background

Experiments can be conducted on various strategies. One approach to experimental design is to choose a random selection of factors and then test them to see what happens. This can be conducted indefinitely by continually changing one or two factors in order to determine an optimum configuration. This approach is called the best-guess approach (Montgomery, 1997: 3). Another approach to conduct experiments is to select a base case of factors and then to vary one factor at a time while keeping the other constant. This is called the one-factor-at-a-time approach. This approach does not consider any interaction between the factors (Montgomery, 1997: 4). The correct approach to experimental design of several variables is to conduct a factorial experiment. In this experimental strategy the factors are varied together, instead of one at a time. An experimental design with two factors that are varied at two levels is called a 2^2 factorial design (Montgomery, 1997: 5).

The factorial design investigates all the possible combinations of the levels of the factors in each complete trial or replication. The main effect of a factor is the change produced in the response by a change in the level of the factor (Montgomery, 1997: 228). The factorial design forms part of response surface methodology (RSM), which is defined as a collection of statistical and mathematical techniques. RSM provides a scientist or engineer with the relationship between the response of a product, process or system and the controllable input variables (Meyers & Montgomery, 1995: 1).

The results obtained from a 2k factorial design can be expressed in terms of a regression model. The first order regression model is:

$$y = \beta_0 + \beta_1 x_1 + \beta_2 x_2 + \varepsilon \tag{B.1}$$

where x_i is coded variables, ε is the error of the model and β_i are regression coefficients. The relationship between the coded variables and the natural variables are (Montgomery, 1997: 296):

$$x_i = \frac{\xi_i - \left(\xi_{Low} + \xi_{Hi}\right)/2}{\left(\xi_{Hi} - \xi_{Low}\right)/2} \tag{B.2}$$

The variables $\xi_1, \xi_2, \ldots, \xi_k$ in equation B.2 are called the natural variables, because they are the measured variables such as temperature, time, etc. In order to take into

account curvature in the results, interaction terms are added to the main effects or first-order model, resulting in (Montgomery, 1997: 336):

$$y = \beta_0 + \sum_{j=1}^{k} \beta_i x_i + \sum\sum_{i<j} \beta_{ij} x_i x_j + \varepsilon \tag{B.3}$$

The interaction term $\beta_{ij}x_ix_j$ produces a twist in the plane. In some cases the curvature in the response function may not be adequately modelled by equation B.3 and a second-order model must be used. The second-order equation is (Montgomery, 1997: 336):

$$\eta = \beta_0 + \sum_{j=1}^{k} \beta_j x_j + \sum_{j=1}^{k} \beta_{jj} x_j^2 + \sum\sum_{i<j} \beta_{ij} x_i x_j + \varepsilon \tag{B.4}$$

The addition of centre points to a 2^k factorial design provides protection against curvature from second-order effects and allows an independent estimate of error to be obtained. This is done by n replicates at the points $x_i = 0$ ($i = 1, 2,\ldots,k$). The addition of the centre points does not impact the usual effect estimates in a 2^k design (Montgomery, 1997: 336). In order to help with the solution of the regression model, the 2^k can be augmented by adding four axial runs. The resulting design is called the central composite design (CCD). Figures B.1 and B.2 shows the CCD for k = 2 and k = 3 factors, respectively.

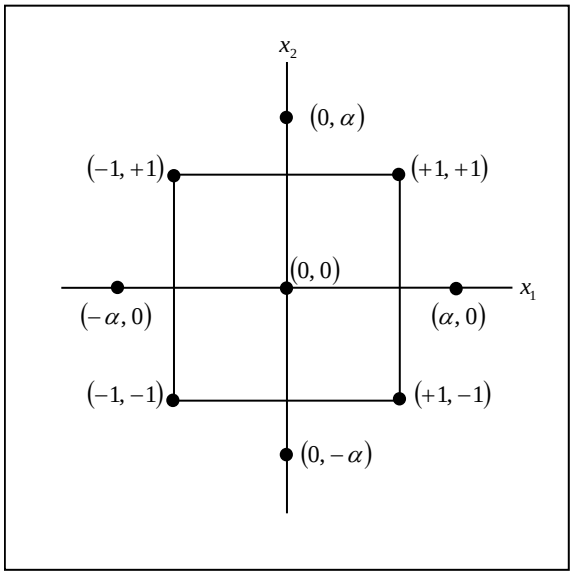

Figure B. 1: Central composite design for k = 2 factors (Montgomery, 1997: 601).

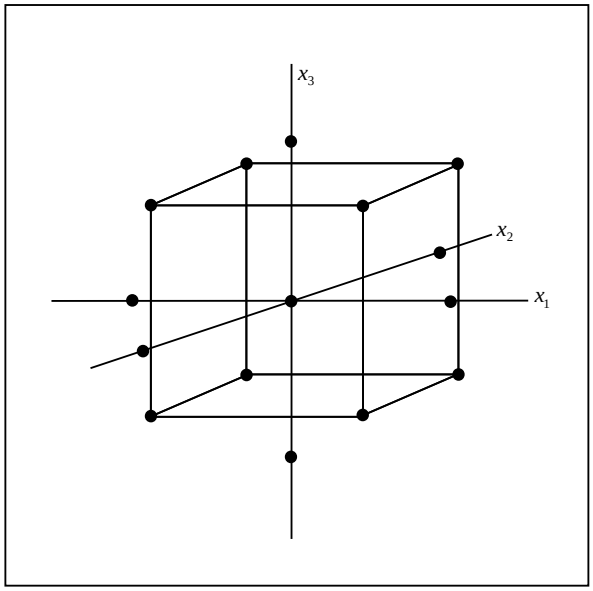

Figure B. 2: Central composite design for k = 3 factors (Montgomery, 1997: 601).

The central component design (CCD) generally consists of a 2k factorial design with n_f runs, 2k axial or star runs and n_c centre runs (Montgomery, 1997: 601). The total number of runs required for a CCD is therefore

$$n_t = 2^k + 2k + n_c \tag{B.5}$$

The value of *α*, depicted in Figure B.1, is the distance of the axial points from the centre point and the choice of *α* produces a variety of CCD's. A spherical CCD puts all the factorial and axial design points on the surface of a sphere of radius $\sqrt{k}$. Therefore, for a spherical CCD the value of *α* is $\sqrt{k}$ (Montgomery, 1997: 602). A face-centered CCD or face-centered cube locates the axial points on the faces of the cube and has an *α* value of 1 (Montgomery, 1997: 605). Figure B.3 shows a face-centered CCD for k = 3 factors.

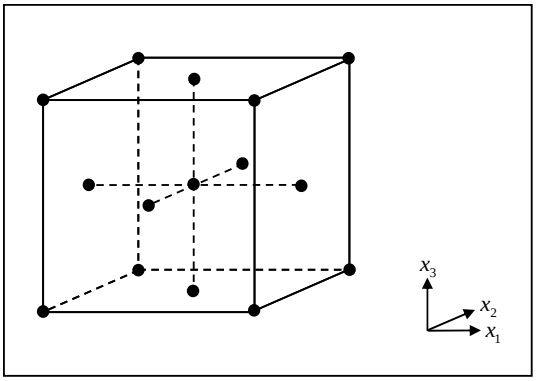

Figure B. 3: Face-centered CCD for k = 3 factors (Montgomery, 1997: 605).

In this study a face-centered CCD was used with 3 factors. The experimental design therefore correlates with Figure B.3.

B.2 Application of CCD on experimental data

Design-Expert® Version 7.1.5 was used to complete an analysis of variance (ANOVA). Section B.2.1 evaluates the ANOVA of the oil yield, whereas Section B.2.2 evaluates the ANOVA of the oil composition. In Section B.1 it is noted that the natural variables should be transformed to coded variables according to Equation B.2. Table B.1 shows the relationship between the natural variables and their coded variables.

Table B. 1: Assigned variables for ANOVA analysis and their coded levels.

Manipulated variable	**Assigned**	**Coded levels**		
	Variable	**-1**	**0**	**1**
Temperature (°C)	X_1	260	300	340
Catalyst load (wt%)	X_2	0	5	10
Residence Time (min)	X_3	15	30	45

Second degree polynomials where used to model the predicted response. These polynomials include all the interaction terms as follows:

$$Y = \beta_0 + \sum \beta_i X_i + \sum \beta_{ii} X_i^2 + \sum \beta_{ij} X_i X_j \,, \qquad \text{(B.6)}$$

where Y represents the response variable, β_0 is the interception coefficient, β_i is the coefficient of linear effect, β_{ii} is the coefficient of quadratic effect and β_{ij} is the coefficient of interaction effect. These coefficients were determined through multiple regressions and may be evaluated in terms of their magnitude and sign to evaluate

their influence on the response variable. Table B.2 shows the various response variables evaluated in this study as well as variables that have been assigned to them by Design-Expert® Version 7.1.5.

Table B. 2: Response variables evaluated in study.

Response variable	Assigned Variable
Oil yield (wt%)	Y_1
Oil composition (wt% C_{16} methyl esters)	Y_2

In order to determine the oil yield (Y_1) the following equation is used:

$$Oil\ yield\ (wt\%) = \frac{Mass\ oil}{Mass\ of\ algae} \times 100\% \qquad (B.7)$$

An F-test was employed to determine the statistical significance of the quadratic polynomial. The performance of the quadratic polynomial obtained from regression was evaluated by determining the determination coefficient of correlation, R^2.

Table B.3 shows the data that was entered into Design-Expert® Version 7.1.5 in order to obtain the various analyses of variance.

Table B. 3: Data entered in Design-Expert®.

	Coded variables			Response variables	
Run number	**X_1**	**X_2**	**X_3**	**Yield (wt%)**	**wt% C_{16}**
1	-1	1	1	10.50	6.72%
2	1	1	1	12.77	10.66%
3	-1	-1	-1	14.20	4.35%
4	0	0	0	14.50	6.98%
5	-1	1	-1	11.40	5.84%
6	1	-1	1	14.47	6.51%
7	-1	-1	1	15.13	5.14%
8	0	0	0	14.27	6.55%
9	0	0	0	14.80	7.43%
10	1	1	-1	12.83	9.14%
11	1	0	0	13.30	5.96%
12	0	0	0	15.77	4.81%
13	0	0	1	16.03	6.01%
14	0	1	0	14.07	6.72%
15	0	0	0	15.07	6.19%
16	-1	0	0	14.70	3.10%
17	0	-1	0	15.60	5.63%
18	1	-1	-1	14.00	9.34%
19	0	0	0	14.17	5.93%
20	0	0	-1	13.77	4.92%

B.2.1 Oil yield ANOVA

A suitable model is required to perform an analysis of variance on the oil yield. Design-Expert® Version 7.1.5 suggested a quadratic model for the ANOVA of the oil yield. The quadratic model has the ability of evaluating the interaction between the various manipulated variables. Table B.4 shows the ANOVA results obtained from Design-Expert® Version 7.1.5.

Table B. 4: ANOVA for fitted quadratic polynomial model of the oil yield.

	Sum of Squares	**Mean Square**	**F Value**	**p-value Prob > F**
Model	29.798	3.311	5.071	0.009[a]
X_1	0.207	0.207	0.318	0.586
X_2	13.995	13.995	21.436	0.001[a]
X_3	0.729	0.729	1.117	0.316
X_1X_2	2.599	2.599	3.981	0.074[c]
X_1X_3	0.018	0.018	0.028	0.871
X_2X_3	0.696	0.696	1.066	0.326
X_1^2	3.597	3.597	5.509	0.041[b]
X_2^2	0.262	0.262	0.401	0.541
X_3^2	0.163	0.163	0.250	0.628
Residual	6.529	0.653		
Lack of Fit	4.755	0.951	2.681	0.152
Standard deviation		0.81		
Mean		14.07		
Coefficient of variation		5.74		
R^2		0.820		
Adjusted R^2		0.659		
Adequate Precision		7.946		

a. Statistically significant at 99% probability level; b. Statistically significant at 95% probability level; c. Statistically significant at 90% probability level.

The ANOVA assigns a p-value to every parameter in the model. These p-values are used to evaluate the significance of the parameters on the response. From Table B.4 the p-value of the total model is 0.009. This indicates that the quadratic model is statistically significant at a 99% probability level, i.e. the quadratic model fits the data.

The evaluation of the p-value assigned to the lack of fit (0.152) reaffirms the fit of the quadratic model and indicates that the lack of fit is not statistically significant. The validity of the model is also confirmed by a coefficient of variation of 5.74% and a R^2 value of 0.820. The coefficient of variation is defined as the error of the model expressed as a percentage of the mean, whereas the R^2 value is a measure of the variation around the mean that is explained by the model.

Various statistical methods were used to validate the quadratic model. Figure B.4 shows that the Normal plot of residuals may be approximated by a straight line. This indicates a good model correlation. Evaluation of the standardized error values (studentized residuals) in correlation with the predicted values from the model in Figure B.5 show significant scatter, which indicates that the model fits the data in whole design range.

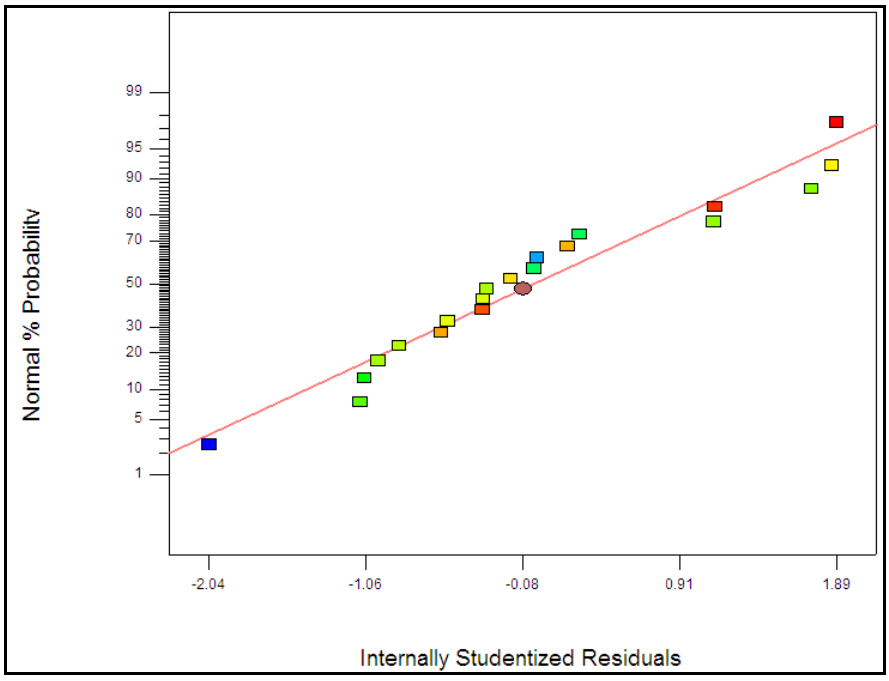

Figure B. 4: Normal plot of residuals for oil yield.

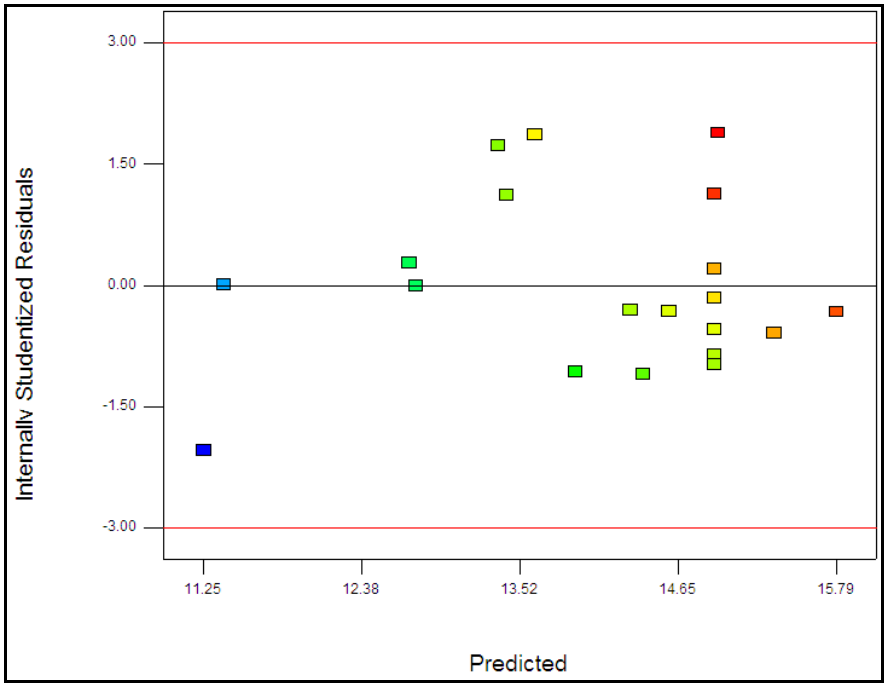

Figure B. 5: Internally studentized residuals versus predicted values for the oil yield.

Multiple regression of Equation B.6 by Design-Expert® Version 7.1.5 produces the following quadratic equation that relates the coded variables to the oil yield:

$$\begin{aligned} Oil\ yield\ (wt\%) = {} & 14.915 + 0.144X_1 - 1.183X_2 + 0.27X_3 + 0.57X_1X_2 + 0.048X_1X_3 \\ & - 0.295X_2X_3 - 1.144X_1^2 - 0.209X_2^2 - 0.244X_3^2 \end{aligned} \quad \text{(B.8)}$$

Equation B.8 may be rewritten in order to take into account the units of the variables. This produces the following equation:

$$\begin{aligned} Oil\ yield\ (wt\%) = {} & -46.737 + 0.416 \times Temperature - 0.850 \times Catalyst\ load \\ & + 0.079 \times \mathrm{Re}\,sidence\ Time + 0.003 \times Temperature \times Catalyst\ load \\ & + 7.92 \times 10^{-5} \times Temperature \times \mathrm{Re}\,sidence\ Time \\ & - 0.004 \times Catalyst\ load \times \mathrm{Re}\,sidence\ Time - 0.001 \times Temperature^2 \\ & - 0.012 \times Catalyst\ load^2 - 0.001 \times \mathrm{Re}\,sidence\ Time^2 \end{aligned} \quad \text{(B.9)}$$

B.2.2 Oil composition analysis of variance

A quadratic model was also selected for the oil composition in order to evaluate the interaction between the various manipulated variables. Table B.5 shows the ANOVA results obtained from Design-Expert® Version 7.1.5.

Table B. 5: ANOVA for fitted quadratic polynomial model of the oil composition.

	Sum of Squares	Mean Square	F Value	p-value Prob > F
Model	45.834	5.093	3.912	0.022[b]
X_1	27.093	27.093	20.814	0.001[a]
X_2	6.577	6.577	5.053	0.048[b]
X_3	0.210	0.210	0.162	0.696
X_1X_2	0.097	0.097	0.074	0.791
X_1X_3	1.110	1.110	0.853	0.378
X_2X_3	2.464	2.464	1.893	0.199
X_1^2	0.556	0.556	0.427	0.528
X_2^2	3.930	3.930	3.019	0.113
X_3^2	0.648	0.648	0.498	0.497
Residual	13.017	1.302		
Lack of Fit	8.847	1.769	2.122	0.214

Standard deviation	1.14
Mean	6.40
Coefficient of variation	17.84
R^2	0.779
Adjusted R^2	0.580
Adequate Precision	7.712

a. Statistically significant at 99% probability level; b. Statistically significant at 95% probability level

The ANOVA results in Table B.5 show a p-value of 0.022 for the quadratic model. This shows that the quadratic model is statistically significant at a 95% probability level. In Table B.5 a p-value of 0.214 is assigned to the lack of fit, which indicates that the lack of fit is not significant, i.e. the model fits the liquefaction data. The soundness of the model is also confirmed by a coefficient of variation of 17.84% and a R^2 value of 0.779. R^2 and coefficient of variation are defined as in Section B.2.1.

The strength of the model may also be evaluated by various statistical methods. Figure B.6 shows that the Normal plot of residuals may be approximated by a straight line, which indicates a good model correlation and the evaluation of the standardized error values (internally studentized residuals) in correlation with the predicted values from the model in Figure B.7 shows noteworthy scatter. As mentioned in Section B.2.1 the scatter shows that the model fits the data in the whole design range.

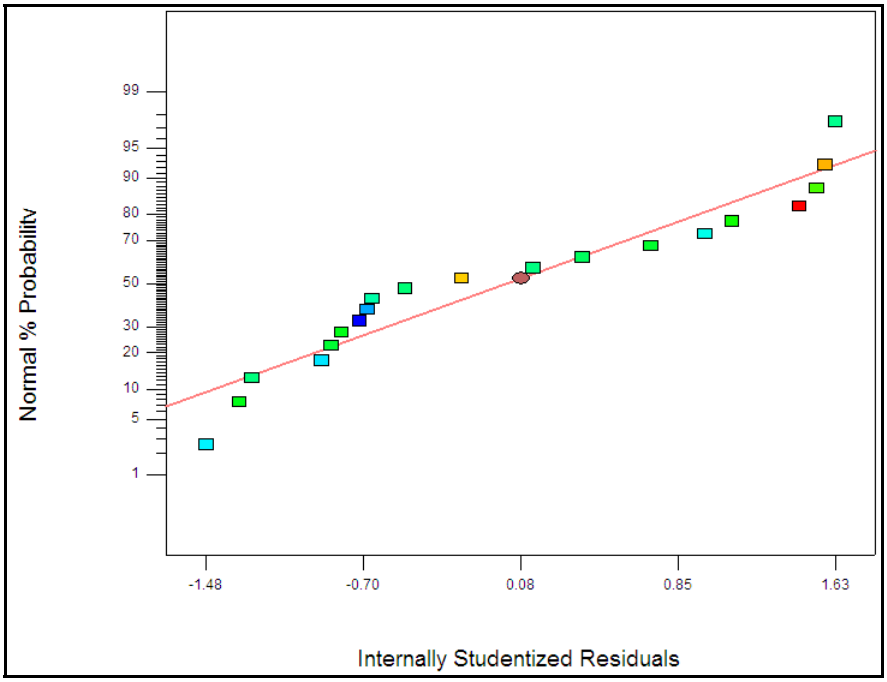

Figure B. 6: Normal plot of residuals for oil composition.

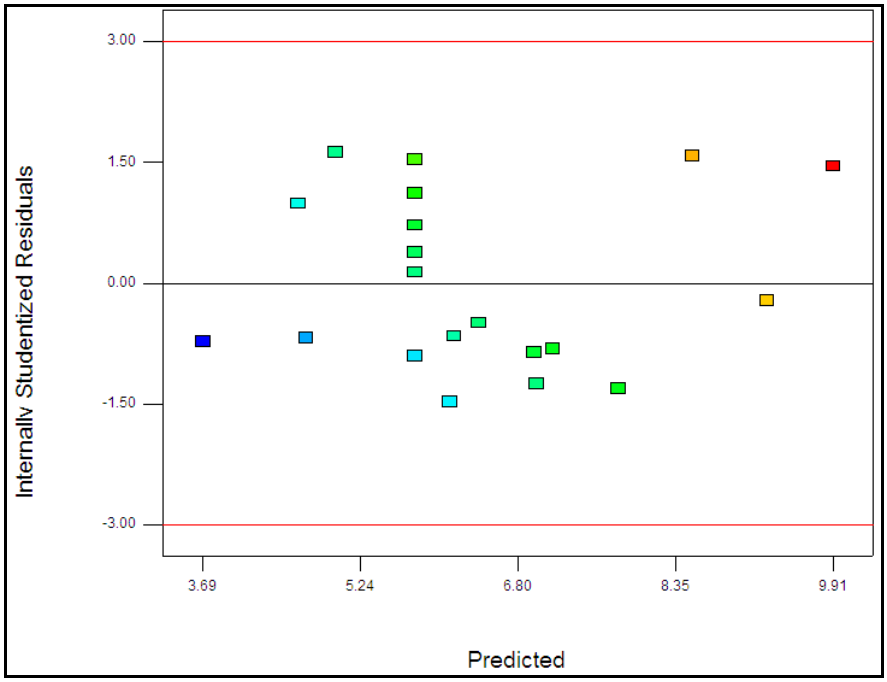

Figure B. 7: Internally studentized residuals versus predicted values for the oil composition.

Multiple regression of Equation B.6 by Design-Expert® Version 7.1.5 produces the following quadratic equation that relates the coded variables to the oil composition:

$$\begin{aligned} Wt\%\ C_{16}\ esters = {} & 5.781 + 1.646X_1 + 0.811X_2 + 0.145X_3 + 0.11X_1X_2 \\ & - 0.373X_1X_3 + 0.555X_2X_3 - 0.450X_1^2 + 1.195X_2^2 \\ & + 0.485X_3^2 \end{aligned} \tag{B.10}$$

Equation B.10 may be rewritten in order to take into account the units of the variables. This produces the following equation:

$$\begin{aligned} Wt\%\ C_{16}\ esters = {} & -33.467 + 0.226 \times Temperature - 0.703 \times Catalyst\ load \\ & + 0.029 \times \mathrm{Re}\, sidence\ Time \\ & + 0.001 \times Temperature \times Catalyst\ load \\ & - 0.001 \times Temperature \times \mathrm{Re}\, sidence\ Time \\ & + 0.007 \times Catalyst\ load \times \mathrm{Re}\, sidence\ Time \\ & - 2.810 \times 10^{-4} \times Temperature^2 + 0.048 \times Catalyst\ load^2 \\ & + 0.002 \times \mathrm{Re}\, sidence\ Time^2 \end{aligned} \tag{B.11}$$

B.3 Summary of CCD results

The ANOVA for the oil yield and the oil composition produced Equations B.8 and B.10 as stated below. These equations relate the oil yield and oil composition to the manipulated variables as defined in Section B.2.

$$\begin{aligned} Oil\ yield\ (wt\%) = {} & 14.915 + 0.144X_1 - 1.183X_2 + 0.27X_3 + 0.57X_1X_2 + 0.048X_1X_3 \\ & - 0.295X_2X_3 - 1.144X_1^2 - 0.209X_2^2 - 0.244X_3^2 \end{aligned} \tag{B.12}$$

$$\begin{aligned} Wt\%\ C_{16}\ methyl\ esters = {} & 5.781 + 1.646X_1 + 0.811X_2 + 0.145X_3 + 0.11X_1X_2 \\ & - 0.373X_1X_3 + 0.555X_2X_3 - 0.450X_1^2 + 1.195X_2^2 \\ & + 0.485X_3^2 \end{aligned} \tag{B.13}$$

The sensitivity analysis in Figure B.8 identifies the manipulated variables which affect the oil yield the most, while Figure B.9 shows the sensitivity analysis that was conducted for the oil composition.

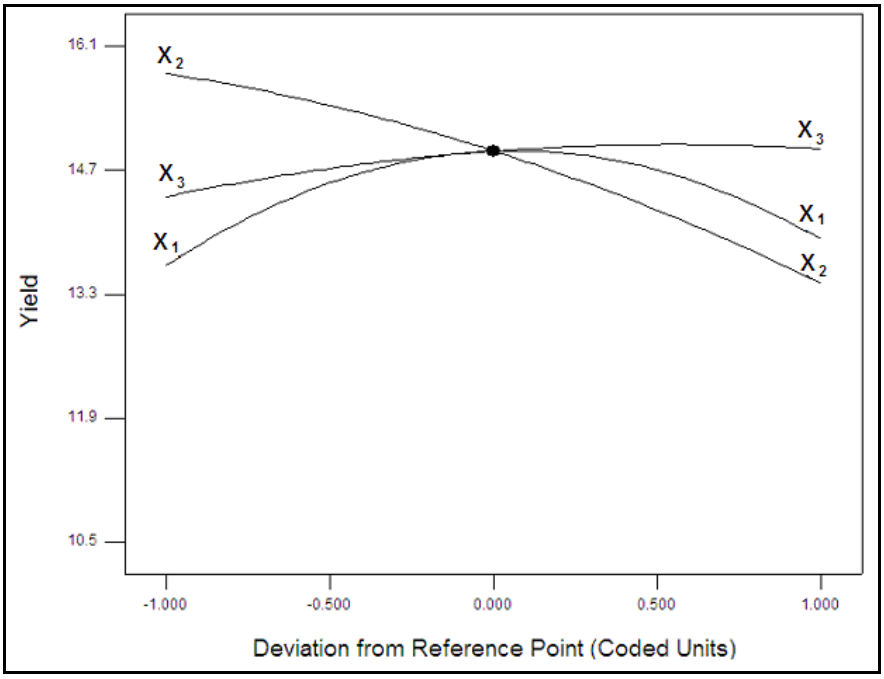

Figure B. 8: Sensitivity analyses for the oil yield.

(A – Temperature; B – Catalyst load; C – Residence Time)

Figure B.8 indicates that the catalyst load had the biggest effect on the oil yield that was obtained from the thermochemical liquefaction experiments. This is confirmed by the magnitude of the coefficient for the catalyst load in Equation B.8. The oil yield has a quadratic dependence on the reaction temperature as can be seen from the shape of the curve in Figure B.8 and by the magnitude of the coefficient of the square of the reaction temperature in Equation B.8. The residence time is the manipulated variable which had the smallest effect on the oil yield.

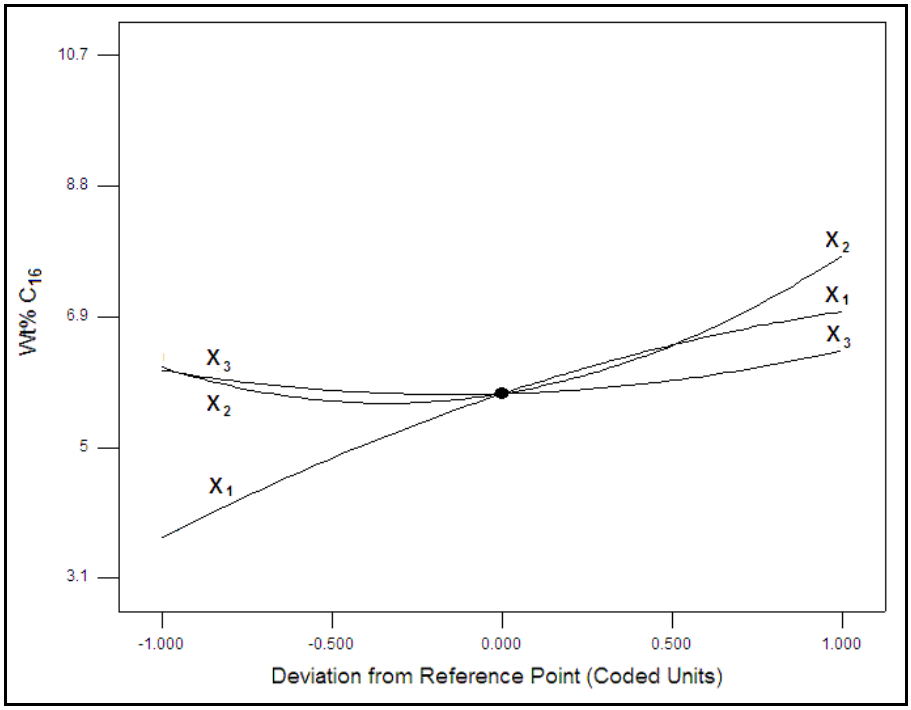

Figure B. 9: Sensitivity analyses for the oil composition.

(A – Temperature; B – Catalyst load; C – Residence Time)

The shape of the curves in Figure B.9 shows that there was a significant quadratic influence of the catalyst load on the oil composition. The reaction temperature is the manipulated variable that had the biggest effect on the oil composition. This is confirmed by the magnitude of the coefficient of the reaction temperature in Equation B.10. The catalyst load had the second largest effect on the oil composition. The catalyst load had an inverse effect on the oil composition compared to the oil yield. An increase in the catalyst load produced an increase in the C_{16} ester content of the algal oil. The residence time had a negligible effect on the composition of the algal oil.

The CCD study showed that from the three manipulated variables evaluated in this study, the reaction temperature and the catalyst load where the only two variables that significantly influenced the thermochemical liquefaction process.

B.4 References

Montgomery, D.C. 1997. Design and Analysis of Experiments. 4th ed. New York: John Wiley & Sons. 704 p.

Myers, R.H. & Montgomery, D.C. 1995. Response Surface Methodology: Process and product optimization using designed experiments. New York: John Wiley & Sons, Inc. 700 p.

Appendix C. – Design of autoclave

C.1 Pressure requirement of autoclave

The pressure generated inside the autoclave is dependent on the reaction temperature. This is illustrated by the phase diagram of water as given in Figure C.1 (Peterson *et al.,* 2008: 35).

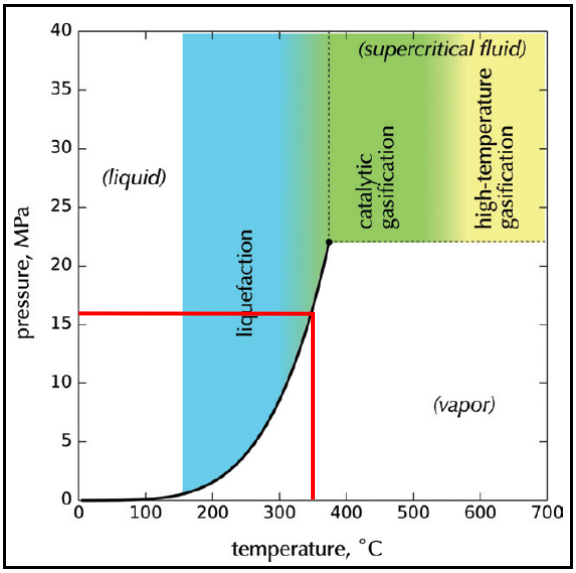

Figure C. 1: Phase diagram of water.

The highest temperature at which thermochemical liquefaction is performed, is 340 °C. From Figure C.1 an estimate of the operating pressure of the autoclave may be obtained. At 340 °C the theoretical operating pressure is approximately 155 bar. Therefore the autoclave is designed for a maximum operating pressure of 200 bar.

C.2 Design of vessel shell

The thickness of the vessel shell under internal pressure was calculated using equations from UG-27 of ASME VIII (ASME, 1983). The shell of the autoclave is constructed from stainless steel 316 and the material form is a seamless pipe. The required shell thickness is the maximum of the longitudinal and the circumferential stress thicknesses as calculated by the following equations:

$$t_{longitudinal} = \frac{PR_i}{2SE + 0.4P} \qquad \text{(C.1)}$$

$$t_{cicumferential} = \frac{PR_i}{SE - 0.6P} \quad \text{(C.2)}$$

where: P = Internal design pressure (bar)

R_i = Inside radius of shell (mm)

S = Maximum allowable stress value at 400 °C

E = Joint efficiency (E = 1, typical)

Table C.1 shows the information of the maximum allowable stress at various temperatures for stainless steel 316 as obtained from ASME VIII (ASME, 1983). Interpolation in Table C.1 produces the maximum allowable stress for stainless steel at 400 °C.

Table C. 1: Maximum allowable stress at various temperatures.

Temperature (°F)	**Maximum allowable stress (ksi)**
300	20
400	19.3
500	18
600	17
650	16.6
700	16.3
750	16.1
800	15.9
850	15.7
900	15.6
950	15.4
1000	15.3
1050	15.1
1100	12.4

Table C.2 shows the dimensions of the autoclave.

Table C. 2: Dimensions of the autoclave.

Dimension	Size
Length	150 mm
Inside radius	45 mm
Volume	0.954 L

The autoclave was designed for an internal pressure of 200 bar and a reaction temperature of 400 °C. At this temperature the maximum allowable stress value of stainless steel 316 is 1109.5 bar. The longitudinal and the circumferential stress thicknesses are calculated by Equations C.1 and C.2 to be 3.915 mm and 9.095 mm respectively. The shell thickness must therefore be 9.095 mm in order to withstand the conditions as specified above. A corrosion allowance of 3 mm is added to the shell thickness, which results in a theoretical shell thickness of 12.095 mm. The nominal shell thickness to be used is 15 mm. Figures C.2 and C.3 show mechanical drawings of the body of the autoclave and the lid of the autoclave, respectively.

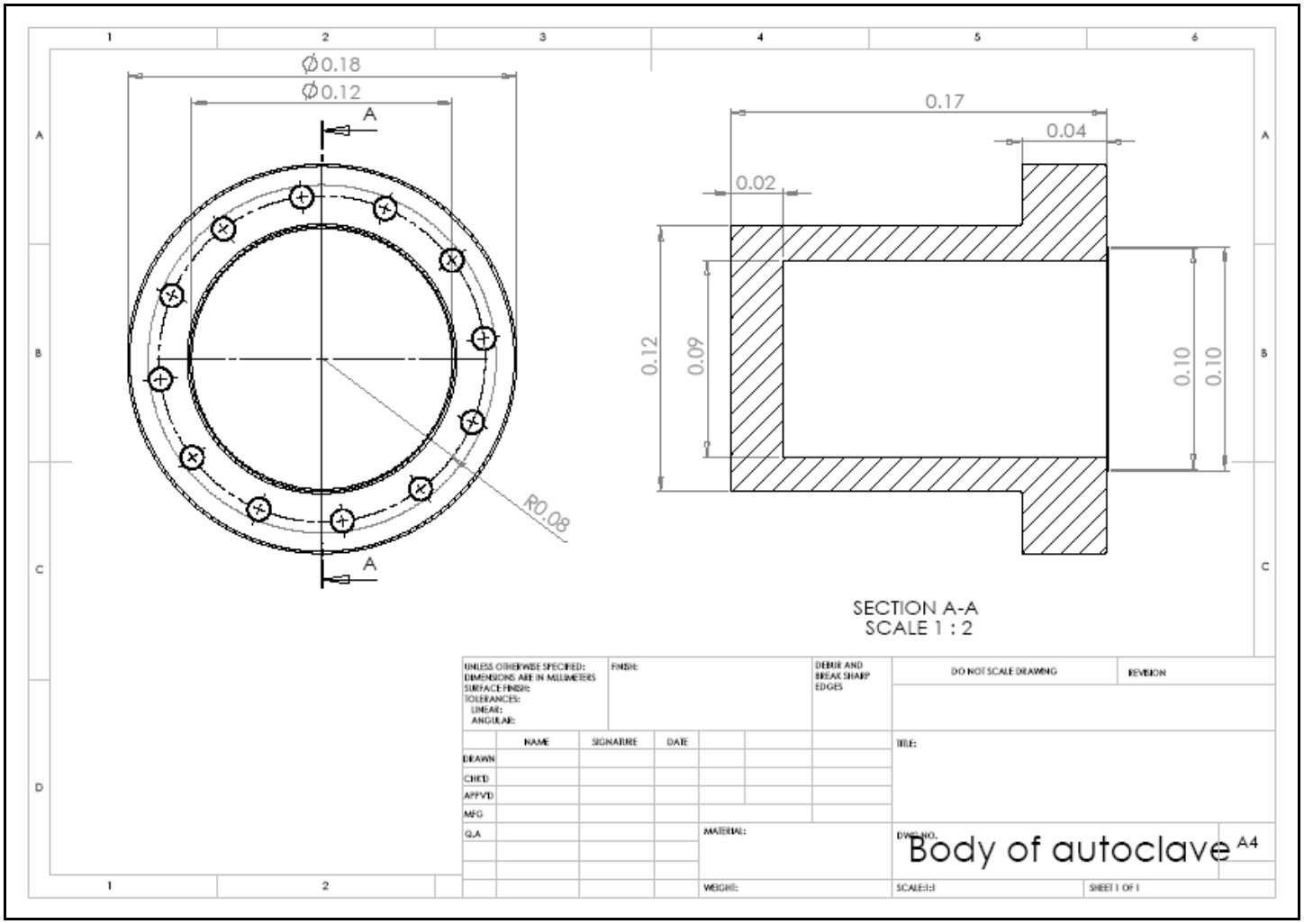

Figure C. 2: Body of the autoclave.

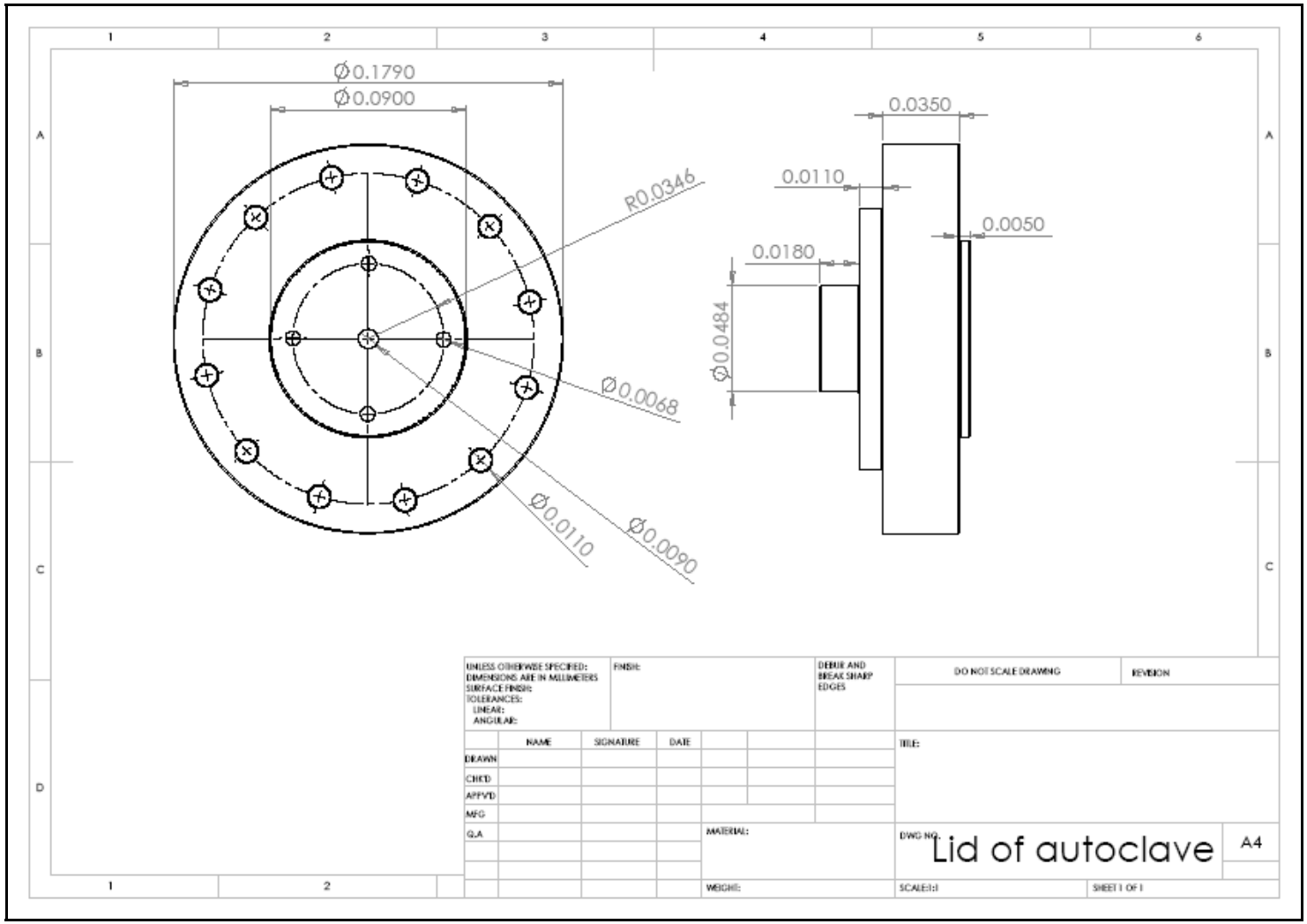

Figure C. 3: Lid of autoclave.

C.3 Bolt requirement

In order to determine the amount of bolts that is required for the top plate the forces that are exerted on the top plate must be evaluated. Table C.3 shows the calculations to obtain the force exerted on the top plate.

Table C. 3: Force exerted on top plate.

Property	Value
Maximum design pressure	200 bar
Area of lid under pressure	0.0064 m^2
Force exerted on top plate	127.23 kN

The bolts that are used are constructed from high-tensile steel. The bolts are M10 allen cap bolts with a length of 60 mm. One bolt has a tensile strength of 47 kN. The autoclave is equipped with 12 bolts. This produces a total tensile strength of 564 kN, which is greater than the force that is exerted on the top plate.

C.4 References

ASME (American Society of Mechanical Engineers). 1983. ASME boiler and pressure vessel code: an American national standard. Section VIII, Rules for construction of pressure vessels. Division 1. New York.

Peterson, A.A., Vogel., F., Lachance, R.P., Fröling, M., Antal., M.J. & Tester, J.W. 2008. Thermochemical biofuel production in hydrothermal media: A review of sub- and supercritical water technologies. Energy and Environmental Science, 1: 32 – 65.

Appendix D. – Gas chromatography

D.1 Identification of fatty acids

Gas chromatography standards of the fatty acids were obtained from Sigma Aldrich. In order to determine the retention time of the various fatty acids on the gas chromatograph 10 $g.L^{-1}$ solutions of the fatty acids in chloroform was prepared. These solutions were methylated according to the procedure discussed in section 3.4.3.2 and injected into the gas chromatograph. Table D.1 shows the retention times of fatty acids.

Table D. 1: Retention times of fatty acids.

Carbon number	Fatty acid	RetentionTime (min)
C6:0	Caproic acid	4.784
C7:0	Enanthic acid	6.269
C8:0	Caprylic acid	7.968
C9:0	Pelargonic acid	9.674
C10:0	Capric acid	11.466
C11:0	Undecylic acid	12.890
C12:0	Lauric acid	14.190
C13:0	Tridecylic acid	15.333
C14:0	Myristic acid	16.471
C15:0	Isopalmitic acid	17.470
C16:0	Palmitic acid	18.408
C16:1	Palmitoleic acid	17.914
C17:0	Margaric acid	19.417
C18:0	Stearic acid	20.374
C18:1 Trans	Elaidic acid	20.145
C18:1	Oleic acid	19.733
C18:1	Petroselinic acid	20.119
C18:2	Linoleic acid	19.660
C18:3	Linolenic acid	19.757
C19:0	Nonadecanoic acid	21.175
C20:0	Arachidic acid	22.038
C20:4	Arachidonic acid	21.147
C21:0	Heneicosanoic acid	22.807
C22:0	Behenic acid	23.600
C22:1	Erucic acid	23.406
C22:6	Docosahexanoic acid	22.670

D.2 Choice of external standard

The external standard used to quantify the components of the algal oil must be similar in structure to the components of the algal oil and it must have a similar retention time as the components of the algal oil. In the literature study it was found that even numbered fatty acids the only acids of any significance in algal cells (Miller, 1962: 358) and that these fatty acids range from C_{12} to C_{24} (Miller, 1962: 358) with the majority of the fatty acids that occur as C_{16} and C_{18} fatty acids (National Renewable Energy Laboratory, 1998: 31). To this end decanoic acid (C_{10} saturated fatty acid) was selected as an external standard.

D.3 Calibration of gas chromatograph

As mentioned in section D.2 the prevalent fatty acids in algal cells are C_{16} and C_{18} fatty acids (National Renewable Energy Laboratory, 1998: 31). Therefore calibration curves of the saturated C_{16} (palmitic acid) and C_{18} (stearic acid) fatty acids were obtained for the gas chromatograph. The calibration curves were prepared with a standard 5 $g.L^{-1}$ decanoic acid solution in chloroform.

In order to obtain the calibration curves for palmitic and stearic acid, solutions with varying concentrations of palmitic and stearic acid was injected on the gas chromatograph for analysis. The solutions therefore contain a fixed, known decanoic acid concentration and a varying palmitic and stearic acid concentration, respectively.

The detector of the gas chromatograph produces a peak of the relevant fatty acid at the corresponding residence time according to the abundance of the component in the sample. The gas chromatograph determines the areas of the various peaks. These areas may be used to quantify the components of the sample according to a mass balance. Table D.2 shows the concentrations of the various palmitic acid solutions as well as the corresponding areas, while Table D.3 shows the concentrations of the various stearic acid solutions as well as the corresponding areas.

Table D. 2: Palmitic acid solution concentrations and areas.

Concentration of C_{10} [g.L^{-1}]	Mass of C_{10} [g]	C_{10} Area [pA*s]	Concentration of C_{16} [g.L^{-1}]	Mass of C_{16} [g]	C_{16} Area [pA]
		Average			Average
5.000	0.050	**896.614**	1.000	0.010	**232.584**
5.000	0.050	**701.628**	2.000	0.020	**259.270**
5.000	0.050	**842.7096**	5.000	0.050	**886.525**
5.000	0.050	**1064.857**	10.000	0.100	**2392.162**
5.000	0.050	**1613.205**	20.000	0.200	**7154.055**
5.000	0.050	**1470.162**	40.000	0.400	**15398.633**

Table D. 3: Stearic acid solution concentrations and areas.

Concentration of C_{10} [g.L^{-1}]	Mass of C_{10} [g]	C_{10} Height [pA]	Concentration of C_{16} [g.L^{-1}]	Mass of C_{16} [g]	C_{16} Height [pA]
		Average			Average
5.000	0.050	**1223.279**	1.000	0.010	**0.000**
5.000	0.050	**1337.465**	2.000	0.020	**859.149**
5.000	0.050	**1473.745**	5.000	0.050	**1946.228**
5.000	0.050	**1787.216**	10.000	0.100	**4303.199**
5.000	0.050	**2163.564**	20.000	0.200	**10076.593**
5.000	0.050	**2813.206**	40.000	0.400	**30103.042**

The concentration of the decanoic acid remains constant for all the solutions noted in Tables D.2 and D.3. The mass balance for the palmitic, stearic and decanoic acids are as follows:

$$mass_{C_{10}\ solution} = mass_{C_{10}\ detected} \quad \text{(D.1)}$$

$$mass_{C_{16}\ solution} = mass_{C_{16}\ detected} \quad \text{(D.2)}$$

$$mass_{C_{18}\ solution} = mass_{C_{18}\ detected} \quad \text{(D.3)}$$

Mass can not be created nor destroyed, therefore the ratios of the palmitic and stearic acid to the decanoic acid in the solutions remains constant as well as the ratio of the areas determined by the gas chromatograph. Table D.4 shows the ratios of the palmitic and stearic acid to the decanoic acid for the various solutions.

Table D. 4: Mass and area ratios of the palmitic and stearic acids for the various solutions.

Concentration of C_{16} [g.L^{-1}]	$\frac{Mass\,C_{16}}{Mass\,C_{10}}$	$\frac{C_{16}\,area}{C_{10}\,area}$	Concentration of C_{18} [g.L^{-1}]	$\frac{Mass\,C_{18}}{Mass\,C_{10}}$	$\frac{C_{18}\,Area}{C_{10}\,Area}$
1.000	0.200	0.259	1.000	0.200	0.000
2.000	0.400	0.370	2.000	0.400	0.642
5.000	1.000	1.052	5.000	1.000	1.321
10.000	2.000	2.246	10.000	2.000	2.408
20.000	4.000	4.435	20.000	4.000	4.657
40.000	8.000	10.474	40.000	8.000	10.701

Plotting the area ratios of the palmitic and stearic acid respectively against the respective mass ratios produces a straight line through the origin. Figures D.1 and D.2 show the plots of the area and mass ratios for palmitic and stearic acid, respectively.

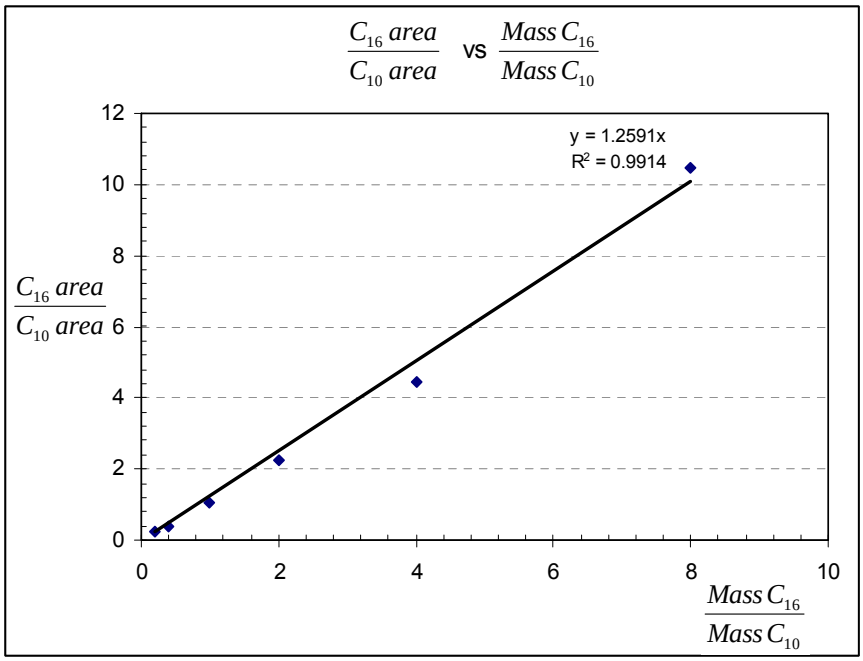

Figure D. 1: Area ratio of palmitic acid versus mass ratio of palmitic acid.

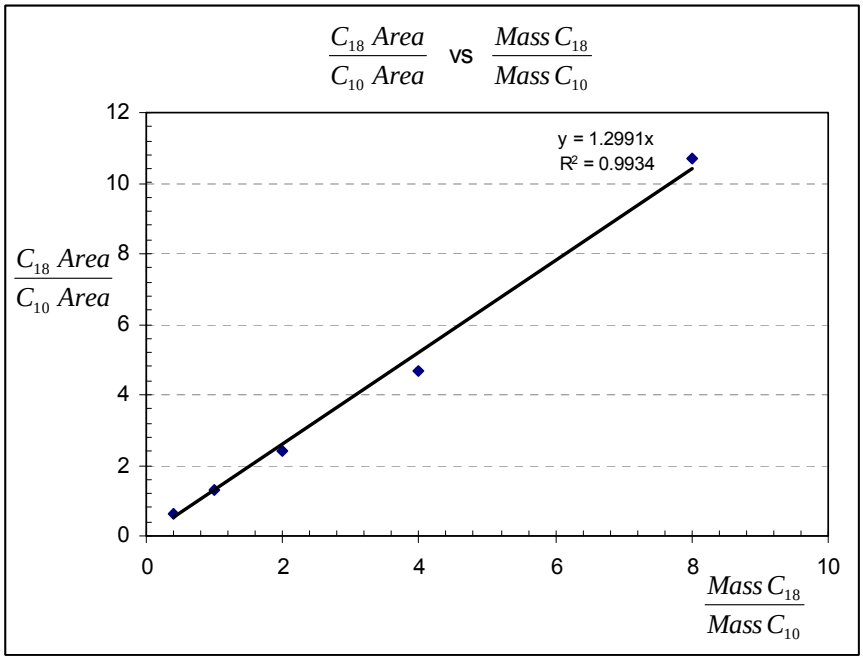

Figure D. 2: Area ratio of stearic acid versus mass ratio of palmitic acid.

From the mass balance the following holds true for the palmitic and stearic acid:

$$\frac{Mass\ C_{16}}{Mass\ C_{10}} = slope\ of\ \ curve\ of\ \ \frac{Mass\ C_{16}}{Mass\ C_{10}}\ vs\ \frac{Area\ C_{16}}{Area\ C_{10}}\ curve = \frac{Area\ C_{16}}{Area\ C_{10}} \quad \text{(D.4)}$$

$$\frac{Mass\ C_{18}}{Mass\ C_{10}} = slope\ of\ \ curve\ of\ \ \frac{Mass\ C_{18}}{Mass\ C_{10}}\ vs\ \frac{Area\ C_{18}}{Area\ C_{10}}\ curve = \frac{Area\ C_{18}}{Area\ C_{10}} \quad \text{(D.5)}$$

The slopes of the concerned curves are constant and determined from figures D.1 and D.2 for palmitic and stearic acid, respectively. Therefore the quantity of palmitic and stearic acid in a sample with an unknown composition can be calculated, seeing as the palmitic and stearic acid quantities are the only unknowns in equations D.4 and D.5, respectively.

D.4 References

Miller, J.D.A. 1962. Fats and Steroids. (In Lewin, R.A., ed. Physiology and Biochemistry of Algae. New York: Academic Press. p. 357 – 370.)

National Renewable Energy Laboratory. 1998. www.**nrel**.gov/docs/legosti/fy98/24190.pdf. Date of access: 22 May 2008.

Appendix E. – Calculations

Appendix E demonstrates the various calculations that were made to process the experimental data that was obtained. Section E.1 illustrates the calculation of the oil yield, whereas Section E.2 describes the calculation of the experimental error. Section E.3 shows the calculations for the gas chromatography. Section E.4 shows the calculation of the calorific value of the oil.

E.1 Calculation of the oil yield

The oil yield was calculated by the following equation:

$$Oil\ yield(wt\%) = \frac{m_{oil}}{m_{algae}} \qquad [B.1]$$

where m_{oil} is the mass of oil obtained from the experiment and m_{algae} is the mass of the algae with which the autoclave was charged.

E.2 Experimental error

In this section the methodology that was followed to calculate the various experimental errors are discussed. Section E.2.1 provides a description of the calculations that were used for the calculation of an experimental error of the thermochemical liquefaction experiments, whereas Sections E.2.2 and E.2.3 provides the calculations used to obtain the experimental error of the bomb calorimeter and elemental analyzer, respectively.

E.2.1 Experimental error for thermochemical liquefaction experiments

The experimental error was calculated for the experiments as stipulated in Section 4.2.1. The experimental error was calculated as follows:

- Step 1: Calculate the mean of the data set. This is done by the following equation:

$$\bar{x} = \frac{1}{N}\sum_{i=1}^{N} x_i \qquad [B.2]$$

  where N is the total number of data points and x_i is a individual data point.

- Step 2: Calculate the standard deviation of the data set as follows:

$$s = \sqrt{\frac{\sum_{i=1}^{N}\left(x_i - \bar{x}\right)^2}{N-1}} \qquad [B.3]$$

- Step 3: Calculate the standard error of the mean with the following equation:

$$standard\ error\ of\ the\ mean = SE = \frac{s}{\sqrt{N}} \qquad [B.4]$$

- Step 4: Calculate the z critical value for a 95% confidence level, i.e. there is a 95% probability the data points obtained from the experiments lies within the range of the calculated confidence interval. The z critical value is calculated as follows:

$$z = \frac{\bar{x} - \mu}{s/\sqrt{n}} \qquad [B.5]$$

  Where μ is the mean value for continuous variable x and n is the amount of data points.

- Step 5: Calculate the confidence interval with the following equation:

$$confidence\ interval = \bar{x} \pm \left(SE \times z\right) \qquad [B.6]$$

- Step 6: Calculate the experimental error with:

$$Experimental\ error = \frac{2 \times Confidence\ interval}{\bar{x}} \times 100 \qquad [B.7]$$

Table E.1 shows the calculation of the experimental error.

Table E. 1: Calculation of the experimental error.

Run number	Yield (wt%)	wt% C_{16}-methyl esters
Run 4	14.50	6.98%
Run 8	14.27	6.55%
Run 9	14.80	7.43%
Run 12	15.77	4.81%
Run 15	15.07	6.19%
Run 19	14.17	5.93%
Average	14.76	6.32
Standard deviation	0.60	0.91
z critical value	2.45	2.45
Experimental error (%)	8.06	28.82

E.2.2 Experimental error of bomb calorimeter

In order to determine the experimental error of the bomb calorimeter, a sample was analyzed three times. Table E.2 shows the calculations for the experimental error of the bomb calorimeter according to the procedure discussed in Section E.2.1.

Table E. 2: Experimental error of bomb calorimeter.

	Calorific value ($MJ.kg^{-1}$)
Run 1	20.723
Run 2	20.713
Run 3	20.715
Average	20.717
Stdev	0.005
z value	3.182
±	0.019
%Error	0.094

E.2.3 Experimental error of elemental analyzer

In order to determine the experimental error of the elemental analyzer, a sample was analyzed five times. Table E.3 shows the calculations for the experimental error of the elemental analyzer according to the procedure discussed in Section E.2.1.

Table E. 3: Experimental error of elemental analyzer.

Sample	wt% N	wt% C	wt% H	wt% S
N1 (1)	6.484	75.032	8.602	0.454
N1 (2)	6.449	74.797	8.574	0.436
N1 (3)	6.392	74.628	8.581	0.335
N1 (4)	6.454	74.649	8.669	0.417
N1 (5)	6.241	72.371	8.302	0.260
Average	6.4041	74.2955	8.5454	0.3803
Standard deviation	0.0969	1.0881	0.1413	0.0810
z critical value	2.5706	2.5706	2.5706	2.5706
±	0.2227	2.5016	0.3250	0.1863
% Error	3.4782	3.3672	3.8029	48.9856
Average weighted error			3.03419	%

Appendix F. – Experimental data

In this appendix the experimental data that was used in the study is listed. Section F.1 lists the oil yield data obtained from the thermochemical liquefaction experiments. In Section F.2 the gas chromatograph data is listed, whereas Section F.3 shows the data obtained from the elemental analyzer. Section F.4 lists the data obtained from the bomb calorimeter.

F.1 Oil yield data of thermochemical liquefaction experiments

Tables F.1.1, F.1.2 and F.1.3 list the oil yield data obtained from the thermochemical liquefaction experiments conducted on *M. aeruginosa, C. meneghinia and N. pusilla*, respectively.

Table F.1. 1: Oil yield data for thermochemical liquefaction of *Microcystis aeruginosa*.

Run number	Temperature (°C)	Wt% Catalyst	Residence Time (min)	Yield (wt%)
Run 1	260	10.00	00:45	10.50
Run 2	340	10.00	00:45	12.77
Run 3	260	0.00	00:15	14.20
Run 4	300	5.00	00:30	14.50
Run 5	260	10.00	00:15	11.40
Run 6	340	0.00	00:45	14.47
Run 7	260	0.00	00:45	15.13
Run 8	300	5.00	00:30	14.27
Run 9	300	5.00	00:30	14.80
Run 10	340	10.00	00:15	12.83
Run 11	340	5.00	00:30	13.30
Run 12	300	5.00	00:30	15.77
Run 13	300	5.00	00:45	16.03
Run 14	300	10.00	00:30	14.07
Run 15	300	5.00	00:30	15.07
Run 16	260	5.00	00:30	14.70
Run 17	300	0.00	00:30	15.60
Run 18	340	0.00	00:15	14.00
Run 19	300	5.00	00:30	14.17
Run 20	300	5.00	00:15	13.77

Table F.1. 2: Oil yield data for thermochemical liquefaction of *Cyclotella meneghinia.*

Run number	Temperature (°C)	Wt% Catalyst	Residence Time (min)	Yield (wt%)
Run 1	260	0.00	00:30	11.93
Run 2	300	0.00	00:30	15.53
Run 3	340	0.00	00:30	12.83
Run 4	260	5.00	00:30	12.40
Run 5	300	5.00	00:30	15.53
Run 6	340	5.00	00:30	16.03
Run 7	260	10.00	00:30	12.87
Run 8	300	10.00	00:30	13.77
Run 9	340	10.00	00:30	13.37
Run 10	280	5.00	00:30	11.70
Run 11	320	5.00	00:30	15.60

Table F.1. 3: Oil yield data for thermochemical liquefaction of *Nitzschia pusilla.*

Run number	Temperature (°C)	Wt% Catalyst	Residence Time (min)	Yield (wt%)
Run 1	260	5.00	00:30	10.63
Run 2	300	5.00	00:30	14.10
Run 3	340	5.00	00:30	15.53
Run 4	260	0.00	00:30	12.20
Run 5	300	0.00	00:30	14.70
Run 6	340	0.00	00:30	15.33
Run 7	260	10.00	00:30	9.30
Run 8	300	10.00	00:30	13.80
Run 9	340	10.00	00:30	13.93
Run 10	280	5.00	00:30	11.57
Run 11	320	5.00	00:30	14.17

F.2 Gas chromatograph data

Tables F.2.1, F.2.2 and F.2.3 list the gas chromatograph data obtained from the thermochemical liquefaction experiments conducted on *M. aeruginosa, C. meneghinia and N. pusilla*, respectively.

Table F.2. 1: Gas chromatograph data for thermochemical liquefaction of *Microcystis aeruginosa*.

Run number	Temperature (°C)	Wt% Catalyst	Residence Time (min)	Area C_{10}		Area C_{16}		Average wt% C_{16}
				Analysis 1	Analysis 2	Analysis 1	Analysis 2	
Run 1	260	10.00	00:45	5366.80	7567.55	2374.15	3155.95	6.72%
Run 2	340	10.00	00:45	5086.55	6525.71	2374.15	3155.95	10.66%
Run 3	260	0.00	00:15	4665.64	5120.79	1831.24	2031.69	4.35%
Run 4	300	5.00	00:30	6570.59	4906.79	4181.70	3235.59	6.98%
Run 5	260	10.00	00:15	6637.10	4598.46	2577.37	1968.37	5.84%
Run 6	340	0.00	00:45	5470.16	7722.95	3354.32	4634.17	6.51%
Run 7	260	0.00	00:45	5959.38	7964.02	3129.45	3986.71	5.14%
Run 8	300	5.00	00:30	5884.99	6135.55	3883.69	3730.24	6.55%
Run 9	300	5.00	00:30	9260.06	4937.38	6487.40	3602.83	7.43%
Run 10	340	10.00	00:15	8706.73	6073.74	6196.05	4562.63	9.14%
Run 11	340	5.00	00:30	6006.21	4758.41	2946.75	2460.99	5.96%
Run 12	300	5.00	00:30	4017.33	5609.80	2035.24	2636.91	4.81%
Run 13	300	5.00	00:45	6467.09	6005.96	3877.24	3652.23	6.01%
Run 14	300	10.00	00:30	8093.05	7594.91	4848.75	4562.15	6.72%
Run 15	300	5.00	00:30	7375.65	7520.82	4445.12	4586.76	6.19%
Run 16	260	5.00	00:30	9048.85	9304.86	2548.57	2890.79	3.10%
Run 17	300	0.00	00:30	6164.03	6640.27	3217.97	4071.61	5.63%
Run 18	340	0.00	00:15	7326.86	5658.83	5369.16	4373.18	9.34%
Run 19	300	5.00	00:30	8086.39	7272.05	4209.12	3835.76	5.93%
Run 20	300	5.00	00:15	4225.40	5771.87	1842.94	2445.72	4.92%

Table F.2. 2: Gas chromatograph data for thermochemical liquefaction of *Cyclotella meneghinia.*

Run number	Temperature (°C)	Wt% Catalyst	Residence Time (min)	Area C_{10}		Area C_{16}		Average wt% C_{16}
				Analysis 1	Analysis 2	Analysis 1	Analysis 2	
Run 1	260	0.00	00:30	9905.89	10065.00	5492.24	5444.75	7.63%
Run 2	300	0.00	00:30	10040.70	9460.81	5325.25	5257.32	5.89%
Run 3	340	0.00	00:30	11670.30	12278.80	6860.34	7190.69	7.68%
Run 4	260	5.00	00:30	9143.72	9335.70	5121.43	5302.10	7.69%
Run 5	300	5.00	00:30	9732.20	9806.29	7380.90	7492.45	8.41%
Run 6	340	5.00	00:30	8286.24	9509.42	8303.11	8309.81	9.77%
Run 7	260	10.00	00:30	9507.44	7584.76	5826.78	5965.26	9.76%
Run 8	300	10.00	00:30	7589.35	9869.28	6062.49	7750.75	9.74%
Run 9	340	10.00	00:30	10165.70	9730.69	8198.20	6524.07	9.78%
Run 10	280	5.00	00:30	9774.07	10251.10	5978.36	6260.76	9.31%
Run 11	320	5.00	00:30	10096.70	10231.10	7890.30	8023.13	8.99%

Table F.2. 3: Gas chromatograph data for thermochemical liquefaction of *Nitzschia pusilla.*

Run number	Temperature (°C)	Wt% Catalyst	Residence Time (min)	Area C_{10}		Area C_{16}		Average wt% C_{16}
				Analysis 1	Analysis 2	Analysis 1	Analysis 2	
Run 1	260	5.00	00:30	1412.65	1177.91	933.60	687.18	9.38%
Run 2	300	5.00	00:30	1460.01	1193.97	1095.84	1028.95	9.78%
Run 3	340	5.00	00:30	1201.64	1477.23	1171.70	1458.88	10.43%
Run 4	260	0.00	00:30	1123.98	1581.32	813.56	1018.95	9.07%
Run 5	300	0.00	00:30	1549.26	829.55	1442.25	945.91	10.86%
Run 6	340	0.00	00:30	1307.23	840.05	1439.44	955.79	11.07%
Run 7	260	10.00	00:30	962.99	626.21	681.96	449.92	13.99%
Run 8	300	10.00	00:30	383.38	442.50	427.46	522.37	13.07%
Run 9	340	10.00	00:30	586.32	459.08	808.12	654.01	15.81%
Run 10	280	5.00	00:30	869.68	467.22	575.40	335.02	9.71%
Run 11	320	5.00	00:30	958.49	376.11	937.29	370.96	10.96%

F.3 Elemental analyzer data

Tables F.3.1, F.3.2 and F.3.3 list the elemental analyzer data of the oil obtained from the thermochemical liquefaction experiments conducted on *M. aeruginosa, C. meneghinia and N. pusilla*, respectively. Tables F.3.4, F.3.5 and F.3.6 list the average elemental analyzer data and calorific values of the oil obtained from the thermochemical liquefaction experiments conducted on *M. aeruginosa, C. meneghinia and N. pusilla*, respectively.

Tables F.3.7, F.3.8 and F.3.9 list the average elemental analyzer data of the *M. aeruginosa, C. meneghinia and N. pusilla*, respectively.

Table F.3. 1: Elemental analyzer data for the oil obtained from thermochemical liquefaction of *Microcystis aeruginosa*.

SAMPLE NAME	DATE	WEIGHT	Wt% N	Wt% C	Wt% H	Wt% S
H1 (1) Run1	09/02/2009	0.002069	5.0316515	66.0308456	7.4962578	0.1617035
H2 (1) Run 2	09/02/2009	0.002834	3.5197923	68.5225754	8.2410679	0.0000000
H3 (1) Run 3	09/02/2009	0.002618	5.7001495	66.9659195	7.8326998	0.3659711
H4 (1) Run 4	09/02/2009	0.003690	4.7901001	64.6084900	7.9385591	0.2988086
H5 (1) Run 5	09/02/2009	0.002463	5.7197614	66.8977280	7.7838430	0.0000000
H6 (1) Run 6	09/02/2009	0.003435	4.3698487	69.0341187	8.0227337	0.0000000
H7 (1) Run 7	09/02/2009	0.002061	5.6428585	70.1536942	8.1155777	0.3309947
H8 (1) Run 8	09/02/2009	0.002119	4.9180908	65.1677704	7.8808975	0.0000000
H9 (1) Run 9	09/02/2009	0.003555	5.2281165	67.4255600	8.0405102	0.2798102
H10 (1) Run 10	09/02/2009	0.002820	3.8656912	66.6356659	7.8963900	0.2848931
H11 (1) Run 11	09/02/2009	0.002993	4.4598112	66.1453552	7.7737870	0.2836767
H12 (1) Run 12	09/02/2009	0.003781	5.4326077	68.5446930	8.0437908	0.3018445
H13 (1) Run 13	09/02/2009	0.003856	4.7259450	63.9069939	7.6025157	0.3920666
H14 (1) Run 14	09/02/2009	0.002683	4.6616278	66.2729034	7.9918103	0.2901791
H15 (1) Run 15	09/02/2009	0.002588	4.7701092	65.1082687	8.0150270	0.2701890
H16 (1) Run 16	09/02/2009	0.003967	5.8363171	62.5150070	7.6102695	0.2618107
H17 (1) Run 17	09/02/2009	0.002489	4.9892054	66.0386810	7.7591386	0.3264862
H18 (1) Run 18	09/02/2009	0.003609	4.4001722	68.6893692	8.3967924	0.3546009
H19 (1) Run 19	09/02/2009	0.002213	4.8757286	63.1356163	7.4087510	0.2788026
H20 (1) Run 20	09/02/2009	0.003685	5.0083265	62.4511833	7.3601532	0.2527805
H1 (2) Run1	09/02/2009	0.002670	4.9177217	63.9406815	7.5891604	0.2001775
H2 (2) Run 2	09/02/2009	0.002002	3.6056886	68.8176422	8.0898972	0.1816783
H3 (2) Run 3	09/02/2009	0.002818	5.6362033	66.5368271	7.8359571	0.3659824

Table F.3.1 continued

SAMPLE NAME	DATE	WEIGHT	Wt% N	Wt% C	Wt% H	Wt% S
H4 (2) Run 4	09/02/2009	0.003215	4.7342238	64.1587601	7.8110800	0.3214295
H5 (2) Run 5	09/02/2009	0.002980	5.4515600	63.7286377	7.6500487	0.2581735
H6 (2) Run 6	09/02/2009	0.003310	4.4621463	70.0844193	7.9028082	0.2301034
H7 (2) Run 7	09/02/2009	0.002332	5.6856675	69.4759064	8.0746193	0.3794813
H8 (2) Run 8	09/02/2009	0.003513	4.8907166	64.3348007	8.0019045	0.3483879
H9 (2) Run 9	09/02/2009	0.002528	5.2942686	69.1378860	7.9227591	0.3164523
H10 (2) Run 10	09/02/2009	0.004111	3.8856840	65.7748947	7.9493012	0.2752533
H12 (2) Run 11	09/02/2009	0.002860	5.2628937	68.5495605	7.9583035	0.3583824
H11 (2) Run 12	09/02/2009	0.003446	4.5094299	66.7257385	7.8943992	0.3349567
H13 (2) Run 13	09/02/2009	0.002808	4.7276354	65.3927078	7.6324716	0.3842283
H14 (2) Run 14	09/02/2009	0.002424	4.5619240	65.2741165	7.9981451	0.3734330
H15 (2) Run 15	09/02/2009	0.002530	4.4790397	63.1596260	8.0065727	0.3111326
H16 (2) Run 16	09/02/2009	0.003102	5.4945836	60.3985138	7.4150915	0.3218639
H17 (2) Run 17	09/02/2009	0.003766	4.8038945	61.4901848	7.6126337	0.3297460
H18 (2) Run 18	09/02/2009	0.002842	4.6329303	71.2128143	8.1839924	0.3131927
H19 (2) Run 19	09/02/2009	0.003200	5.1618485	66.4410629	7.4414368	0.3540063
H20 (2) Run 20	09/02/2009	0.002995	5.3414712	65.2372513	7.3708739	0.3639946
H1 (3) Run 1	09/09/2009	0.002489	4.8143482	61.5828018	7.5093155	0.0000000
H2 (3) Run 2	09/09/2009	0.002531	3.5444953	69.3377457	8.2118549	0.0000000
H3 (3) Run 3	09/09/2009	0.003742	5.5478449	64.9661789	7.8576765	0.3288887
H4 (3) Run 4	09/09/2009	0.003024	4.6271276	63.1657791	7.9621639	0.3724626
H5 (3) Run 5	09/09/2009	0.002335	5.9819427	70.7046051	7.7977719	0.0000000
H6 (3) Run 6	09/09/2009	0.002631	4.4845347	69.8838043	7.9330807	0.2886692
H7 (3) Run 7	09/09/2009	0.003051	5.5968027	68.7494049	8.1567955	0.4201284
H8 (3) Run 8	09/09/2009	0.003454	5.0056434	65.5820313	8.1152134	0.3847342
H9 (3) Run 9	09/09/2009	0.002947	4.8089533	64.8329315	7.8395314	0.3108690
H10 (3) Run 10	09/09/2009	0.002889	4.3570995	68.8944473	7.8792396	0.3074187
H11 (3) Run 11	09/09/2009	0.003411	4.7375946	67.3020630	7.8908753	0.3670895
H12 (3) Run 12	09/09/2009	0.002748	5.4721899	68.8180008	8.0159683	0.3991916
H13 (3) Run 13	09/09/2009	0.002756	4.3499770	62.2586136	7.6865034	0.3328798
H14 (3) Run 14	09/09/2009	0.002758	4.5494075	65.3958893	8.0703611	0.3425453
H15 (3) Run 15	09/09/2009	0.003846	4.5863686	61.5981445	7.7733068	0.3626043
H16 (3) Run 16	09/09/2009	0.003053	6.2705011	69.3101807	7.6835027	0.4003536
H17 (3) Run 17	09/09/2009	0.003597	5.2424769	65.4224014	7.6962576	0.3815302
H18 (3) Run 18	09/09/2009	0.002402	4.4958940	71.4509964	8.3254194	0.3751805
H19 (3) Run 19	09/09/2009	0.002816	4.7581887	62.0879745	7.4402671	0.3436633
H20 (3) Run 20	09/09/2009	0.002691	4.8198485	60.0682182	7.2381968	0.3096713

Table F.3. 2: Elemental anzalyzer data for oil obtained from thermochemical liquefaction of *Cyclotella meneghinia.*

SAMPLE NAME	DATE	WEIGHT	Wt% N	Wt% C	Wt% H	Wt% S
C1 (1)	09/09/2009	0.002586	4.7914486	66.2153320	8.0850372	0.3518044
C2 (1)	09/09/2009	0.002858	4.2797608	65.2903366	8.0907011	0.4039488
C3 (1)	09/09/2009	0.003213	4.5953274	71.0549622	8.1460991	0.3813473
C4 (1)	09/09/2009	0.002638	5.4491982	68.6994781	7.9952040	0.3276030
C5 (1)	09/09/2009	0.003176	5.1372490	69.6649780	8.0908546	0.3870652
C6 (1)	09/09/2009	0.002124	4.4095421	71.1868362	8.0591927	0.3596783
C7 (1)	09/09/2009	0.002885	5.0991049	67.5788422	8.3828907	0.3736836
C8 (1)	09/09/2009	0.003019	4.7112470	69.0713654	8.2253246	0.4332487
C9 (1)	09/09/2009	0.003179	3.9586542	67.5520554	8.3775177	0.4210897
C10 (1)	09/09/2009	0.003581	5.8410931	70.9810867	8.0804310	0.4839067
C11 (1)	09/09/2009	0.002979	4.4846282	69.4170609	8.2174025	0.3594752
C1 (1)	09/30/2009	0.002879	4.0477023	62.1205406	7.9988613	0.3584067
C2 (1)	09/30/2009	0.00271	4.7814307	71.3041687	8.3258324	0.0000000
C3 (1)	09/30/2009	0.003342	4.4398961	66.9254837	8.1548872	0.4188654
C4 (1)	09/30/2009	0.002552	4.4168992	62.6587257	7.7620988	0.3338691
C5 (1)	09/30/2009	0.00262	4.6752019	67.1116028	7.9310994	0.4092592
C6 (1)	09/30/2009	0.003256	3.8712635	65.0612793	7.9884715	0.4475019
C7 (1)	09/30/2009	0.003308	4.7909765	64.1621170	8.1566677	0.5463669
C8 (1)	09/30/2009	0.002381	4.5431266	73.2142029	8.4340439	0.3539589
C9 (1)	09/30/2009	0.003135	3.9898314	66.2370529	8.0625601	0.4902848
C10 (1)	09/30/2009	0.002176	4.7761436	68.8730469	8.0041971	0.0000000
C11 (1)	09/30/2009	0.002565	4.2599254	73.4006271	8.5510654	0.3219006
C1 (2)	09/30/2009	0.002346	4.9593539	67.6391754	7.3274059	0.1197009
C2 (2)	09/30/2009	0.002168	5.7909899	78.4558640	8.5025120	0.0000000
C3 (2)	09/30/2009	0.002947	4.2164426	65.1596680	8.1525793	0.4192259
C4 (2)	09/30/2009	0.002818	5.5981379	72.9915771	8.1359472	0.3807203
C5 (2)	09/30/2009	0.002633	4.5009322	63.7160149	7.6871996	0.0000000
C6 (2)	09/30/2009	0.003794	2.9380863	57.0716858	7.7108774	0.4933580
C7 (2)	09/30/2009	0.002955	5.2092242	70.1183319	8.5011606	0.4555227
C8 (2)	09/30/2009	0.002662	4.6492910	70.3330078	8.2566156	0.4035386
C9 (2)	09/30/2009	0.002809	3.6612771	65.5824738	8.1469841	0.3784041
C10 (2)	09/30/2009	0.002526	4.7845011	67.4897385	8.0341358	0.0000000
C11 (2)	09/30/2009	0.003648	3.7327936	60.4880333	7.8103032	0.4441078

Table F.3. 3: Elemental analyzer data for the oil obtained from thermochemical liquefaction of *Nitzschia pusilla.*

SAMPLE NAME	DATE	WEIGHT	Wt% N	Wt% C	Wt% H	Wt% S
N1 (1)	08/19/2009	0.003248	6.4540610	74.6493378	8.6691360	0.4168115
N2 (1)	08/19/2009	0.002245	5.7376909	77.0728607	8.8339243	0.3229848
N3 (1)	08/19/2009	0.002237	5.0799990	77.9089432	8.7468786	0.2396404
N4 (1)	08/19/2009	0.002885	6.2644529	75.6957397	8.5027647	0.3302890
N5 (1)	08/19/2009	0.002377	5.7616057	77.4576874	8.5458794	0.2950902
N6 (1)	08/19/2009	0.002076	5.3328485	78.8842545	8.6828337	0.2353429
N7 (1)	08/19/2009	0.003213	6.1810374	74.0507126	8.6875124	0.3381871
N8 (1)	08/19/2009	0.002367	5.4846101	76.3910446	8.6835871	0.2823020
N9 (1)	08/19/2009	0.002733	4.7734528	78.4119720	9.0814009	0.3421893
N10 (1)	08/19/2009	0.001959	6.0494423	75.9887695	8.6970587	0.3039861
N11 (1)	08/19/2009	0.003516	5.9417934	86.5567322	9.8947182	0.4021423
N1 (1)	08/26/2009	0.00293	6.2412810	72.3706589	8.3017645	0.2604469
N2 (1)	08/26/2009	0.00245	5.6055298	74.8700943	8.5925217	0.2746161
N3 (1)	08/26/2009	0.002572	4.7901850	74.8398972	8.5181923	0.2449091
N4 (1)	08/26/2009	0.003072	5.9867306	73.6308746	8.3151274	0.2255959
N5 (1)	08/26/2009	0.002356	5.5169988	74.9879990	8.3542128	0.2652737
N6 (1)	08/26/2009	0.003244	5.0503130	75.2755508	8.4543505	0.2618693
N7 (1)	08/26/2009	0.004028	6.0201316	72.0345154	8.6206703	0.3067276
N8 (1)	08/26/2009	0.002794	5.2632046	74.0358887	8.5970697	0.2957650
N9 (1)	08/26/2009	0.004398	4.5312204	74.0637207	8.6809740	0.3205578
N10 (1)	08/26/2009	0.00207	5.8886380	75.1414032	8.3858566	0.2910450
N11 (1)	08/26/2009	0.002044	5.1391630	74.6685028	8.3776731	0.2282969
N1 (2)	08/19/2009	0.002611	6.3921733	74.6278305	8.5807867	0.3347293
N2 (2)	08/26/2009	0.0042	5.4181628	73.3757477	8.5952873	0.3173541
N3 (2)	08/26/2009	0.003837	4.7627230	74.6481857	8.5518932	0.2411677
N4 (2)	08/26/2009	0.002192	5.9916534	74.5984573	8.3143349	0.2135904
N5 (2)	08/26/2009	0.003073	5.4737172	74.2491760	8.3575745	0.2647256
N6 (2)	08/26/2009	0.003367	5.1218004	76.1641464	8.4770231	0.2735613
N7 (2)	08/26/2009	0.003231	5.9384742	72.4176483	8.7178583	0.2849105
N8 (2)	08/26/2009	0.003791	5.2167087	73.7954178	8.6914701	0.2920859
N9 (2)	08/26/2009	0.003011	4.5401902	75.7528763	8.8204889	0.3465375
N10 (2)	08/26/2009	0.00421	5.7997785	73.0860901	8.4811831	0.3011298
N11 (2)	08/26/2009	0.002757	5.0505509	75.0803604	8.4284773	0.2640126

Table F.3. 4: Average elemental analyzer data and calorific value of the oil obtained from thermochemical liquefaction of *Microcystis aeruginosa*.

Run number	wt% C	wt% H	wt% N	wt% S	wt% O*	Calorific value ($MJ.kg^{-1}$)
Run 1	63.8514430	7.5315779	4.9212405	0.1206270	23.5751116	27.1228
Run 2	68.8926544	8.1809400	3.5566587	0.0605594	19.3091874	29.9519
Run 3	66.1563085	7.8421111	5.6280659	0.3536141	20.0199004	28.6250
Run 4	63.9776764	7.9039343	4.7171505	0.3309002	23.0703385	27.5938
Run 5	67.1103236	7.7438879	5.7177547	0.0860578	19.3419760	28.9112
Run 6	69.6674474	7.9528742	4.4388433	0.1729242	17.7679109	30.1830
Run 7	69.4596685	8.1156642	5.6417762	0.3768681	16.4060230	30.4279
Run 8	67.7976939	8.0374374	5.4001870	0.2665366	18.4981451	29.5378
Run 9	67.1321259	7.9342669	5.1104461	0.3023772	19.5207840	29.1025
Run 10	67.1016693	7.9083103	4.0361582	0.2891884	20.6646738	28.9458
Run 11	66.7243856	7.8530205	4.5689452	0.3285743	20.5250744	28.7796
Run 12	68.6374181	8.0060209	5.3892304	0.3531395	17.6141911	29.9056
Run 13	63.8527718	7.6404969	4.6011858	0.3697249	23.5358207	27.2564
Run 14	65.6476364	8.0201055	4.5909864	0.3353858	21.4058858	28.4665
Run 15	63.2886798	7.9316355	4.6118391	0.3146420	23.8532036	27.2935
Run 16	64.0745672	7.5696212	5.8671339	0.3280094	22.1606682	27.4075
Run 17	64.3170891	7.6893433	5.0118589	0.3459208	22.6357879	27.5579
Run 18	70.4510600	8.3020681	4.5096655	0.3476580	16.3895484	30.9515
Run 19	63.8882179	7.4301516	4.9319220	0.3254907	23.4242178	27.0773
Run 20	62.5855509	7.3230747	5.0565488	0.3088155	24.7260102	26.3793

* Calculated by difference.

Table F.3. 5: Average elemental anzalyzer data and calorific value of oil obtained from thermochemical liquefaction of *Cyclotella meneghinia.*

Run number	wt% C	wt% H	wt% N	wt% S	wt% O*	Calorific value ($MJ.kg^{-1}$)
Run 1	65.3250160	7.8037682	4.5995016	0.2766373	21.9950769	28.0807
Run 2	71.6834564	8.3063485	4.9507271	0.1346496	14.9248183	31.5208
Run 3	67.7133713	8.1511885	4.4172220	0.4064795	19.3117386	29.5448
Run 4	68.1165937	7.9644167	5.1547451	0.3473975	18.4168471	29.5982
Run 5	66.8308652	7.9030512	4.7711277	0.2654415	20.2295144	28.8887
Run 6	64.4399338	7.9195139	3.7396306	0.4335127	23.4674090	27.7403
Run 7	67.2864304	8.3469063	5.0331019	0.4585244	18.8750370	29.6306
Run 8	70.8728587	8.3053281	4.6345549	0.3969154	15.7903430	31.1712
Run 9	66.4571940	8.1956873	3.8699209	0.4299262	21.0472716	28.9648
Run 10	69.1146240	8.0395880	5.1339126	0.1613022	17.5505732	30.0918
Run 11	67.7685738	8.1929237	4.1591157	0.3751612	19.5042256	29.5801

* Calculated by difference.

Table F.3. 6: Average elemental analyzer data and calorific value of oil obtained from thermochemical liquefaction of *Nitzschia pusilla.*

Run number	wt% C	wt% H	wt% N	wt% S	wt% O*	Calorific value ($MJ.kg^{-1}$)
Run 1	74.6914775	8.6078278	6.4316991	0.3958781	9.8731175	33.4221
Run 2	75.1062342	8.6739111	5.5871278	0.3049850	10.3277418	33.5732
Run 3	75.7990087	8.6056547	4.8776356	0.2419057	10.4757952	33.7304
Run 4	74.6416906	8.3774090	6.0809457	0.2564918	10.6434630	33.0915
Run 5	75.5649541	8.4192222	5.5841072	0.2750298	10.1566866	33.5090
Run 6	76.7746506	8.5380691	5.1683207	0.2569245	9.2620352	34.1391
Run 7	72.8342921	8.6753470	6.0465477	0.3099417	12.1338714	32.5857
Run 8	75.3932699	8.7003819	5.0960016	0.3082015	10.5021451	33.6812
Run 9	76.0761897	8.8609546	4.6149545	0.3364282	10.1114730	34.1172
Run 10	74.7387543	8.5213661	5.9126196	0.2987203	10.5285397	33.2781
Run 11	74.8744316	8.4030752	5.0948570	0.2461548	11.3814814	33.1191

* Calculated by difference.

Table F.3. 7: Elemental analyzer data of *Microcystis aeruginosa*.

	Analysis 1	Analysis 2	Analysis 3	Average
wt% C	42.373	43.462	40.318	42.0508
wt% H	6.383	6.588	6.431	6.4673
wt% N	7.843	8.034	7.989	7.9555
wt% S	0.230	0.199	0.285	0.2379
wt% O*	43.170	41.718	44.977	43.2885
H/C	0.151	0.152	0.160	0.1539
O/C	1.019	0.960	1.116	1.0314

* Calculated by difference.

Table F.3. 8: Elemental analyzer data of *Cyclotella meneghinia*.

	Analysis 1	Analysis 2	Analysis 3	Average
wt% C	47.248	50.030	37.306	44.8612
wt% H	6.658	6.644	6.318	6.5401
wt% N	7.139	8.229	6.216	7.1946
wt% S	2.327	1.086	0.673	1.3622
wt% O*	36.628	34.010	49.487	40.0418
H/C	0.141	0.133	0.169	0.1477
O/C	0.775	0.680	1.327	0.9272

* Calculated by difference.

Table F.3. 9: Elemental analyzer data of *Nitzschia pusilla*.

	Analysis 1	Analysis 2	Analysis 3	Average
wt% C	41.499	46.021	47.589	45.0365
wt% H	6.405	6.401	6.708	6.5048
wt% N	6.142	6.887	7.088	6.7055
wt% S	0.336	0.550	0.529	0.4716
wt% O*	45.617	40.141	38.086	41.2816
H/C	0.154	0.139	0.141	0.1448
O/C	1.099	0.872	0.800	0.9239

* Calculated by difference.

F.4 Bomb calorimeter data

Tables F.4.1, F.4.2 and F.4.3 list the bomb calorimeter data of the *M. aeruginosa, C. meneghinia and N. pusilla* algae, respectively.

Table F.4. 1: Bomb calorimeter data of *Microcystis aeruginosa*.

	Calorific value ($MJ.kg^{-1}$)
Run 1	20.723
Run 2	20.713
Run 3	20.715
Average	20.717
Stdev	0.005
z value	3.182
±	0.019
%Error	0.094

Table F.4. 2: Bomb calorimeter data of *Cyclotella meneghinia*.

	Calorific value ($MJ.kg^{-1}$)
Run 1	18.938
Run 2	18.740
Run 3	18.938
Average	18.872
Stdev	0.114
z value	3.182
±	0.420
%Error	2.226

Table F.4. 3: Bomb calorimeter data of *Nitzschia pusilla*.

	Calorific value ($MJ.kg^{-1}$)
Run 1	17.416
Run 2	17.242
Run 3	17.548
Average	17.402
Stdev	0.153
z value	3.182
±	0.564
%Error	3.241

Appendix G. – Calculation of the ECR

In this appendix the experimental data that was used for the calculation of the ECR is listed. Table G.1 lists the experimental data that was obtained from the liquefaction experiment used to determine the ECR. Table G.2 lists the calculation of the ECR.

Table G. 1: Experimental data for ECR calculation.

Reaction Time	Voltage (V)	Ampere (A)
00:10	1.331	13.310
00:20	2.188	21.880
00:30	0.010	0.100
00:40	1.332	13.320
00:50	0.907	9.070
01:00	1.325	13.250
01:10	0.010	0.100
01:20	1.314	13.140
01:30	0.903	9.030
01:40	0.908	9.080
01:50	0.910	9.100
02:00	1.330	13.300
02:10	1.324	13.240
02:20	1.323	13.230
02:30	1.324	13.240
Average for experiment	1.096	10.959
Average for heating time	1.039	10.390
Average for reaction time	1.324	13.237

Table G. 2: Calculation of ECR.

C_v of oil	28.42	$kJ.g^{-1}$
Mass oil extracted	0.435	g
Energy from oil	12.3627	kJ
Energy used for reaction	2912.067	Watt
	2.912067	kW
	2912.067	$J.s^{-1}$
Time necessary for reaction	1800	s
Energy used for reaction	5241720	J
	5241.72	kJ
ECR	423.99	